Characterization of Autologous Cell Sources for Alternatives to Aortic Valvular Interstitial Cells in Tissue Engineered Heart Valves

by

Emma Claire Ambrose

A Thesis Submitted to the Faculty of Graduate Studies of

The University of Manitoba

in partial fulfillment of the requirements for the degree of

MASTER OF SCIENCE

Department of Physiology and Pathophysiology

University of Manitoba

Winnipeg

FOR MY FATHER, CHRISTOPHER FREYE HAUCH

TABLE OF CONTENTS

ACKNOWLEDGEMENTS

I would first and foremost like to express my gratitude for my supervisor Dr. Ian M.C. Dixon for his mentorship, encouragement, and endless support. Your belief in my abilities as a student and a scientist has given me the strength to persevere through challenges and strive for greatness. You inculcated in me the importance to think critically, to ask questions and to approach science with great fervor. I am grateful to you for the opportunities provided to me and the experiences I have gained throughout my training. I would also like to acknowledge the current and former members of the Dixon lab for their encouragement, support and friendship. I would most especially like to thank Sunil Rattan whose constancy and leadership I admire, and whose expertise and support facilitated my research.

I would like to acknowledge my committee members, Drs. Peter Cattini, Jeffery Wigle, Andrew Halayko and Darren Freed for their guidance and insight and for fostering an environment that encouraged me to look forward and expand my boundaries. Most of all I am grateful for the stimulating scientific discourse that incited my true passion for research.

I would like to extend my gratitude to Dr. Michael Czubryt, Dr. Rushita Bagchi and Patricia Roche for their assistance in performing the microarray and RT-qPCR assays. I would also like to thank Dr. Christopher White for his training in large animal surgical techniques.

I am extremely grateful to Gail McIndless and Judith Olfert for their incredible support. I would also like to thank all of the wonderful members of the Institute of Cardiovascular Sciences, especially my fellow graduate students who truly made this experience one to value and remember.

I gratefully acknowledge the funding agencies that supported our research and made our work possible, including Research Manitoba, CANUSA, Graduate Enhancement of Tri-Council Stipends, and the Institute of Cardiovascular Sciences.

Lastly I would like to thank all of my friends and family who supported me through this endeavor.

"*Have the courage to follow your heart and your intuition. They somehow know what you truly want to become.*" – Steve Jobs

LIST OF ABBREVIATIONS

2D	Two-dimensional
3D	Three-dimensional
α-SMA	Alpha-smooth muscle actin
A-fib	Atrial fibroblast
ADAM	A disintegrin and metalloproteinase domain-containing protein
AF	Atrial fibrillation
ALP	Alkaline phosphatase
AR	Aortic regurgitation
AS	Aortic stenosis
AVA	Aortic valve annulus
AVD	Aortic valve disease
aVIC	Activated valvular interstitial cell
BCA	Bicinchoninic acid
bHLH	Basic helix-loop-helix
BMC	Bone marrow-derived progenitor cell
BMP-2	Bone morphogenetic protein-2
BSA	Bovine serum albumin
BSP	Bone sialoprotein
cGMP	Cyclic guanosine monophosphate
CAVD	Calcific aortic valve disease
D-fib	Dermal fibroblast
DAPI	4',6-diamidino-2-phenylindole

DDR2	Discoidin domain receptor 2
DHV	Decellularized heart valves
DLL	Delta-like
DMEM	Dulbecco's modified eagle's medium
DNA	Deoxyribonucleic acid
DSL	Delta or Jagged/Serrate
ECM	Extracellular matrix
EDA-FN	Extra domain A fibronectin
EDTA	Ethylenediaminetetraacetic acid
ELISA	Enzyme-linked immunosorbent assay
EMT	Epithelial-to-mesenchymal transition
emVIC	Embryonic valvular interstitial cell
EndMT	Endothelial-to-mesenchymal transition
ESC	Embryonic stem cell
F-actin	Filamentous actin
FBS	Fetal bovine serum
FGF	Fibroblast growth factor
FSC	Fetal-derived stem cell
GAG	Glycosaminoglycan
GAPDH	Glyceraldehyde-3-phosphate dehydrogenase
GPa	Gigapascal
HES	Hairy and enhancer-of-split
HEY	Hairy and enhancer-of-split related with YRPW motif
HLA	Human leukocyte antigen

HSC	Hematopoietic stem cell
iCPC	Induced cardiac progenitor cells
IE	Infective endocarditis
INR	International normalized ratio
iPSC	Induced pluripotent stem cell
iTRAQ	Isobaric tagging for relative and absolute quantification
IV	Intravenous
JAG	Jagged
KIT	v-kit Hardy-Zuckerman 4 feline sarcoma viral oncogene
KLF-4	Kruppel-like factor 4
kPa	Kilopascal
LAA	Left atrial appendage
LC	Liquid chromatography
MMP	Matrix metalloproteinase
mRNA	Messenger ribonucleic acid
MSC	Mesenchymal stem cell
MS/MS	Tandem mass spectrometry
MYC	Avian myelocytomatosis virus oncogene cellular homolog
NG2	Neural/glial antigen 2
NICD	NOTCH intracellular domain
OB-CDH	Osteoblastic cadherin
obVIC	Osteoblastic valvular interstitial cell
OCN	Osteocalcin
OCT3/4	Octamer-binding transcription factor 3/4

ODSC	Organ-derived stem cells
OPN	Osteopontin
P0/P1	Passage 0/passage 1
PAGE	Polyacrylamide gel electrophoresis
PBS	Phosphate buffered saline
PCL	Polycaprolactone
PG	Proteoglycan
PGA	Polyglycolic acid
PGS	Polyglycerol sebacate
PKG	cGMP-dependent protein kinase
PSEN	Presenilin
pVIC	Progenitor valvular interstitial cell
qVIC	Quiescent valvular interstitial cell
PFA	Paraformaldehyde
RBPJ	Recombination signal binding protein for immunoglobulin kappa J region
RAS	Rheumatic aortic stenosis
RCF	Relative centrifugal force
RER	Rough endoplasmic reticulum
RGD	Arginine-glycine-aspartate
RIN	Ribonucleic acid integrity number
RT-qPCR	Quantitative reverse-transcriptase polymerase chain reaction
RUNX2	Runt-related transcription factor 2
SAVR	Surgical aortic valve replacement
SEM	Standard error of the mean

SMC	Smooth muscle cell
SMEM	Minimum essential media
SMEMB	Embryonic smooth muscle myosin heavy chain
SOX2	Sex determining region Y-box2
SSEA-4	Stage-specific embryonic antigen-4
TAVI	Transcatheter aortic valve implantation
TEHV	Tissue-engineered heart valve
TGF-β	Transforming growth factor beta
TGF-β_1	Transforming growth factor beta-1
TIMP	Tissue inhibitor of matrix metalloproteinase
UCBC	Umbilical cord blood cell
VEGF	Vascular endothelial growth factor
VIC	Valvular interstitial cell
VIM	Vimentin
VKA	Vitamin K antagonist

LIST OF TABLES

LIST OF FIGURES

ABSTRACT

Aortic valve disease (AVD) represents a spectrum of etiologies and pathologies; however, all severe cases lead to similar disease sequelae, including decompensated cardiomyopathy, reduction of forward blood flow, dyspnea and heart failure. The gold standard treatment for patients with AVD is surgical replacement of the aortic valve with either mechanical or fixed tissue prostheses. These implants have a limited lifespan and are associated with serious adverse events; thus, providing the rationale to develop superior alternative devices. Patient autologous tissue engineered heart valves (TEHVs) offer a solution, as tissue valves would mitigate some of the issues that arise with current implants. Vital to the development of a TEHV is determining a source of donor tissue(s) that most closely mimics the native valve tissue. The main cellular component found in aortic valve cusps are valvular interstitial cells (VICs). These cells are responsible for the synthesis, degradation and maintenance of the extracellular cellular matrix. In pursuit of determining an alternative cell source for patient autologous TEHVs we compared a number of phenotypic and genotypic characteristics of atrial fibroblasts (A-fibs), dermal fibroblasts (D-fibs) and differentiated bone marrow-derived progenitor cells (BMCs) and made a comparison to VICs. We demonstrate that while VICs share some phenotypic similarities with fibroblasts and BMCs, they also possess unique characteristics and demonstrate differential mRNA expression of key regulatory pathways that may influence their phenotype.

We conclude that a greater understanding of the genes that mediate phenotypic differences between VICs and A-fibs, D-fibs and BMCs is a first step towards determining a patient autologous cellular source for valve implants, which would advance TEHV technology and improve therapeutic options for patients with aortic valve disease.

1. INTRODUCTION

1.1. Aortic valve

The aortic valve is positioned between the left ventricular outflow tract and the aorta, and posterior to the pulmonic valve (1). The aortic valve facilitates unobstructed, unidirectional blood flow during systole and prevents the regurgitation of blood back into the left ventricle during diastole (2). The aortic valve has two main components: the annulus, and the cusps (or leaflets). The annulus is a thick fibrous ring that lies at the aortic root and provides the structure to the valve orifice. Three thin leaflets (right, left and posterior) are attached to the annulus and form a valve opening between 3 and 4 cm^2 (3). The aortic valve leaflets form the physical boundary between the left ventricle and the aorta. During systole, the pressure within the left ventricle generated by the contracting myocardium forces the aortic valve to open (4). During diastole, the reversed hemodynamic pressure pushes the leaflets towards the center of the annulus, closing the valve (4). Tight coaptation of the leaflets prevents backflow into the heart during diastole (Figure 1) (2). The leaflets of the aortic valve form three distinct layers: 1) ventricularis; 2) fibrosa; and 3) spongiosa, each defined by a unique extracellular matrix (ECM) composition (5, 6) (Figure 2). The ventricularis lies on the inflow side of the valve, proximal to the left ventricle, and consists mainly of radially aligned elastin fibers (7). Elastin provides the valve leaflet with the elasticity required to stretch during diastole, allowing for proper coaptation. The collagen-dense fibrosa layer lies on the outflow tract of the aortic valve (8). The collagen fibers of the fibrosa are arranged circumferentially and lie perpendicular to the elastin fibers (8, 9). The strength provided by the collagen fibers prevents the leaflets from prolapsing into the

ventricle during diastole (2). The spongiosa consists of hygroscopic glycosaminoglycans (GAGs) and proteoglycans (PGs), which act to resist compression, provide flexibility, and transmits shear forces between the outer two valve layers (7-10).

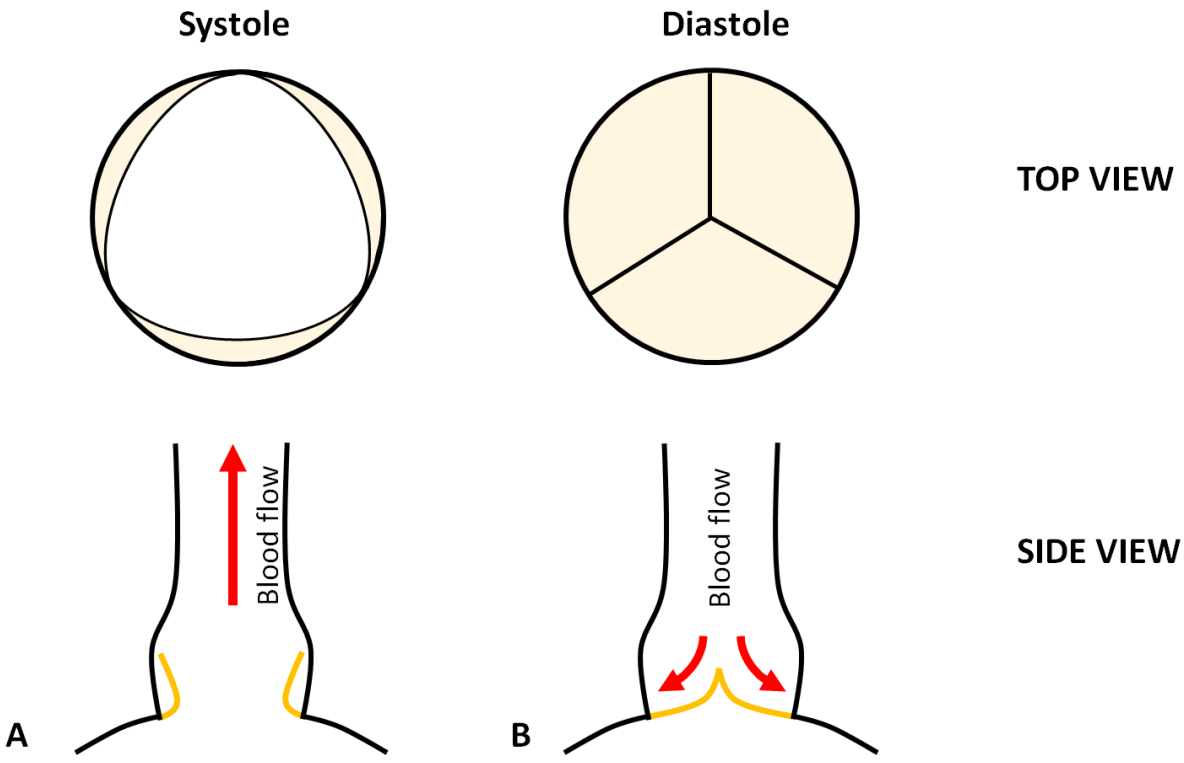

Figure 1: Aortic valve structure and function during the cardiac cycle
(A) During systole, the aortic valve opens and allows forward blood flow through the left ventricular outflow tract. **(B)** In diastole, the aortic valve leaflets close and prevent backflow into the heart. Adapted with permission from Hutcheson *et al* (2).

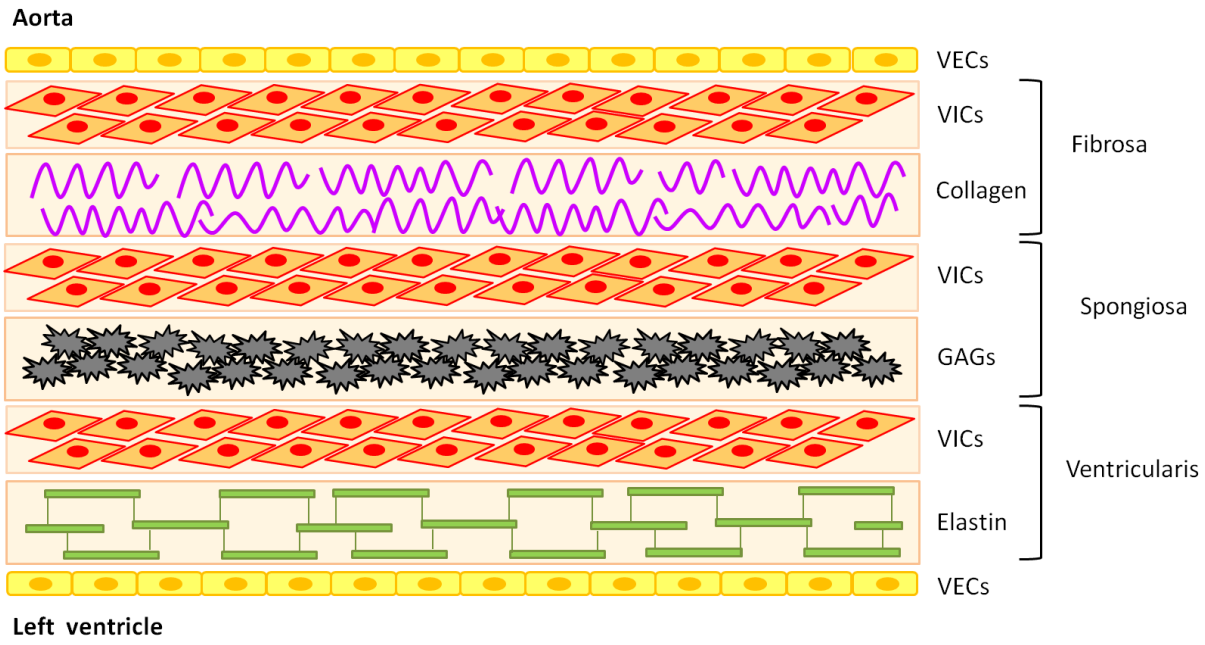

Figure 2: Cross-section depicting the trilaminar structure of the aortic valve leaflet
A monolayer of valvular endothelial cells (VECs) line the aortic valve leaflet. Valvular interstitial cells (VICs) are the main cellular component of the aortic valve and are found in all three layers: 1) fibrosa, 2) spongiosa, and 3) ventricularis. Collagens, glycosaminoglycans, and elastin are found in high abundance in the fibrosa, spongiosa, and ventricularis, respectively. Abbreviations: glycosaminoglycans (GAGs), valvular endothelial cells (VECs) and valvular interstitial cells (VICs). Adapted with permission from Leopold (11).

1.2. Aortic valve disease

The aortic valve open and closes with every cardiac cycle, a remarkable 3 billion times over the course of a lifetime (7). These repetitive mechanical and hemodynamic stresses can cause to physical damage of the aortic valve and subsequently lead to aortic valve disease (12). Individuals can live asymptomatically with a degree of valvular impedance; however those who progress to decompensated aortic valve disease may suffer from irreversible LV dysfunction, pulmonary hypertension, atrial fibrillation, stroke, dyspnea and heart failure (13, 14). There are several causes of decompensated aortic valve disease, most of which will be discussed below.

1.2.1. Aortic stenosis

Aortic stenosis is a hemodynamic narrowing of the left ventricular out flow tract and is often accompanied by aortic sclerosis (fibrotic thickening and calcification of the leaflets) (15). Individuals can live with AS asymptomatically for a number of years prior to being diagnosed (16). Once the disease has progressed to symptomatic AS, patients will commonly present with angina, syncope and/or heart failure and the onset of these symptoms typically occurs once the aortic valve area (AVA) is ≤ 1 cm^2 (15). There are three main types of aortic valve stenosis: 1) degenerative calcific aortic stenosis; 2) rheumatic aortic stenosis; and 3) congenital aortic stenosis (15, 17-19).

Degenerative calcification of the aortic valve is the most common cause of aortic stenosis in industrialized countries and is most frequently seen in adults 65 years or older, with an estimated 5% of the population acquiring moderate to severe degenerative calcific disease by the age of 75 (20-24). Calcific aortic valve disease (CAVD) is a dynamic process that involves biological,

chemical and physical changes. Hemodynamic "wear and tear" of the valve leaflets, as well as inflammation, lipid accumulation, mineralization and fibrosis are all processes that have been implicated in the progression of CAVD (17, 18, 25-27). Typically, the valve undergoes fibrocalcific remodeling over the period of years to decades, leading to an over-abundance collagen accumulation and calcium deposition on the leaflets (2). However, an exception to this is the observation of rapid calcification of the aortic valves seen in end-stage renal disease patient undergoing dialysis (28).

Rheumatic aortic stenosis (RAS) is a secondary complication to an untreated group A streptococci infection that leads to an abnormal autoimmune response causing pancarditis and valvular fibrosis (29, 30). RAS remains the most common cause of AS in low-middle income countries and is estimated to be responsible for more than 300 000 deaths worldwide each year (19, 30-32) However, RAS continues to be a concern amongst the Indigenous populations of Australia, New Zealand and Canada (33, 34).

Congenital aortic stenosis is a condition in which infants are born with a bicuspid, unicuspid, or quadricuspid valve, predisposing these individuals to valvular damage and aortic insufficiency (35, 36). More specifically, bicuspid aortic valve disease is the most common form of congenital heart defects affecting 1-2% of the global population (37, 38). This disease, found predominantly in males, puts patients at a 10 fold greater risk of suffering from aortic dissection as well as an additional risk of endocarditis, aortic coarctation, dilation of the proximal ascending aorta and aortic aneurysm (37, 39). The complications secondary to congenital valve stenosis can drastically increase the financial burden of the disease (37).

Congenital valvular malformations and rheumatic valve disease predispose the aortic valve to fibrocalcific remodeling and stenosis (15, 35).

Individuals diagnosed with severe aortic stenosis have a 50% mortality rate at 1 year, and 90% mortality at 5 years, if the disease if left untreated (24). This underscores the importance of early surgical intervention.

1.2.2. Aortic regurgitation

Aortic regurgitation (AR) is characterized by failure of the leaflets to coapt during diastole, resulting in reflux of blood into the left ventricle (40, 41). Bicuspid aortic valves (or congenital valve defects), calcific valve disease and rheumatic heart disease are common etiologies of AR; however, AR can also be a secondary sequelae arising from diseases that cause dilation of the aortic root or ascending aorta, such as Marfan's syndrome (40, 42-44). Similar to AS, most patients with AR experience a slow progression in their disease and are at risk of left ventricular volume overload and heart failure (14, 45).

1.2.3. Infective endocarditis

Infective endocarditis (IE) is an infection of the endocardial lining of the heart, most commonly caused by persistent bacteremia (46-52). Risks factors of the disease include: intravenous (IV) drug use, degenerative CAVD, nosocomial infections, valves prostheses and implantable devices and/or intravascular catheters (49, 50, 52, 53). Individuals with in degenerative CAVD are at a high risk of developing IE as the fibrocalcific remodeling provides a nidus for bacteria to form vegetative lesions on the valve leaflets (46, 53). Vegetations on native

valves or valves prostheses can cause severe AS or AR, leading to congestive heart failure (46, 47, 51, 52).

1.3. Treatment of aortic valve disease

The standard treatment for severe aortic valve disease is surgical replacement of the aortic valve with a mechanical or fixed-tissue prosthesis (54). Despite advances in quality and design, the current options for valve implants continue to have substantial limitations (55). Mechanical heart valves are made with metal disks that confer long durability and have a low likelihood of reoperation; however, these implants put patients at high risk of hemolysis and thromboembolism, which requires life-long anti-coagulation therapy (55-57). The guideline-determined medical therapy for post-surgical aortic valve replacements (SAVR) with mechanical prosthesis is anti-coagulation therapy with Warfarin (Coumadin), a vitamin K antagonist (VKA) (14, 57). VKAs have many drug-drug interactions and are affected by dietary levels of vitamin K and blood alcohol content; thus patients prescribed VKAs have alcohol and dietary limitations (58-61). Monthly monitoring for dose titration are required to ensure that international normalized ratio (INR) levels remain in the therapeutic range, which may be challenging for patients with limited access to healthcare facilities. Patients on anti-coagulation therapy are at high risk of bleeding events – with intracranial hemorrhage being of great concern (62, 63). Massive bleeding events are of particular concern for children and young adults who participate in sports and/or other rigorous activities (61). In addition, women of child bearing age may not be suitable candidates for mechanical heart valves as VKAs are associated with increased fetal death and hemorrhagic sequelae (64).

Bioprosthetic valves made from fixed porcine or bovine pericardial tissue do not require anticoagulation therapy; however, these implants are susceptible to structural deterioration and calcification and typically require reoperation within 10-15 years, with accelerated degeneration of bioprosthetic valves seen in children and young adults (65-67). As such, bioprosthetic valves are more commonly used in patients aged 65 or over, or in those for which anti-coagulation therapy is contraindicated (65). In addition, bioprosthetic valves, similar to mechanical valves, are rigid and do not compensate for cardiac growth and or remodeling, necessitating repeat surgeries for pediatric patients (68). In addition to the emotional and physical impacts that a patient endures by undergoing re-replacement surgery, there is also a substantial financial burden placed of the health care system with each repeat procedure (69).

Other surgical interventions include transcatheter aortic valve implantation (TAVI), which is a minimally invasive endocatheter approach for valve replacement (70, 71). A relatively new procedure, TAVI is only used for those individuals who are considered too high risk for SAVR (71-74). The Ross procedure – replacement of the aortic valve with a pulmonic autograft – is used in infants and young children (75, 76). Although this procedure has the best hemodynamic outcome, there are high rates of prosthetic pulmonic valve stenosis and higher operative risk (77).

As there are considerable risks with surgical intervention, physicians adopt a “watch and wait” philosophy towards managing patients with asymptomatic aortic stenosis (16). This is not without concern as the early stages of aortic stenosis are concomitant with irreversible left ventricular remodeling is response to pressure overload, which can lead to additional complications such as mitral regurgitation and atrial fibrillation (72, 78).

The long-term outcome for patients suffering from AVD remains poor, despite surgical and medical intervention. This necessitates the development of an alternative valve prosthesis that would have fewer associated risks and quality of life limitations. Such a prosthesis may then be indicated for those patients with early asymptomatic AVD and prevent complicated disease sequelae.

1.4. Tissue engineered heart valves

Tissue engineering is an interdisciplinary field that provides a potential solution to the limited supply of donor organs and inadequacy of modern implants (68, 79). To date, this area of research is poised for significant advances and has covered nearly all mammalian tissue, including: cornea, skin, cartilage, bone, liver, intestine, ureter/urinary bladder, nervous system, myocardium, and heart valves (80-88). The practice of tissue engineering and regenerative medicine includes any and all biological substitutes that use either: 1) cells alone; 2) biocompatible, biodegradable substrates alone; 3) or a combination of both cells and biomaterials (89). Successful construction of implantable tissue-engineered heart valves (TEHVs) requires both a biocompatible scaffold as well as an appropriate cellular alternative to native VICs (79, 90, 91).

1.4.1. Scaffolds for tissue engineered heart valves

Scaffolds for TEHVs can be categorized as either biodegradable synthetic matrices or natural (or biologic) scaffolds (68, 81, 90-92). Natural scaffolds are made by exposing donated human

tissue or non-human mammalian tissue to chaotropic agents that remove the cellular components while leaving the extracellular matrix intact (80, 93, 94). Decellularized allografts are less immunogenic than non-human mammalian matrices; however, the limited supply of human cadaveric donor tissue precludes widespread clinical use of allografts at this time. As such, decellularized xenogenic scaffolds are more widely studied, and are becoming promising candidates for tissue-engineered valve replacements (92, 95, 96).

Synthetic matrices are made using biodegradable, polymeric substrates to construct scaffolds that resemble native valve tissue. Although synthetic scaffolds are currently limited by insufficient biomechanical properties, the polymeric substrates used are non-immunogenic, non-antigenic and are less thrombogenic than decellularized valve scaffolds (92).

1.4.1.1. Decellularized scaffolds

Decellularized heart valves (DHVs) share similar hemodynamic and biomechanical properties to that of native heart valves. Usually, the decellularization process maintains the structural integrity of the matrix, including the microvasculature, which is challenging to recreate with modern technology (90, 95, 97). DHVs also contain a rich course of signaling molecules that support the adhesion of cells to the matrix and promote cellular proliferation. For example, ECM proteins collagen and fibronectin contain RGD sequences, or cellular adhesion motifs, that can bind to cellular transmembrane proteins, such as integrins (80, 98). In addition, the ECM contains matrix-bound growth factors and chemoattractants that facilitate cellular division and differentiation (92).

The immunogenicity of allogeneic and xenogeneic scaffolds remains an obstacle in using biologic scaffolds for tissue engineering. Theoretically, the removal of native cells should eliminate host immune rejection without chemically fixing the tissue; however, studies have shown that decellularization does not completely abrogate antigenicity (90, 95, 99, 100). This is attributable to incomplete removal of cellular debris and antigenic epitopes found on matrix proteins (100). Although matrix proteins are well conserved amongst species there are some antigens found on xenographs that elicit a robust immune response in humans: for example, the ECM component galactose-alpha-1,3-galactose (α-gal) found in porcine tissue (100, 101). This has led to studies using α-gal knockout animals or pre-treatment of the valve scaffold with α-galactosidase (98, 102-107). Residual cytosolic and membrane proteins as well as associated genetic material can also elicit an inflammatory response, leading to rapid breakdown and/or calcification of the decellularized scaffold (43, 108-110).

Another drawback to native matrices is that the decellularization process can breakdown the ECM, altering the biomechanical and hemodynamic properties of the biologic scaffolds – although this can be minimized by avoiding the use of harsh chaotropic agents (80, 97, 108, 111-113). Chemically crosslinking decellularized scaffolds maintains valve integrity and reduces both antigenicity and immunogenicity, but it decreases reseeding potential by lowering the bioavailability of ECM adhesion motifs (92). Further, repopulation of DHVs with donor cells remains largely unsuccessful. New methods for reseeding or scaffold preparation will be required to increase the effective delivery of cells into the collagen-dense matrix (94, 114).

1.4.1.2. Bioprinted scaffolds

Bioprinting is a technique that allows for the creation of complex, patient-specific 3D structures through a process of depositing layers of material and fusing them together (115, 116). Unlike other valve scaffolds that must be seeded once the structure is formed, ECM components, proteins, cytokines and/or living cells can be deposited into the 3D scaffold simultaneously (117). Osteoblasts, pluripotent cells, endothelial cells and cardiac cells have been successfully bioprinted; however, survival of printed cells over the duration of lengthy procedures remains a challenge (118). Biomimetic hydrogels and gelatinous proteins are commonly used materials in bioprinted heart valves (119-122). These biodegradable synthetic materials have tunable porosities and pore size, and can be made with varying levels of stiffness (123). Despite the versatility of bioprinted structures, reproducing the mechanical strength, flexibility and intricate structure of semilunar hearts valves using 3D bioprinting methods remains a challenge (118). Notably pre-vascularization of tissues cannot yet be done reliably and requires the improvement of nanoscale bioprinting (115, 124). The aforementioned constraints of bioprinted heart valves have precluded clinical use, and vast improvements in technology are required before bioprinted scaffolds become a reasonable option for TEHVs.

1.4.1.3. Electrospun scaffolds

Electrospinning technology produces nanofibrous scaffolds by applying a high voltage to a polymeric liquid while the substance is being ejected through a syringe pump (125, 126). Once ejected from the syringe, the polymeric nanofibers adhere to a mold and create a fibrous mesh (125, 127). This technology is easy to perform and can create scaffolds with high levels of

structural and mechanical anisotropy, which is crucial when trying to imitate the unique structural layers found in native semilunar heart valves (127-132). Polyglycolic acid (PGA), polyglycerol sebacate (PGS) and polycaprolactone (PCL) are commonly used due to their biocompatibility and their ability to be degraded without the release of harmful toxins (133-137). Previous studies have shown that electrospun valves can support the growth of VICs and MSCs and that these cells can degrade the polymeric substrate and replace the scaffold with ECM deposition (134). However, similar to bioprinted constructs, electrospun valve scaffolds have failed to recapitulate the mechanical strength and flexural modulus of the native heart valve (127, 138, 139).

1.4.2. Cellular alternatives for TEHVs

Numerous cellular sources have been investigated for their potential use in bioengineering, including: stem cells, progenitor cells, and committed non-parenchymal cells (82, 140-149). In regenerative medicine, stem cells or progenitor cells refer to any of the following: embryonic stem cells (ESCs), fetal-derived stem cells (FSCs), adult-derived stem cells or progenitor cells, as well as adult induced pluripotent stem cells (iPSCs) (97). Depending on the stage in development in which the stem cells are isolated, they may have varying degrees of differentiation potential (i.e. totipotent, pluripotent or multipotent) (150-152). Totipotent stem cells have the greatest differentiation potential and can generate any embryonic tissue, as well as give rise to the placenta. Pluripotent and multipotent stem cells, on the other hand, are restricted to embryonic tissue only (151). The distinction between pluripotency and multipotency is that pluripotent stem cells can give rise to cell types in any of the three germ layers (ectoderm, mesoderm and

endoderm), whereas multipotent stem cells are committed to a single germ layer (151). Progenitor cells, another cell type with regenerative potential, are even further differentiated and are typically restricted to only a single cell lineage (153).

To determine whether or not a cellular source(s) is appropriate for bioengineered tissue, there are several characteristics that must be considered, such as: a) the urgency of need of the tissue replacement; b) the feasibility of cellular harvest and expansion; and c) the requirement of differentiation potential (97). Imminent need for organ replacement requires readily available cells, such as allogeneic adult stem cells, ESCs or potentially banked iPSCs (97). Non-emergent cases are more conducive to using autologous cell sources including committed, primary cells or adult-derived stem or progenitor cells (97).

As aortic heart valve replacements are commonly non-emergent cases and patients are treated medically for an extended length of time prior to surgical intervention, the flexible timeframe permits the use of autologous cells for TEHVs and warrants greater investigation towards patient-specific cellular alternatives (97).

1.4.2.1. Embryonic stem cells

Embryonic stems cells (ESCs) are isolated from the inner cell mass of a blastocyst (154). Isolated shortly after fertilization, ESCs retain totipotency and can thus give rise to the placenta, embryo, and all post-embryonic tissues. The ability of ESCs to differentiate into all three germ layers, namely, the ectoderm, mesoderm and endoderm, has great implications in regenerative medicine (154). ESCs demonstrate an extraordinary proliferative capacity – they can undergo several hundred passages without becoming senescent, *in vitro* (155). Additionally, as ESCs are

derived from early stage embryos and have had little environmental influence, they lack many epigenetic modifications. As a result, they may be more easily programmable than stem cells derived from adult tissues (97).

There are, however, several drawbacks regarding the use of ESCs in tissue engineering. Firstly, cells derived from embryos are allogeneic in origin and face immune rejection if they are transplanted into non-gamete providers (144, 156). However, this genetic mismatch can be overcome through somatic cell nuclear transfer to create cells that are immunologically identical to the recipient (156, 157). Secondly, ESCs can form teratomas if they are implanted in an undifferentiated state. Consequently, these cells require further *in vitro* processing prior to use (158). To overcome this barrier, studies investigating cellular alternatives for VICs have shown that exposure of ESCs to cardiopoietic factors such as bone morphogenetic protein 2 (BMP-2), transforming growth factor-beta (TGF-β) and vascular endothelial growth factor (VEGF) can differentiate ESCs towards a cardiac lineage (154, 158-163). Lastly, there remains a moral opposition towards the use of ESCs in tissue engineering and/or research; therefore, a resolution of this ethical dilemma is required prior to practical application (114, 156, 157, 164-166).

1.4.2.2. Fetal-derived cells

Fetal stem cells (FSCs) are not yet widely used in tissue engineering; however more recently there have been advancements in the isolation of mesenchymal stem cells (MSCs) from fetal tissue (97). FSCs derived from first trimester fetal tissue retain a high proliferative capacity and express pluripotent stem cell markers, indicating multi-lineage potential (167). Nevertheless, FSCs demonstrate a reduced propensity towards teratoma formation. Not surprisingly, isolation

of cells directly from fetal tissue remains an ethically debated subject; however, fetal stem cells can be derived from a less contentious source: amniotic fluid (156, 164). Fetal stem cells isolated from amniotic fluid are more readily accessible, easily expandable and can be reprogrammed to pluripotent stem cells (97). Given that amniotic fluid-derived progenitors are easy to obtain and retain self-renewal properties *in vitro*, the use of fetal derived cells in tissue engineering will likely increase.

1.4.2.3. Adult-derived stem cells and progenitor cells

Adult-derived stem cells pertain to any multipotent cell source that has been isolated from post-nascent tissue, including umbilical cord blood, bone marrow and organ-derived progenitor cells (97). Unlike embryonic and fetal stem cells, adult-derived progenitors and have a reduced proliferative capacity and are committed to one lineage, i.e. multipotent (97). Umbilical cord blood cells (UCBCs) are isolated from placental blood shortly after parturition and can be expanded as a source of mesenchymal stem cells (97, 168). An advantage of using MSCs derived from cord blood over other allogeneic adult sources is that UCBCs express only the class I human leukocyte antigen (HLA), not class II HLA. As a result, they are far less immunogenic and can be transplanted with a greater degree of genetic mismatch (169-172). For this reason, UCBC are becoming more popular in TEHV research (173).

Bone marrow-derived mesenchymal stem cells or progenitors (BMCs) are another source of mulitpotent mesenchymal cells, and are characterized by their plastic adherent capacity, fibroblast-like morphology and their ability to differentiate into osteoblasts, chondrocytes, and adipocytes (153, 174, 175). Although BMCs are most commonly isolated directly from bone

marrow, BMCs can also be found in the circulation and these cells have been shown to replenish cells in various tissues in the body, including heart valves (175, 176). For this reason, there has been a substantial amount of research investigating the *in vitro* manipulation of BMCs towards a VIC phenotype (142, 177-189). Studies have shown that exposure to mechanical stretch and fibroblast growth factors (FGFs) mitigate BMC osteogenic differentiation and that these cells share similar levels of collagen expression to that of native aortic VICs (143, 180).

Organ-derived stem cells (ODSCs) or progenitors are multipotent cells with self-renewal properties that maintain the regeneration of the tissue in which they reside (174). As these cells are derived directly from the tissue of interest, organ-derived progenitors require less *in vitro* manipulation to create phenotypically similar cellular donors for bioengineered tissue (174). Despite the instinctive advantage of tissue-derived stem cells, they are often found in low abundance and require considerable *in vitro* expansion for clinical application, which is costly and laborious (190). Additionally, isolation of ODSCs for autologous transplantation may not be feasible as retrieval may reduce or abolish tissue function, causing harm to the patient (190). For example, cardiac stem cells may be a phenotypically compatible cellular source for VICs due to their cardiogenic differentiation potential, but extraction of cardiac progenitor cells for patient autologous TEHVs is impractical (190-193). This has prompted the development of induced cardiac progenitor cells (iCPCs), a more committed variation of induced pluripotent stem cells (194).

Induced pluripotent stem cells (iPSCs) are adult-derived cells that have been de-differentiated via genetic manipulation to become pluripotent (195-197). iPSCs have been genetically reprogrammed to an embryonic-like state via induction of four transcription factors: *MYC*, *KLF-4*, *OCT3/4* and *SOX2* (196, 197). This allows that creation of patient-specific cell

lines that can generate nearly any cell type, and circumvents the risk of immune rejection and ethical concerns regarding use of human embryos; however, reprogramming does not completely reverse epigenetic modifications of the DNA, which may hinder practical use (97, 198, 199). Additionally, human iPSCs are costly and take considerable time to produce, and if implanted in an undifferentiated state can cause teratomas (198, 200). The teratogenic risk may be mitigated if pluripotent stem cells are differentiated into iCPCs prior to implantation (201, 202). Albeit, a superior method may be developing cardiac progenitors directly from stromal cells via expression of cardiogenic transcription factors, circumventing the iPSCs stages (194). For example, fibroblast are non-parenchymal cells that have been be reprogrammed into iCPCs (201). An advantage of using stromal cells, such as fibroblasts, in regenerative medicine is their accessibility and abundance, increasing TEHV feasibility (201). Likewise, as previously mentioned, VICs are often characterized as phenotypically similar to fibroblasts (203). This provides a rationale to pursue the investigation of directly using fibroblasts for recapitulating scaffolds for biological valve implants.

1.4.2.4. Adult-derived stromal cells

Non-parenchymal cells such as fibroblasts and endothelial cells are important in maintaining the structure of the tissue and providing non-thrombotic barriers, respectively (204, 205). Fibroblasts secrete and remodel the ECM and act as supporting cells to parenchymal cells; for example, cardiac fibroblasts are mechanically and electrically coupled to cardiomyocytes, supporting the contraction of, and electrical impulse through, the myocardium (206-208). Cardiac fibroblasts have also been shown to share several phenotypic characteristics to VICs,

including matrix remodeling. Intuitively, harvesting cardiac fibroblast from live donors may appear to be challenging and/or unsafe; however there is an autologous source of cardiac fibroblasts that may be able to be acquired via a minimally invasive procedure. The left atrial appendage (LAA) is a small sac of myocardium that protrudes from the wall of the left atrium and consists of resident cells equivalent to that of the left atrium, including cardiac fibroblasts (209, 210). The function of the LAA remains largely unknown; however, recent data has shown that the LAA can be a stroke risk for patients with atrial fibrillation (AF) (211-217). For this reason, several studies have investigated the safety of occluding of the LAA via cardiac plug (AMPLTZER and WATCHMAN) and percutaneous suture (LARIAT) (218-222). Positive long-term patient outcomes from the LARIAT trial could justify the removal of the left atrial appendage for use in patient autologous TEHVs (218).

Dermal fibroblasts have been another investigated source of cells for TEHVs (149, 223-225). Although previous studies have shown that cellular sources such as vascular fibroblasts have greater phenotypic similarity to native VICs than dermal fibroblasts, this disparity may be mitigated by variations within studies and among studies with respect to *in vitro* culturing conditions (149, 224). The easy access of dermal fibroblasts through a minimally invasive, low risk biopsy further justifies investigation for the use of dermal fibroblasts for TEHVs.

1.5. Valvular interstitial cells

Cardiac valve leaflets contain interstitial tissue amongst the dense extracellular scaffold. The majority of this dynamic tissue consists of valvular interstitial cells (VICs), which are responsible for maintaining the steady-state of valve matrix remodeling (226, 227). Although

VICs are found throughout the trilaminar leaflet, they are most concentrated within the spongiosa (228).

While VICs are recognized to be a unique mesenchymal cell type, they possess phenotypic characteristics of both smooth muscle cells (SMCs) and fibroblasts (203, 229, 230). VICs resemble both fibroblasts and SMCs *in vitro*, with the majority exhibiting a spindle-like morphology with elongated processes; however, distinctions can be made in post-confluent, overgrowth conditions (231). Cultured VICs, like fibroblasts, form an orthogonal monolayer and lack the typical hill and valley appearance observed with SMCs (227, 228). Additionally, both VICs and fibroblasts have an incomplete basal lamina, allowing direct contact with the ECM proteins (231). This is distinct from SMCs which have a fully developed basal lamina and intact basement membrane (227, 231). Despite morphological similarities, SMCs and fibroblasts can be easily distinguished by the presence or absence of the intermediate filament, desmin, respectively (232). Some studies observed weak, diffuse expression of desmin in a small percentage of VICs – suggesting desmin expression, but incomplete filament organization (228, 233, 234). In addition, VICs demonstrate aligned actin filaments that shorten when stimulated with epinephrine (231). VICs have also been shown to compress collagen matrices *in vitro*, indicating contractile properties similar to SMCs (126, 228, 230). Furthermore, unlike fibroblasts, VICs have also been shown to express cGMP-dependent protein kinase (PKG) and myosin light chain, both of which are found in smooth muscle cells (231). As VICs demonstrate characteristics of both fibroblasts and smooth muscle cells, it was previously unknown as to whether VICs were a singular cell type (muscle-like fibroblasts or myofibroblasts), or if they represented a heterogeneous group of distinct cells (203). However, experiments aimed to characterize VICs, such as a particular study, which observed that VICs secrete significantly greater amounts of

prostacyclin than both fibroblasts and SMCs when exposed to arachidonic acid, indicated their distinctiveness from other mesenchymal cells (229). Therefore, while VICs were considered by some to be a heterogeneous mixture of cells (fibroblasts, myofibroblasts, progenitors and smooth muscle cells), VICs are now considered to be a singular, unique mesenchymal cell type (235, 236).

Due to their plasticity and specific contribution to valve development, homeostasis and pathological remodeling, VICs have been categorized into five identifiable phenotypes: 1) quiescent VICs, 2) activated VICs, 3) osteoblastic VICs, 4) progenitor VICs, and 5) embryonic progenitor endothelial/ mesenchymal cells. Quiescent VICs (qVICs) resemble fibroblasts (vimentin positive, α-SMA negative cells) and under normal, physiological conditions qVICs maintain homeostatic matrix remodeling. However during pathological conditions, such as valvular injury or hemodynamic stress, qVICs become activated, adopting a myofibroblast-like phenotype (237). Similar to fibroblast-myofibroblast activation, TGF-β mediates VIC activation in a dose dependent manner that is seen through elevated stress fiber protein expression, predominantly α-SMA (238, 239). Removal of TGF-β stimulation reduces both VIC activation as well as proliferation, and also mitigates apoptosis (240). In response to injury, aVICs secrete high levels of matrix metalloproteinases (MMPs) and their inhibitors, tissue inhibitors of MMPs (TIMPs), which initiates wound healing and matrix repair (241, 242). Subsequent to ECM remodeling, the majority of aVICs are eliminated via TGF-β mediated apoptosis. However, a dysfunction in the apoptotic process can lead to excess ECM deposition, inflammation and formation of fibrocalcific nodules (230, 243). These calcific lesions are a result of aVICs differentiating into osteoblastic VICs (obVICs).

obVICs are characterized by the presence of cellular markers alkaline phosphatase (ALP), bone sialoprotein (BSP), BMP-2, osteocalcin (OCN) and osteopontin (OPN); congruency is observed between OPN expression levels and the degree of calcification and VIC osteogenesis (230, 244-246). Osteogenic differentiation of aVICs occurs in the event of elevated TGF-β and BMP-2 in the presence of mechanical tension (235). Interestingly, increasing mechanical tension alone or TGF-β alone showed little effect on osteoblastic differentiation, suggesting a synergistic effect; this evidence is congruent with the model of CAVD (235). While aVICs may differentiate into an osteogenic phenotype secondary to pathological sequelae, it has been shown that VICs do not have to pass through the activated phenotype prior to osteoblastic differentiation (244). One particular study demonstrated that VICs exposed to mineralizing media underwent osteogenesis without expressing elevated levels of α-SMA, indicating direct conversion from a quiescent to osteogenic phenotype (244). While osteogenic differentiation of VICs occurs via a similar process to that of osteogenesis in skeletal bone formation, obVICs are distinct from osteoblasts as demonstrated via differential protein expression of osteoblast cell markers (244, 247, 248).

VIC turnover primarily occurs through the proliferation of qVICs; however a small number of progenitor cells have been found within the valve leaflet and have been shown to contribute to VIC replenishment (176, 249). Progenitor VICs (pVICs) are valvular stem cells that are derived from circulating BMCs and hematopoietic stem cells (HSCs) (176, 237). These cells express cellular markers for pericyte progenitors (neural/glial antigen 2; NG2), mesenchymal stem-cells (stage-specific embryonic antigen-4; SSEA-4), and myofibroblast-like/osteogenic progenitors (osteoblastic cadherin; OB-CDH) and respond to signaling molecules such as VEGF and TGF-β (237, 250). pVICs are distinct from embryonic progenitor endothelial/mesenchymal VICs (emVICs). emVICs are endothelial cells that appear during early aortic valve development.

Initially overlying the endocardial cushions, emVICs invade the cardiac jelly and undergo endothelial to mesenchymal transition (EndMT), a process regulated by TGF-β superfamily members (TGF-β1, BMPs, NOTCH1 and VEGF) (237, 251). emVICs express high levels of α-SMA – an intercellular protein that is likewise highly expressed in adult aVICs isolated from diseased, myxomatous valves (252). Similarly, in comparison to VICs isolated from long-term pulmonary autografts, VICs from short-term pulmonary autografts also showed elevated α-SMA expression (252). These findings suggest that elevated levels of α-SMA are expressed by cells within valves that are undergoing development, disease or remodeling. Furthermore, cell-cell contact has been shown to inhibit VIC activation, as α-SMA expression decreases concurrently with increased cell density (240). The absence of cell-cell contact appears to promote VIC activation via TGF-β mediated wound healing response (240). These findings suggest that VICs adopt a myofibroblast-like phenotype during development and disease states, and assume a quiescent, fibroblast-like phenotype in homeostatic conditions.

VICs in culture have been shown to have two distinct morphologies: small islands of cuboidal/cobblestone cells and the more predominant elongated, spindle-shaped cells (126). Cuboidal VICs are less-motile, more contractile and have a prominent Golgi apparatus and rough endoplasmic reticulum (RER), whereas elongated VICs have prominent microfilaments and are more proliferative and demonstrate greater motility (227, 237). Spindle-shaped VICs have long slender processes and express cell-cell junctional proteins such as cadherins, gap junctions and integrins that allow for cell-cell and cell-matrix contact (230, 231). Gap junctions allow VICs to transduce intercellular signals through direct connection of the cytoplasm between to cells, whereas integrins are transmembrane proteins that allow for cell-cell and cell-matrix interactions (231, 232). Integrins act as both adhesion proteins as well as a mechanotransducers, mediating

mechanical signal transduction and providing the VICs with environmental information, such as hemodynamic stress or flexural tension (126).

1.5.1. Cell-matrix communication

The aortic valve is a trilaminar structure that contains numerous extracellular matrix proteins (9). Collagen I and chondroitin sulfate are found predominantly in the fibrosa or outermost layer of the aortic valve (253). Elastin, fibronectin and vitronectin are expressed strongly in the ventricularis, or innermost layer (253). Proteoglycans and GAGs are found throughout the trilaminar cusp, but are highly concentrated in the spongiosa, or central layer of the leaflet (253). Collagen III, keratin sulfate and decorin are expressed ubiquitously (253).

Although the ECM largely is responsible for maintaining the mechanical properties of the valve, it is also implicated in the mediation of cellular pathways, such as VIC adhesion, proliferation, and differentiation (254). Communication between the matrix and VICs is primarily accomplished through focal and fibrillar adhesions in conjunction with integrins (255). The valve matrix also binds and localizes growth factors and chemokines (referred to as matrikines), which can be solubilized and then utilized by interstitial cells in the event of valvular injury or hemodynamic stress (254, 256). These molecules can regulate cellular behaviour, function and differentiation (257).

Increased mechanical tension causes VICs to secrete MMPs and TIMPs into the extracellular environment. VICs express several MMPs and TIMPs, but predominantly MMP-1 and -2, and TIMP-1, -2 and -3 (237, 258). MMPs and TIMPs are responsible for repairing and modeling the extracellular matrix post-injury. Consequently, dysfunction in matrix remodeling can have

deleterious effects (230). For example, connective tissue diseases such as Marfan's syndrome and myxomatous valve disease lead to inappropriate ECM remodeling and lead to reduced matrix integrity (126, 258). Conversely, overt remodeling secondary to wound healing can result in excess matrix deposition and increased valve stiffness (242). Thickening and stiffening of the valve has a direct influence on VIC phenotype (259). Decreased ECM compliance promotes VIC activation, propagating pathological ECM deposition, leading to aortic fibrosis and CAVD (259).

1.5.1.1. Matrix compliance

Matrix compliance unequivocally alters VIC phenotype, which is clearly observed via *in vitro* culture methods (6, 260-262). VICs plated on standard plastic dishes – which have a substrate modulus of ~1 GPa – demonstrated high levels of activation through elevated expression of α-SMA and were highly contractile and proliferative (260, 262). Conversely, myofibroblast-like VICs cultured on matrices with elastic moduli ≤15 kPa not only mitigate cell activation, but reverts VICs from an activated to quiescent phenotype (194, 242, 261, 263). This cause and effect relationship between mechanical stiffness and VIC activation is mimicked in fibroblasts (Figure 3) (264). Hemodynamic stress in conjunction with the presence of TGF-β promotes fibroblast to myofibroblast activation in a dose dependent manner (265). Similarly, substrate compliance directly affects stem cell and progenitor cell behaviour and mesenchymal stem cells (MSCs) cultured on substrates with varying elasticity display distinct phenotypes (257, 266-268). For example, MSCs subjected to 0.1-1 kPa differentiate into neuronal-like cells, whereas stem cells cultured on 10 kPa or 100 kPa promote myogenic or osteogenic differentiation, respectively; further demonstrating the effects of matrix stiffness on cell-fate

(266, 267). While, cell-matrix communication is critical in regulating cellular differentiation, neighbouring cells can also communicate with one another directly to drive processes such as proliferation, activation, and termination (269).

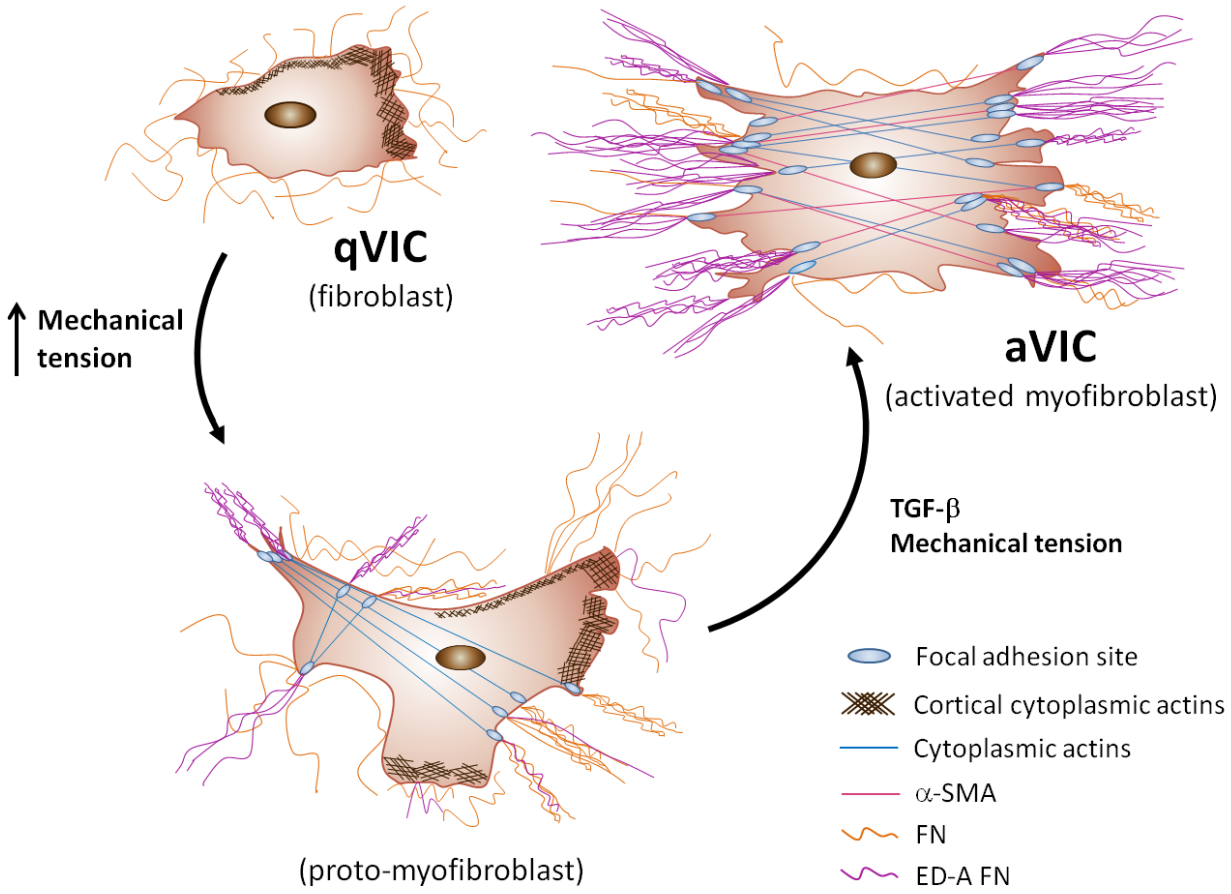

Figure 3: Mechanical tension regulates cellular activation
Increased mechanical tension and TGF-β mediate the activation of valvular interstitial cells (VICs) and fibroblasts, leading to a loss of cortical actin filaments and increased expression of α-SMA, FN and EDA-FN and stress fiber alignment. Abbreviations: activated valvular interstitial cell (aVIC), quiescent valvular interstitial cell (qVIC), alpha smooth muscle actin (α-SMA), extra domain A fibronectin (EDA-FN), fibronectin (FN) and transforming growth factor beta (TGF-β). Adapted with permission from Tomasek *et al* (264).

1.5.2. Cell-cell communication

VICs can communicate with adjacent cells through paracrine or juxtacrine signaling, which are forms of cell-cell communication that can occur through release and uptake of signaling molecules or via direct contact, respectively (242). Juxtacrine signaling can direct cellular proliferation, function and survival, and is responsible for regulating numerous cellular pathways, including those implicated in epithelial-mesenchymal transition (EMT) and valvulogenesis (269). Furthermore, the interplay between VIC intercellular signaling can determine VIC behaviour and these cell-cell interactions may be vital in directing and maintaining VIC phenotype (242).

1.6. NOTCH signaling pathway

The NOTCH signaling pathway is an evolutionarily conserved signaling pathway that regulates cell-fate determination, differentiation, proliferation and apoptosis through a cell-cell dependent mechanism (270-273). Transmembrane receptors of the NOTCH family (NOTCH1-4) are activated via direct binding with transmembrane Delta or Jagged/Serrate (DSL) ligands: Jagged (JAG) and Delta-like (DLL) families (JAG 1, 2 and DLL 1, 3 and 4) (274, 275). NOTCH-DSL binding leads to cleavage of the extracellular portion of NOTCH by ADAMs 10 and 17 (276). Subsequently, presenilin-1 dependent gamma-secretase (PSEN1) cleaves the intracellular region, releasing the NOTCH intracellular domain (NICD) into the cytoplasm (276). The NICD translocates to the nucleus where it binds with cotranscription factor recombining binding protein suppressor of hairless (RPBJ; also known as CBF1, CSL, or Su(H)) (271, 277-279). NICD-RBPJ binding converts the RBPJ complex from a repressor to an activator, leading

to the transcription of NOTCH target genes, HES/HEY family members (273, 278, 280). Hairy/enhancer of split (HES) and hairy/enhancer or split related with YRPW motif (HEY) proteins are basic helix-loop-helix (bHLH) transcription factors belonging to the Orange family of transcriptional regulators (281). HES1 is implicated in neurogenesis and is also responsible for regulating progenitor cell differentiation (272, 278). There are three HEY proteins: HEY1, HEY2 and HEYL, also called HRT1, 2 and 3, HESR1, 2 and 3, HERP2, 1 and 3 and CHF2, 1 and 3, but only HEY1 and 2 are normally expressed during cardiogenesis (275, 278, 282). HEY1 and HEY2 have differential spatial expression within the developing heart. HEY1 expression observed in atrial progenitor cells and atrial myocardium, whereas HEY2 expression is found in ventricular progenitor cells, the ventricular myocardium and the mesenchymal cushion; both are found throughout the endocardium (275, 283).

HEY1 has been demonstrated to be redundant in murine cardiogenesis; *HEY1* null mice were fully viable and exhibited only vascular malformations (282). However, inactivation of both *HEY1* and *HEYL* lead to detrimental cardiac malformations, suggesting that *HEY1* loss of function may be party compensated by *HEYL* (284). In contrast, *HEY2* knockout mice have severe cardiac defects, including ventricular septal defects, tetralogy of Fallot and tricuspid valve atresia, and the majority fail to thrive perinatally (282, 283, 285). Deletion of both *HEY1* and *HEY2* genes is embryonic lethal (286). NOTCH and RBPJ are essential for EMT and deletion of these proteins leads to severe disruptions in both cardiac and valve development (283, 287). NOTCH signaling is also implicated in directing stem cell fate, progenitor expansion and lineage commitment (287). Activation of NOTCH in mesodermal cells prevents the development of cardiac muscle cells, endothelial cells and hematopoietic cells, whereas inhibition of NOTCH promotes cardiomyocytes differentiation (237, 283, 288).

NOTCH1 has also been implicated in the etiology of aortic valve disease and appears to play a critical role in ameliorating VIC osteoblastic differentiation by suppressing pro-osteogenic signaling pathways (283, 289, 290). NOTCH1 represses valvular expression of both *BMP-2* and the master osteogenic regulator, runt-related transcription factor 2 (RUNX2), mitigating calcific nodule formation and CAVD pathogenesis (277, 280, 281, 291, 292). Conversely, derepression of *BMP-2* and *RUNX2* via NOTCH1 inhibition demonstrated valve mineralization and subsequent fibrocalcific remodeling (283). In addition, aortic valve calcification is concomitant with the loss of SOX9, a downstream mediator of NOTCH1. SOX9 expression appears to be mediated by NOTCH target gene, *HEY2*, as adenoviral overexpression of *HEY2* resulted in an increase in SOX9 expression (277). Overexpression of *HEY2* also resulted in decreased levels of OPN in valve leaflets, further suggesting that *HEY2* plays a key role in regulating CAVD pathogenesis.

In summary, the NOTCH signaling pathway is a central regulatory cascade that directs cell fate in numerous tissue types and is a critical player in valve development and disease (292). Disruption in the NOTCH signaling pathway during valvulogenesis has been shown to cause valvular anomalies in humans and non-human mammals, leading to aortic valve disease and subsequent heart failure (273, 285, 286, 293). Furthermore, down regulated NOTCH signaling in human adults has been linked to increased incidences of bicuspid aortic stenosis and CAVD, as well as increased VIC activation and osteoblastic differentiation (281, 284, 294, 295). This finding suggests that NOTCH signaling may be central to maintaining VIC phenotype and/or implicated in VIC differentiation from resident or circulating progenitor cells.

2. RATIONALE, HYPOTHESIS & OBJECTIVES

2.1. A-fibs, D-fibs and BMCs as cellular alternatives for VICs in TEHVs

Determining a patient autologous cellular source that can successfully populate bioengineered valve scaffolds and maintain valve homeostasis is central to the success of TEHVs. Numerous studies have attempted to define a cellular alternative that could be used to build TEHVs. The vast majority of this research has involved allogeneic progenitor cell sources. A major disadvantage in using non-autologous cells in TEHVs is the risk of graft rejection; the use of patient-specific tissue would circumvent this concern. In order to meet the criteria for use in TEHVs, the defined cell type would have to be: 1) autologous-derived; 2) phenotypically similar to VICs; and 3) easily accessible through minimally invasive means. Previous studies have suggested that fibroblasts and bone marrow-derived progenitors demonstrate similar characteristics to VICs. Dermal fibroblasts and bone marrow can be harvested quite easily and with minimal risk to the patient. Atrial fibroblasts are more challenging to isolate, but have previously shown to closely resemble VICs and their use warrants further investigation. ***Our working hypothesis was that atrial fibroblasts, dermal fibroblasts and/or differentiated bone marrow-derived progenitor cells will demonstrate phenotypic similarities to VICs and as such will represent reasonable potential cellular alternative(s) to VICs for valve bioengineering.***

2.1.1. Objective 1 – Optimizing VIC, A-fib, D-fib and BMC culture methods

Optimization of *in vitro* culture methods for VICs, A-fibs, D-fibs and BMCs had to first be established. To achieve this we tested several parameters, such as: the duration of initial cell seeding for excluding non-fibroblast-like cells (i.e., endothelial cells and SMCs), the types of enzymes used for cellular liberation, duration of enzymatic digestion, etc. Our objective was to define cell culture methodologies that would consistently produce an evenly distributed monolayer of cells that reached 60-70% confluency within 48-72 hours (or 5-6 days for BMCs).

2.1.2. Objective 2 – Cell culture purity

Our second objective was to determine the purity of the different types of cells in culture. We needed to establish pure culture in order to be confident that our gene expression studies would be representative of only the cells of interest. Contamination would likely lead to spurious results. To achieve this goal we stained P1 cultures with immunofluorescent probes specific to potential cellular contaminants (i.e. endothelial cell and smooth muscle cell markers). We then analyzed the cell cultures for the presence of these cellular markers to determine the percentage of cellular contaminants in our cell cultures.

2.1.3. Objective 3 – Characterization of cellular marker expression

We hypothesized that VICs would have positive staining for numerous fibroblast markers and have the greatest similarity in cellular marker expression with A-fibs. As such, our third objective was to determine if cultured VICs express key fibroblast/myofibroblast markers and/or

bone marrow progenitor cell markers, as this would give us a general idea whether or not VICs shared phenotypic similarities with these cell types.

We also wished to compare the expression of these markers by VICs to that of the alternative cell types investigated (i.e. A-fibs, D-fibs or BMCs) and look for intercellular similarities. To achieve this objective we stained P1 cell cultures with antibodies against several fibroblast/myofibroblast and BMC markers and detected the presence or absence of fluorescent staining, indicating the presence or absence of protein expression, respectively.

2.1.4. Objective 4 – Characterization of cellular morphology

We hypothesized that VICs would most closely resemble the morphology of A-fibs, followed by D-fibs and BMCs. Therefore, our fourth objective was to characterize the morphology of cultured VICs and to compare VIC morphology to that of A-fibs, D-fibs and BMCs. To do this we cultured P0 cells to 60-70% confluency on standard culture dishes and acquired images using a light microscope.

2.2. Substrate stiffness as a mediator of cellular activation

Several studies have shown that matrix stiffness has a direct effect on cellular phenotype, and that an increase in the substrate modulus promotes cellular activation and differentiation (6, 249-251).

2.2.1. Objective 5 – Effect of substrate stiffness on α-SMA expression

Here we wished to confirm that our model for mimicking physiological aortic valve elasticity via pre-fabricated, compliant (relative to plastic and applicable to stress and strain within cardiac tissues) 2-D silicone-based culture dishes was effective in mitigating cellular activation. To do this we cultured A-fibs on 2-D matrices of varying stiffness, 5 kPa (normal heart compliance), 100 kPa and 1 GPa, and compared relative α-SMA expression between cultures. We also wanted to determine if the softer matrices would maintain cellular quiescence over passage. To determine this we passaged the cell cultures to P1 and again compared relative α-SMA expression.

2.2.2. Objective 6 – Effect of substrates stiffness on cellular morphology

We hypothesized that the softer matrices would promote a quiescent, spindle-like cellular morphology, whereas the relatively stiff (1 GPa) substrates would force the cells to adopt an activated, cuboidal/cobblestone shape. Our sixth objective was to investigate the effect of substrate stiffness on cellular morphology. To do this we cultured P0 VICs, A-fibs, D-fibs and BMCs on substrates with varying stiffness, 5 kPa, 100 kPa and 1 GPa, to 60-70% confluency and acquired images using a light microscope.

2.3. Signaling pathways central to maintaining VIC phenotype

VICs are mesenchymal in origin and undergo cellular differentiation. As A-fibs, D-fibs and BMCs are also mesenchymal in origin we tested the hypothesis that there may key regulatory pathways that may be exploited in these cell types to push them towards a VIC phenotype.

2.3.1. Objective 7 – Differential expression of key regulatory pathway proteins

Finally, we investigated differences in mRNA expression between VICs, A-fibs, D-fibs and BMCs. In particular, we were interested in the differential expression of key regulatory pathways known to be involved in valve development and disease. To accomplish this we extracted mRNA from P0 VICs, A-fibs, D-fibs and BMCs cultured on matrices with a substrate modulus of 5 kPa, which is similar to that of the native valve. We then performed a microarray analysis to obtain a general overview of gene expression, followed by quantitative reverse transcriptase polymerase chain reaction (RT-qPCR) and Western blot on the genes of interest.

3. MATERIALS & METHODS

3.1. Isolation and culture of porcine VICs, A-fibs, D-fibs and BMCs

All animal study protocols were approved by the Animal Care Committee of the University of Manitoba, in accordance with the Canadian Institute of Health Research and the Canadian Council on Animal Care Guidelines (2010). Approval was obtained for the collection of skin, bone marrow, and heart tissue (particularly the left atrial appendage and aortic valve) from female Yorkshire pigs (~40 kg) (Figure 4).

All animals were anesthetized via intramuscular injection of Tiletamine (2.4 mg/kg), Zolazepam (2.4 mg/kg), and Xylazine (4.6 mg/kg). Orotracheal intubation was established for institution of mechanical ventilation and maintenance of general anesthesia using 2% inhalational isoflurane. The animals were mechanically ventilated to maintain a pH of 7.35 to 7.45, PO_2 > 200 mmHg and PCO_2 of 35-45 mmHg. Post induction, a small area of the ventral thoracic region was shaved and cleaned to allow for the removal of a small piece of the dermis (1.0 cm^2), which was immediately placed in a 50 mL conical tube containing 10 mL of phosphate buffered saline (PBS). A median sternotomy was performed and the pericardium opened. Systemic heparinization was established with intravenous delivery of 400 units/kg of heparin. The animals were euthanized via heart excision and exsanguination. The hearts were harvested, after which the aortic valve leaflets and a piece of the left atrial appendage (1.0 x 1.0 x 0.5 cm) were excised.

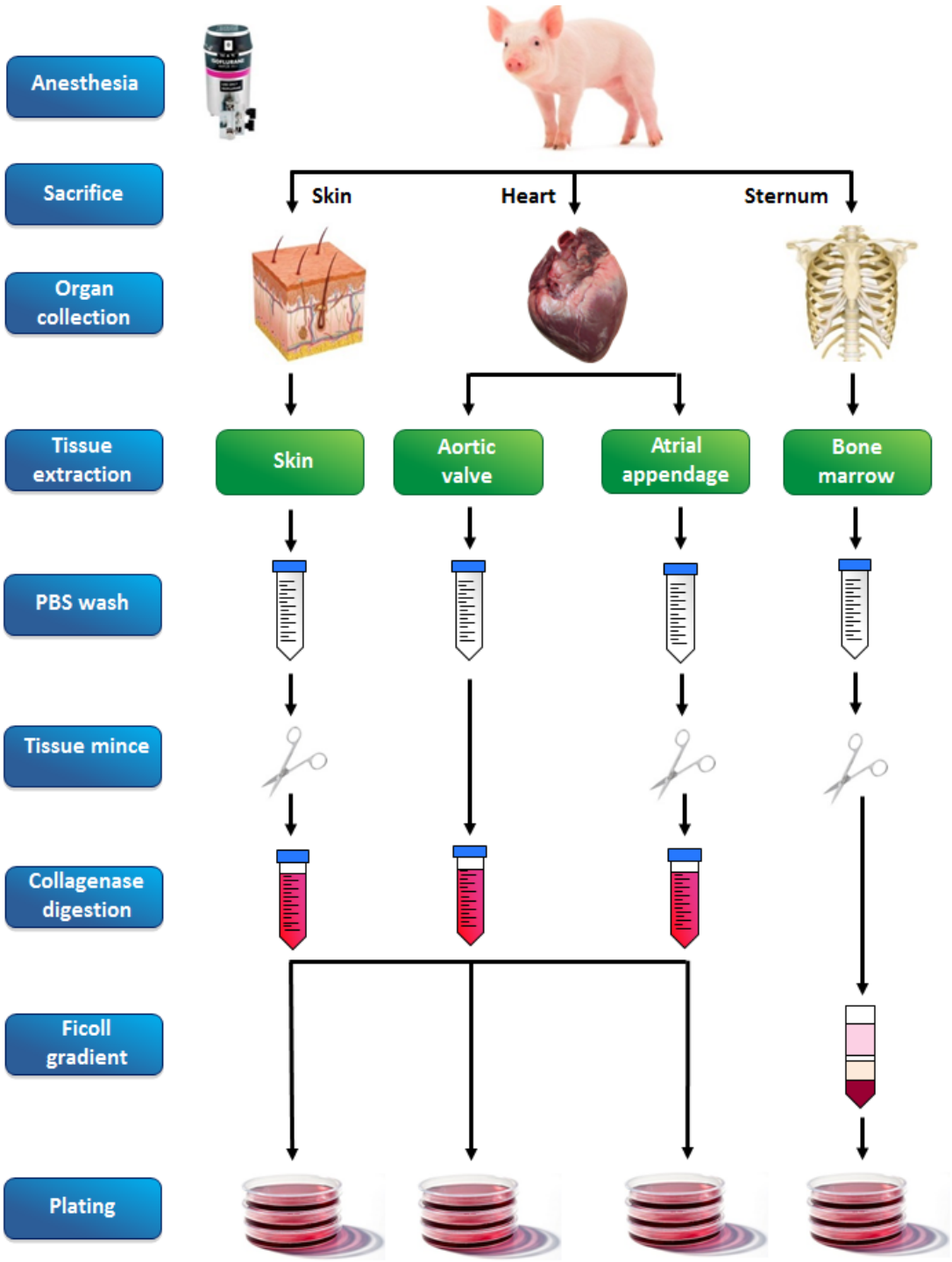

Figure 4: Cellular culture methods for porcine VICs, A-fibs, D-fibs and BMCs
Schematic diagram depicting the main steps involved in the isolation and cell culture preparation of porcine donor tissue.

3.1.1. Dermal, aortic valve and atrial appendage cell isolation

After collection, all tissue samples were immediately placed in individual 50 mL conical tubes containing 10 mL of phosphate buffered saline (PBS). Under sterile conditions, the subcutaneous fat was removed from the dermal tissue. The dermal and atrial tissues were minced into 1 mm^3 pieces. The minced atrial tissue and the aortic valve leaflets were treated with 0.1% w/v collagenase type II (396 U/mg, Worthington Biochemical Corp., USA) in Minimal Essential Medium for suspension cultures (SMEM) for 16 hours at 37 C. The minced dermal tissue was treated similarly, with the addition of 0.05% w/v dispase II protease (0.5 U/mg, Sigma-Aldrich, USA) in the culture medium. Collagenase type II and dispase II were neutralized via the addition of equal volume of growth media (Dulbecco's Modified Eagle Medium F-12 (DMEM-12), supplemented with 10% fetal bovine serum (FBS), 1% penicillin (100 U/mL), 1% streptomycin (100 μM/mL), 0.1% gentamicin (10 mg/mL), and 1% ascorbic acid (100 mM)). The cells were dissociated via trituration and filtered through a 40 μm cell filter, using a 60 mL syringe and plunger. The cellular suspension was centrifuged at 750 rcf for 7 min, the supernatant was removed, and the cells were rinsed once with 1x phosphate buffered saline (PBS) and centrifuged once more at 750 rcf for 7 min. The pellets were re-suspended in fresh growth media and plated onto 100 mm culture dishes for 1-2 hours in a 5% CO_2 incubator at 37 C to allow for cell anchorage. The cells were rinsed twice with PBS to remove all non-adherent cells (i.e. myocytes, endothelial cells and smooth muscle cells). The remaining adherent cells (mainly fibroblasts or VICs) were incubated in fresh growth media for approximately 24 hours at which time the growth media was changed. Cell culture media changed every 48 hours, thereafter. For experiments that required the collection of cellular lysates, cultures were left to grow for 48-72 hours until they reached 60-70% confluency at which point the cells were

liberated from the plates using 0.25% trypsin with ethylenediaminetetraacetic acid (EDTA). Cells were subsequently pelleted and rinsed twice with PBS.

3.1.2. Bone marrow cell isolation

Samples of the bone marrow (1 cm^3) were excised from the sternum of the animals, via the sternal incision. The collected bone marrow was immediately placed in a solution containing 8 mL of growth medium (as described above) and 17 mL of PBS, and then subjected to mechanical disaggregation. The cellular suspension was then filtered through a 40 μm cell filter (as above) and collected in a fresh 50 mL conical tube. Bone marrow-derived stem cells were isolated as previously described (296). Using a 9 inch glass pipette, a total of 15 mL of room-temperature Ficoll-Paque™ (Sigma-Aldrich, USA) was added to the cellular suspension. The pipette tip was gently placed to the bottom of the 50 mL tube, below the marrow-medium-PBS suspension, and the Ficoll was slowly underlain. The layered cell suspension was centrifuged at 400 rcf for 30 min at room temperature, with the brake off. Four layers were formed: 1) bottom layer – predominately red blood cells; 2) the second layer – Ficoll; 3) the third layer – a pink hazy layer, or "buffy coat," which contained the majority of the mononuclear cells; and 4) the uppermost layer – predominately the plasma and DMEM-F12/PBS solution (Figure 5). Using a glass pipette, the uppermost layer was aspirated and discarded. The mononuclear layer was collected via aspiration and transferred into a 10 mL conical tube. The collected cells were centrifuged at 1000 rcf for 10 min at room temperature. After centrifugation, the supernatant was discarded and the cells were rinsed and re-suspended in 10 mL of warm PBS. This washing step was repeated three times. After thorough rinsing the cells were re-suspended in 10 mL of growth

medium, and gently triturated to ensure adequate separation. The cells were plated on a 100 mm culture dish and incubated overnight in a 5% CO_2 incubator at 37 C. After 16-24 hours the cells were gently rinsed with warm PBS and fresh growth media was added. Afterwards, cell culture media changed every 48 hours. For experiments that required the collection of cellular lysates, cultures were left to grow for 5-6 days until they reached 60-70% confluency at which point the cells were liberated from the plates using 0.25% trypsin with EDTA and subsequently pelleted and rinsed twice with PBS.

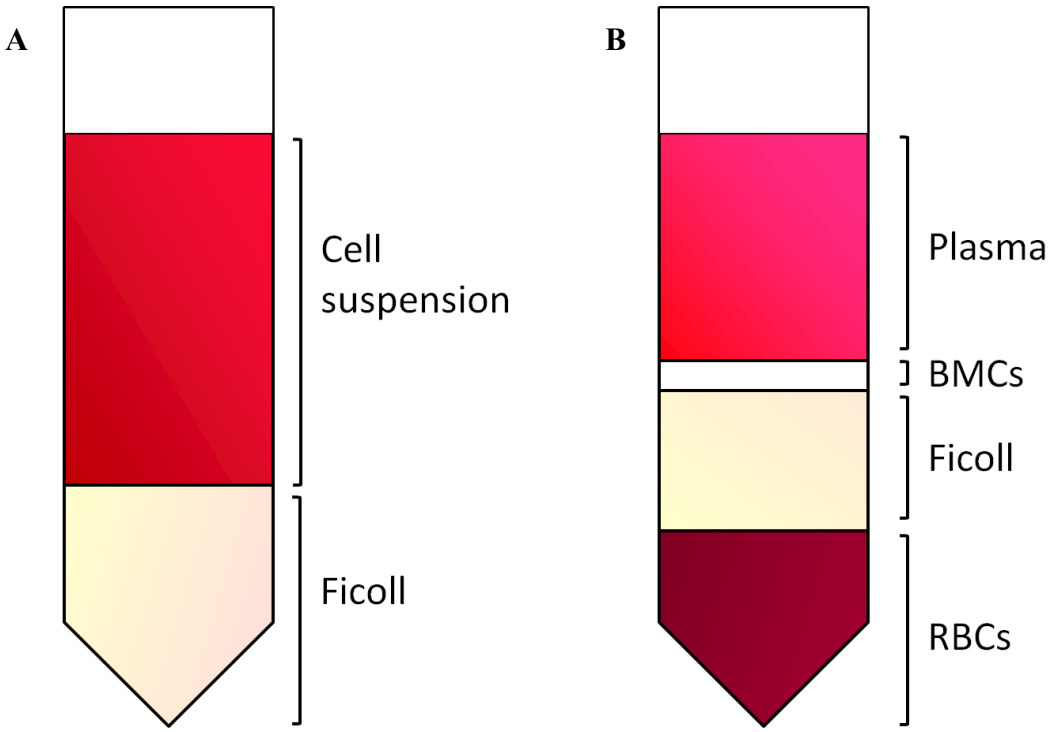

Figure 5: Ficoll gradient before and after centrifugation
Schematic illustrating the layers formed during the isolation of bone marrow mononuclear cells using a Ficoll gradient and centrifugation steps. **(A)** Ficoll was carefully layered beneath the cellular suspension. **(B)** After centrifugation, four layers were formed. The top layer contained plasma; beneath that is the "buffy coat" or mononuclear cells; under the buffy coat is a layer of Ficoll; and the bottom layer consists of red blood cells. Abbreviations: bone marrow-derived progenitor cells (BMCs) and red blood cells (RBCs).

3.2. Immunofluorescence of target genes

Cells cultured in 6-well plates overlaid with glass coverslips were fixed in 4% paraformaldehyde for 15 minutes and permeabilized in 0.2% Triton-X-100 in PBS for 5 minutes. Cultures were washed twice with PBS and blocked with 10% bovine serum albumin (BSA) for 30 min at room temperature. Fixed cells were incubated with 100 μL of the appropriate primary antibody, overnight at 4°C. The coverslips were then gently rinsed three times with PBS, and incubated with a fluorescent secondary antibody for 1 hour at room temperature. All primary and secondary antibodies were diluted in 1% BSA. Cells requiring staining for filamentous actin (F-actin) were blocked, incubated overnight in 1% BSA, washed twice, and incubated with 100 μL of phalloidin for 20 min at room temperature. Once the secondary antibody or the phalloidin stain was applied, the coverslips were protected from the light. *SlowFade*® Gold antifade reagent with 4',6-diamidino-2-phenylindole (DAPI) was used to mount the coverslips. Cells were visualized with an epifluorescent microscope with appropriate filters.

3.3. Cell culture using pre-fabricated silicone-based matrices

VICs, A-fibs, D-fibs and BMCs were isolated as described above. The cells were then plated onto matrices of varying stiffness: 5 kPa, 100 kPa, and ~1 GPa (standard plastic) (Figure 6). The prefabricated silicone-based culture dishes (5 kPa and 100 kPa) were pre-treated with 1% human fibronectin in DMEM-F12 for one hour prior to plating, to support cellular adherence. In order to account for any variability caused by the fibronectin coating, all experiments comparing the various substrates included a fibronectin coated plastic culture dish control. Once the cells

reached 60-70% confluency, the cells were liberated from the substrate via trypsinization, and passaged onto a fresh plate with the same substrate modulus as the previous passage.

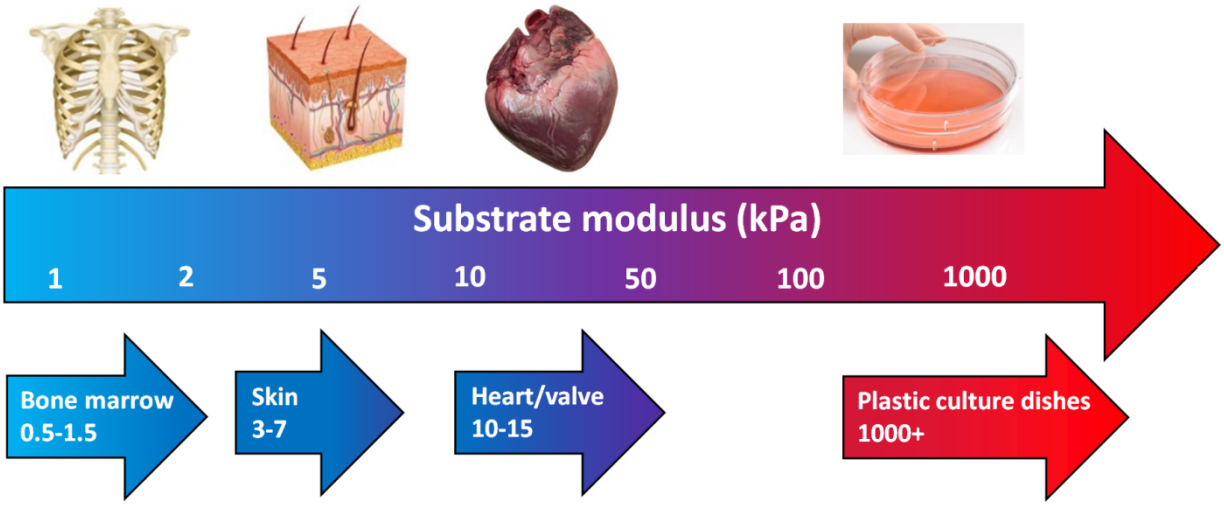

Figure 6: Substrate moduli of bone marrow, skin, heart tissue and standard culture dishes

Biological tissue from various origins demonstrates differences in compliance. Bone marrow, skin and heart-derived tissues have elastic moduli of 0.5-1.5 kPa, 3-7 kPa and 10-15 kPa, respectively, whereas standard plastic culture dishes have a much higher elastic moduli of ~ 1 GPa.

3.4. Western blot analysis

Primary cells cultures were washed twice in cold PBS, and trypsinized using 5 mL of 0.25% trypsin with EDTA. The trypsin reaction was terminated by adding 10 mL of DMEM-F12 (with 10% FBS and supplements) to the cell cultures. Cells were centrifuged at 2000 rpm for 7 minutes, rinsed twice with PBS, and then lyzed in RIPA lysis buffer (150 mM NaCl, 50 mM Tris pH 8.0, 1mM EDTA, 1 mM EGTA, 0.5% sodium deoxycholate, 0.1% SDS, and 1% Triton X-100) supplemented with a protease inhibitor cocktail (0.1 M phenylmethylsulfonyl fluoride, 5 μg/mL leupeptin, 2 μg/mL aprotinin, and 1 μg/mL pepstatin). Protein concentrations of whole cell lysates were determined using the bicinchoninic acid (BCA) method (297). Equal amounts of each protein sample (20 μg) were separated on an 8% sodium dodecyl sulfate-polyacrylamide gel at 180 V for 60 min. Separated proteins were transferred to a polyvinylidene difluoride (PVDF) membrane via electrophoresis for 110 minutes at 100 V. After blocking the membrane with 5% (w/v) dried skim milk powder in PBS for 2 hours at room temperature, the membrane was incubated with primary antibody overnight at 4°C with shaking. The membrane was rinsed three times with 0.1% PBS-Tween for 10 minutes each, followed by one rinse with PBS without tween, and then incubated for 1 hour at room temperature with the respective horseradish peroxidase-conjugated secondary antibody. The membrane was rinsed again, as above, and the protein bands were visualized using Pierce® ECL Plus (according to the manufacturer's instructions) and developed on film. To facilitate probing for the loading control, membranes were either cut stripped and re-probed for β-tubulin. Blot densities were measured using Quantity One software and normalized to β-tubulin blot densities. Only those films that did not have over saturated bands, as assessed by the Quantity One software, were used for analysis.

3.5. Transcriptome analysis

3.5.1. RNA extraction

Passage 0 cell cultures were grown to 60-70% confluency on soft, 5 kPa substrates. The growth medium was removed and the cells were rinsed twice with warm PBS. Cells were detached from the growth surface via trypsinization (0.25% trypsin with EDTA) and collected in a sterile 50 mL conical tube. The trypsin reaction was neutralized by adding 10 mL of growth media, supplemented with 10% FBS. The cellular suspensions were centrifuged for 5 min at 250 x g, and then rinsed with warm PBS to remove any residual growth medium; this step was repeated twice. After a final centrifugation step, the supernatant was removed and the cell pellet was collected in a 1.5 mL RNase free Eppendorf tube. Total RNA was isolated using the GeneJET RNA purification kit, as follows. Cell pellets were resuspended in 600 µL of GeneJet lysis buffer supplemented with 2% v/v of 1.4 M β-mercaptoethanol and vortexed for 10 s, followed by addition of 360 µL of 100% ethanol, mixed via gentle trituration. Cell lysate was transferred into the GeneJet RNA purification column, and subsequently inserted into a collection tube. The column was centrifuged for 1 min at 14 000 rcf. The flow through was discarded and the purification column was inserted back into the collection tube. This step was repeated until all of the lysate was transferred into the column and spun through. The purification column was transferred into a new 2 mL collection tube, after which 700 µL of GeneJet Wash Buffer 1 was added to the column followed by centrifugation for 1 min at 14 000 rcf. The flow through was discarded and the purification column was transferred back into the collection tube. 600 µL of Wash Buffer 2 was added to the column, again followed by a 1 min centrifugation at 14 000 rcf. Flow through was discarded and the column placed back into the collection tube. The

purification tube was then transferred into a sterile, RNase free microcentrifuge tube. 100 µL of nuclease-free water was added to the center of the purification column membrane, and the column was spun for 1 min at 14 000 rcf to elute the RNA. The purified RNA was stored at -80 C until use.

RNA concentration and purity was determined by measuring the nucleic acid concentration at 260 nm and the 260/280 nm ratio, respectively, via the NanoDrop Lite Spectrophotometer. An additional measurement of RNA purity was done using the Aligent 2100 Bioanalyzer – only RNA with a RIN ≥8 was used for experiments.

3.5.2. Microarray analysis

Total RNA samples collected from P0 VICs, A-fibs, D-fibs and BMCs (n=3) were pooled together such that each cell type investigated had equal contribution from each of the three animals. Microarray analysis was performed according to the Affymetrix GeneChip Expression 3'-Amplification Labeling kit directions, with a modification that 5 µg total RNA was used as a starting point. Samples were hybridized to Affymetrix GeneChip Porcine Genome 2.0 microarrays and analyzed using GCOS software, with post-analysis performed using BioConductor and AffylmGUI.

3.5.3. Quantitative reverse transcriptase polymerase chain reaction

The RNA samples used to generate the microarray data were also used for the subsequent q-RT-qPCR experiments; however, the RNA samples used were unpooled and ran as separate samples to allow for statistical analysis. A one-step RT-qPCR analysis was performed using a Bio-Rad iQ5 iCycler and B-R One-Step SYBR Green RT-qPCR kit, with 25 ng RNA and 5 µM of each of the forward and reverse primers. mRNA expression was normalized relative to *GAPDH*. All primers were designed using the PrimerBlast program (Table 1 and Table 2).

Table 1: Primer sequences used in 1-Step RT-qPCR analysis.

Gene Name	Direction	Primer sequence 5' → 3'
HES1	Forward	CAGTTTGCCTTCCTCATCCC
	Reverse	CTGTTGCTGGTGTAGACTGG
HEY1	Forward	AGGTTCCATGTCCCCAACTAC
	Reverse	GGCAGATCCCTGCTTCTCAA
HEY2	Forward	TGTCAGTATCAGCCACGTCC
	Reverse	TGGCTACTTTCAGGGTGCAG
RBPJ	Forward	TACCTACACGCCAGAACCAG
	Reverse	TGTGTAACTTCCCTCGCTGT
GAPDH	Forward	AACGTGTCGGTTGTGGATCT
	Reverse	CCCCAGCATCAAAAGTGGAAG

Table 2: Gene and protein names

Gene Name	Protein Name	Alternative Name
HES1	HES1	
HEY1	HEY1	HRT1/HESR1/HERP2/CHF2
HEY2	HEY2	HRT2/HESR2/HERP1/CHF1
RBPJ	RBPJ	CBF1/CSL/Su(H)
GAPDH	GAPDH	

3.5.4. Western blot analysis of microarray target genes

To investigate the protein expression of the genes of interest selected subsequent to the microarray and RT-qPCR analyses, Western blot analyses were performed. Due to limitations concerning the number of P0 cells that could be isolated from each animal, protein and RNA were not isolated from the same animals. Therefore, cellular lysates of VICs, A-fibs, D-fibs and BMCs from three additional animals were collected for protein extraction. Again, due to limitation regarding the availability of porcine antibodies, antibodies selected for probing included HEY1, HEY2, ADAM10 and ADAM17. Western blots were performed as previously described in the methods section.

3.6. Reagents

Cell culture media (DMEM-F12 and SMEM) and antibiotics (penicillin, streptomycin and gentamycin) were purchased from Gibco, Life Technologies (Grand Island, USA). FBS was purchased from Wisent (St-Bruno, Canada). Plastic cell culture plates were obtained from Corning (Tewksbury, USA) and the silicone, compressible culture dishes were purchased from Excellness (Lausanne, Switzerland). Collagenase type II protease was purchased from Worthington Biochemical Corp. (Lakewood, USA) and the dispase II protease was obtained from Sigma (St. Louis, USA). The GeneJet RNA purification kit, coverslips and *SlowFade*® Gold was purchased from Thermo Fisher Scientific (Canada). The SuperSignal West Pico chemiluminescent substrate was purchased from Thermo Fisher Scientific (Rockford, USA). A BCA kit used for protein assays was obtained from Sigma (St. Louis, USA), and the Western

blot ladders and PVDF membranes were purchased from BIO-RAD (Hercules, USA) and Millipore (Ebicoke, Canada), respectively. The One-Step SYBR Green RT-qPCR kit was purchased from Quanta Biosciences (Gaithersburg, USA).

3.7. Antibodies

Mouse monoclonal desmin (ab8976), ED-A fibronectin (ab6328), PECAM-1 (ab14091), SMEMB (ab684), and vimentin were purchased from Abcam (Cambridge, UK). Rabbit polyclonal alpha smooth muscle actin (ab5694), β-tubulin (ab6046), and osteopontin (ab4884) were also purchased from Abcam (Cambridge, UK). Secondary antibodies used for Western blot analysis (goat anti-rabbit IgG, conjugated to horse radish peroxidase) were purchased from Jackson ImmunoResearch Laboratories (Westgrove, USA). Tetramethylrhodamine isothiocyanate conjugated probe for F-actin was obtained from Molecular Probes, Life Sciences (Rockford, USA). Goat anti-mouse, Alexa Fluor 488 FluoroNanogold and goat anti-rabbit, Alexa Fluor 594 Nanogold secondary antibodies were obtained from Life Technologies (USA).

3.8. Statistical analysis

Results were analyzed by one-way analysis of variance (ANOVA). Newman-Keuls multiple comparison test and Tukey's multiple comparison test were used post hoc for the immunoblot and qRT-PCT data, respectively. All data is expressed as mean ± SEM. A P-value ≤ 0.05 was considered statistically significant.

4. RESULTS

4.1. Optimization of cell culturing methods

Prior to proceeding with experiments comparing the different cell types, protocols for large animal use, harvesting tissue and cell culture had to be defined. Particular care was taken to optimize the cell culture methods to ensure consistency among *in vitro* experiments.

4.1.1. Direct explant *vs*. enzymatic liberation

We compared two commonly used techniques for isolating dermal fibroblasts: direct explant and enzymatic liberation. The direct explant method involves cutting the tissue (in this case skin) into small pieces and placing it directly onto the surface of the culture dish and allowing the cells to migrate out of the tissue and onto the plate, as opposed to the cellular liberation method that uses enzymes to isolate cells prior to plating. Overall we found that the enzymatic liberation method for culturing dermal fibroblasts was less time consuming, easier to execute and produced far better results than the direct explant method for reasons explained below.

Firstly, complete removal of the hypodermis (or subcutaneous fat) was required for the direct explant method. Failure to remove the hypodermis would result in a low yield cell culture. This is likely due to fibroblasts not having contact with the culture dish, resulting in a low percentage of cells migrating out onto the surface of the plate. Additionally, if only a small number of cells migrated from the tissue, this often result in early senescence (i.e. cells

undergoing cell death prior to reaching confluency), possibly due to a lack of intercellular signaling caused by low population density. Conversely, complete removal of the hypodermis was not required in the enzymatic liberation method as any remaining adipose tissue would be removed during the subsequent enzyme digestion steps, prior to plating.

For the direct explant method, placing the tissue onto the culture dish presented a challenge. We had to ensure that the deep side (dermis), as opposed to the epidermis, was adjacent to the surface of the culture dish; otherwise the cells would not migrate out of the tissue. In addition, it was difficult to determine how far apart to space the pieces of tissue and what size the pieces of dermis should be in order to grow cell cultures with an even distribution of cells. We cut the dermal tissue into 4 mm^3 (2 mm x 2 mm x 1 mm) pieces and spaced the tissue between 1 and 2 cm apart. Based on our trials, we were unable to grow P0 cultures that had an even distribution of cells. In addition, our cultures were not reaching confluency within 48-72 hours – a requirement of our experimental studies. For the enzymatic method, as the cells were liberated from the connective tissue and put through a cell filter prior to plating, the P0 cell cultures had a much more even distribution of cells.

As our experiments required the use of P0 cell cultures we abandoned the direct explant method and pursued the enzymatic method of culturing dermal fibroblasts. In addition, as the direct explant method was fairly laborious and did not produce P0 cell cultures that were appropriate for our experiments we chose not to trial the direct explant method on the other tissue types (atrial appendage or aortic valve leaflet).

4.1.2. Types of enzymes used and duration of exposure

As we found the enzymatic liberation method superior to the direct explant method for our experimental design, our next step was to determine which enzyme(s) would be most efficient at digesting the porcine tissues (dermis, atrial appendage and aortic valve leaflets). All tissue was minced into small pieces (between 1 and 8 mm^3), with the exception of the valve leaflets, which were left in their native state. Our initial attempts to establish which enzyme(s) to use and for how long included collagenase type II (0.1% w/v) over 4 hours. We found that after 4 hours of exposure to collagenase II was not sufficient to digest the tissue. As a result, a large percentage of cells were unable to pass through the cell filter and were discarded prior to plating. We extended the duration of enzyme exposure to 6 hours, then to 8 hours. This resulted in only a slight increase in the percentage of cells that were liberated from the tissue. As we wanted to minimize the percentage of cells discarded we tested the addition of dispase II protease (0.05% w/v) to the enzyme cocktail. After 8 hours we found that the dermal tissue was noticeably more disaggregated; however, it was still challenging to pass the cells through the filter and a large percentage of cells were still discarded. In addition, we did not notice any improvement in the percentage of cells liberated from the atrial tissue and valve leaflets; therefore, we increased the duration of enzyme exposure to ~16 hours (or overnight). For logistical reasons we did not test a digestion time between 8 and 16 hours. After 16 hours all tissue types (dermis, atrial appendage and aortic valve leaflets) were sufficiently disaggregated such that only a minimal amount of tissue was discarded after passing through the cell filter. Additionally, as we found that including dispase II appeared to aid in the digestion of the dermal tissue we used a mix of both dispase II and collagenase II for all future dermal fibroblast isolations.

For the isolation of aortic valvular interstitial cells only we also tested the efficacy of a brief (10 min) exposure to collagenase II, followed by gentle removal of the endothelial monolayer with a small sterile sponge, prior to the overnight digestion. This was initially done to minimize endothelial cell growth in our cultures; however, this became redundant once we decreased the initial cell adherence time to 60 min, as less adherent cells (i.e. endothelial and smooth muscle cells) would be removed when the media was changed. Again previously mentioned, mincing the leaflets into small pieces was redundant due to the natural size of the porcine aortic valve leaflets; however, any smooth muscle tissue still attached to the leaflets after excision was removed to minimize smooth muscle cell contamination in our VIC cultures.

4.1.3. Isolation of porcine bone marrow-derived progenitor cells

As stated in the methods section, we used a modified version from a previously described method for culturing porcine bone marrow-derived progenitor cells (296). As this method describes the isolation of rat tibial bone marrow, a number of steps had to be modified for our use. Due to the age of the animals, the bone matrix of the sternum was quite stiff; therefore, we had to minced the tissue into very small pieces (<0.1 mm^3). Failure to sufficiently breakdown the tissue via mechanical disaggregation resulted in a too low yield of cells, such that we could not grow the required number of cell cultures for our experiments. Additionally, mincing the bone marrow into very fine pieces allowed the tissue to be triturated through a glass pipet, which also increased the number of cells released from the tissue.

We also had to optimize the amount of media/salt solution to the cellular suspension prior to differential centrifugation. Adding too much media/salt solution to the cellular suspension prior

to differential centrifugation would result in a diffuse mononuclear layer (or buffy coat), which was not adequate separated from the media/salt solution. We found that this resulted in a substantially lower yield of cells. Typically, a mixed solution consisting of 8 mL of growth media and 17 mL of PBS resulted in optimal cell retrieval for piece of bone marrow; however, this amount was adjusted according to the size of the tissue specimen.

4.1.4. Population doublings

Determining population doubling for our P0 cell cultures presented a challenge. As the cell types were selected for during the culturing procedure, not prior, it was not possible to accurately assess the number of atrial fibroblasts, dermal fibroblasts, VICs and BMCs in the atrial tissue, dermal tissue, valve tissue and bone marrow, respectively, prior to initial plating by using standard cell counters. We attempted to measure cell doubling via flow cytometry using fluorescent cell proliferation assays (Click-iT® EdU Alexa Fluor® 488 Imaging kit, ThermoFisher Scientific, Canada); however, we were unsuccessful in obtaining significant results. Therefore, we were unable to obtain accurate results for cell doublings. Based on the consistency in the methods between cell cultures we assume that the number of cell doublings between cell cultures of the same tissue type were fairly comparable we acknowledge that this was a parameter that we were unable to adequately quantify. In addition, we cannot reasonably determine if the cell doubling between different tissue types was similar or not. This may mean that one tissue type underwent a higher number of cell doublings to reach the desired confluency. Certainly, we acknowledge that due to the number of cells that could be isolated from the bone

marrow tissue that our progenitor cell cultures likely underwent a substantially higher number of cell doublings prior to reaching the desired confluency.

4.1.5. Size of tissue biopsies

As previously mentioned, our goal was to consistently grow cell cultures to a confluency of 60-70% within 48-72 hours. These parameters were chosen to 1) reduce the influence of prolonged *in vitro* culture on gene expression, and to 2) minimize the number of, or prevent the inclusion of, cells in the experiment that were undergoing senescence. We also wished to minimize the presence of cellular contaminants (i.e. smooth muscle cells, myocytes and endothelial cells) in our cell cultures. To achieve this we needed to determine: 1) the minimum sample size for the tissue biopsies (i.e. the amount of tissue required for plating), and 2) the duration of cell seeding (as our method for excluding cellular contaminants was based on fibroblast-like cells adhering to plastic dishes or culture surfaces more quickly than other cells types.

Through trial and error we observed that an atrial tissue biopsy with a size of 0.125 cm^3 (0.5cm x 0.5cm x 0.5cm) was sufficient for seeding four, 100 mm culture dishes. Furthermore, a sample of skin 0.1 cm^3 (1cm x 1cm x 0.1cm) in size was sufficient, as was a bone marrow biopsy 8 cm^3 (2 mm x 2 mm x 2 mm). These samples sizes were large enough to ensure that we had sufficient starting material to grow our cultures to 60-70% within 48-72 hours. Our initial trials used much larger tissue specimens. From this we determined that plating too many cells resulted in overgrowth and a large percentage of cells undergoing senescence within 24 hours. For our

VIC cultures, we used all three leaflets to inoculate four, 100 mm plates. Attempts to grow more than four cultures resulted in our cell cultures reaching 60-70% confluency after 72 hours.

To minimize the growth of other cell types in our cultures we had to determine a length of time for cell seeding that would allow our target cells to attached and proliferate, while excluding other (less adherent) cell types. We found that reducing duration of cell seeding to 1 hour was still a sufficient amount of time to allow our target cells to adhere, with the exception of the bone marrow progenitor cells which required 16 hours. In the event that we used a smaller tissue sample than previously mentioned, we would need to increase the duration of cell seeding for enough target cells to adhere to the cell dish, which would likely lead to a higher percentage of non-target growing in the culture. If the cell seeding time was not increased, the cultures would not reach confluency within 48 hours. By determining the amount of tissue required as well as the duration of cell seeding, we were able to consistently grow cell cultures that had an even distribution of cells and reached 60-70% confluency within 48-72 hours (with the exception of BMCs which required 5-6 days) (Figure 7).

A

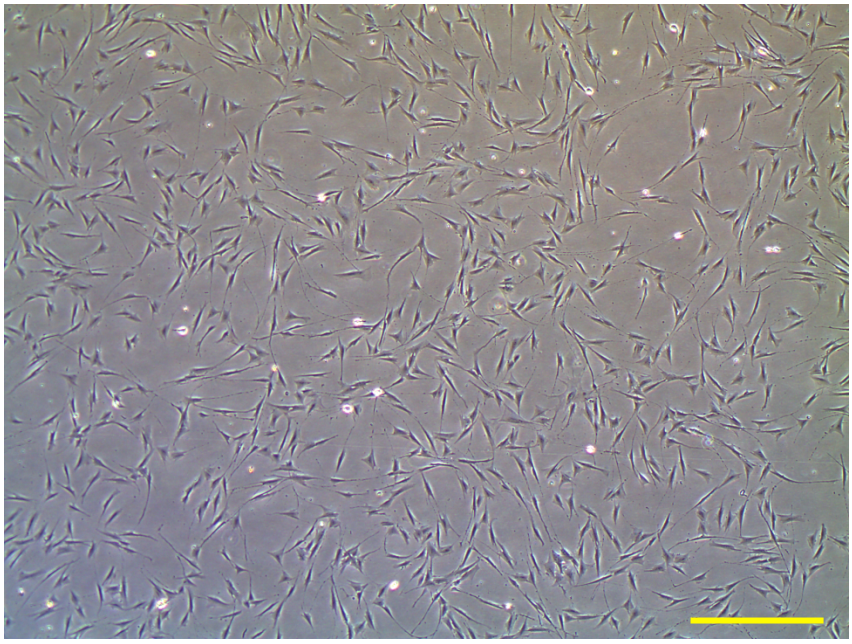

B

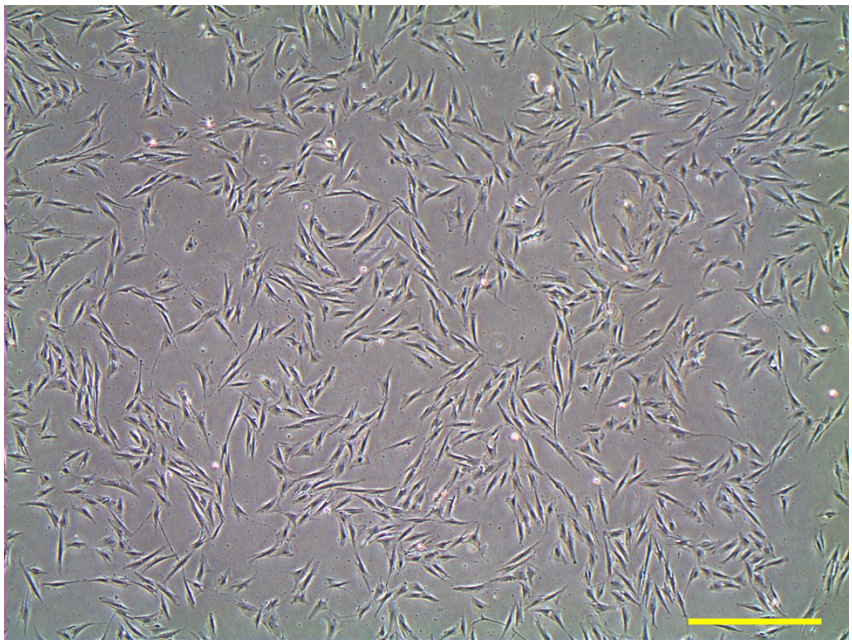

C

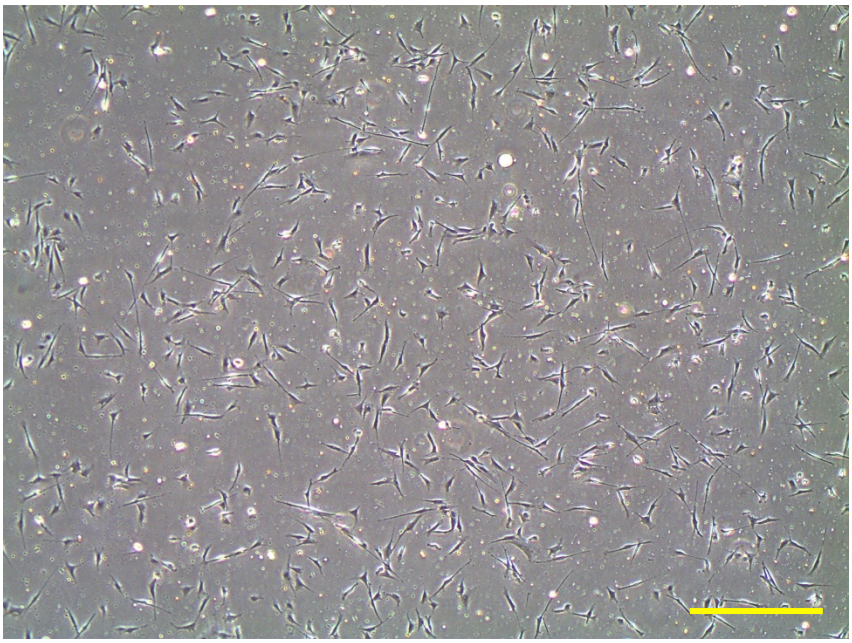

D

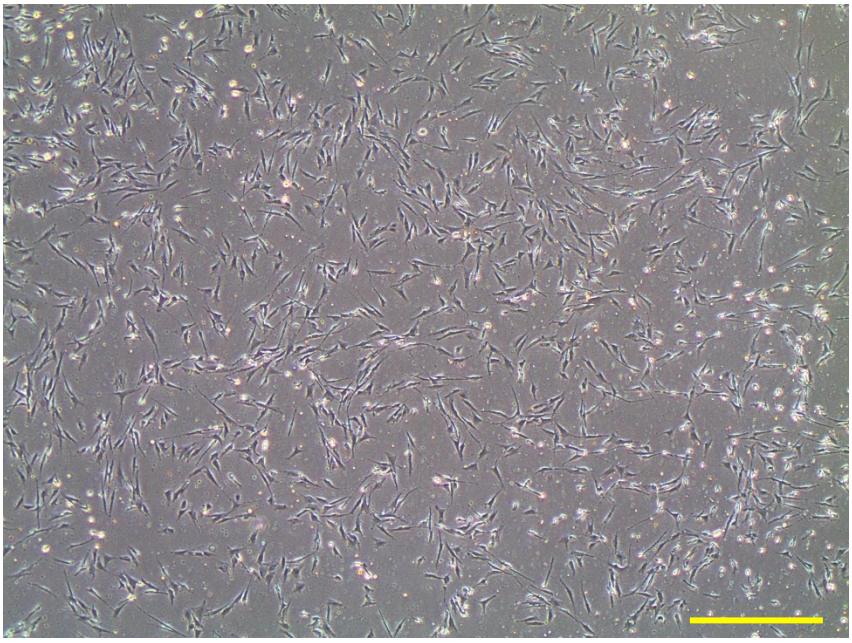

Figure 7: Phase contrast image of cell cultures

Phase contrast image of (A) dermal fibroblasts, (B) atrial fibroblasts, (C) bone marrow-derived progenitor cells, and (D) valvular interstitial cells. Images found in figures A, B and D were taken 68 hours post plating, whereas the image in figure C was taken 120 hours post plating. Magnification 4x. Scale bar 1 mm.

4.1.6. Cell culture purity

We did not find any evidence of cellular staining for platelet endothelial cell adhesion molecule (PECAM-1) or desmin in any of our cell cultures – VICs, A-fibs, D-fibs or BMCs (n=3) (data not shown). This suggests that our methods for cell isolation were successful in excluding endothelial and smooth muscle cell contaminants. We did not culture porcine smooth muscle cells or porcine endothelial cells for a positive control for desmin and PECAM-1 staining, respectively. We recognize that including a positive control for these antibodies would strengthen our results.

4.2. Phenotypic comparison of porcine VICs to porcine A-fibs, D-fibs and BMCs

4.2.1. Cellular marker expression

P1 porcine VICs, A-fibs, D-fibs and BMCs cultured on standard plastic dishes were probed for various fibroblast/myofibroblast and BMCs markers (Figure 8). All cell types stained positive for α-SMA, DDR2, F-actin and vimentin. VICs and BMCs both stained positive for BMC markers KIT and OPN, whereas A-fibs and D-fibs did not. VICs also expressed myofibroblast marker SMEMB, but showed no expression of EDA-FN and POSTN. Both fibroblast cell cultures stained positive for POSTN; however between the fibroblasts only the A-fibs showed expression of SMEMB, whereas the D-fibs expressed EDA-FN. VICs and BMCs had the same expression profile of the cellular markers investigated, with the exception of SMEMB, which was not expressed in the differentiated BMC cultures.

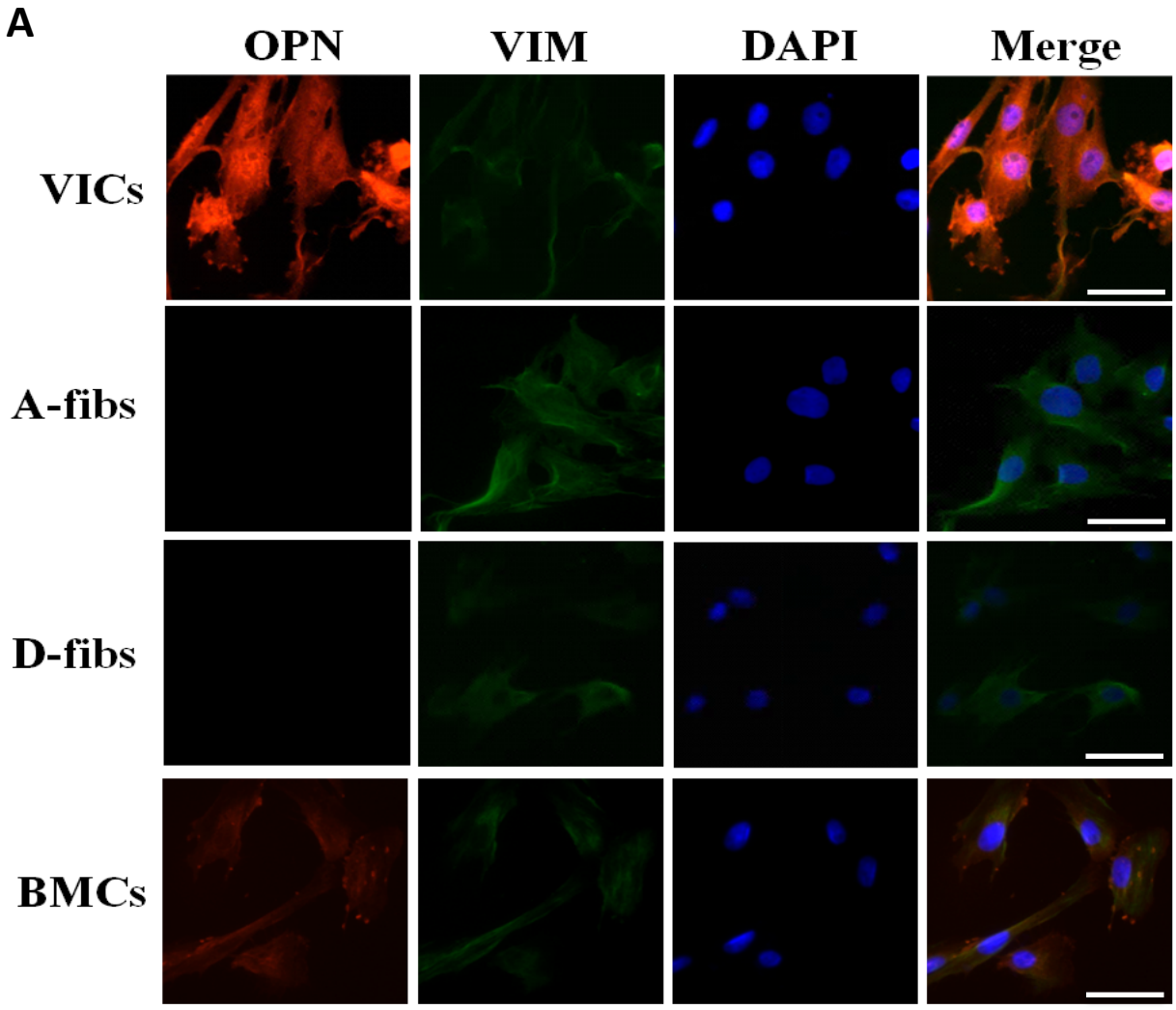

Figure 8: Characterization of cellular marker expression in VICs
Porcine VICs, A-fibs, D-fibs and BMCs were stained for various myofibroblast markers (α-SMA, DDR2, EDA-FN, F-actin, POSTN, SMEMB and VIM), as well as F-actin and differentiated BMC markers (KIT and OPN). These cells were also probed for DES and PECAM-1, but all cells were negative for those markers (data not shown). All cell cultures were P1 and plated on standard rigid plastic dishes.

Figure 8A: Immunofluorescent staining probing for cellular markers OPN and VIM.
Abbreviations: valvular interstitial cells (VICs), atrial fibroblasts (A-fibs), dermal fibroblasts (D-fibs), bone marrow-derived progenitor cells (BMCs), osteopontin (OPN) and vimentin (VIM). Scale bar: 50 μm

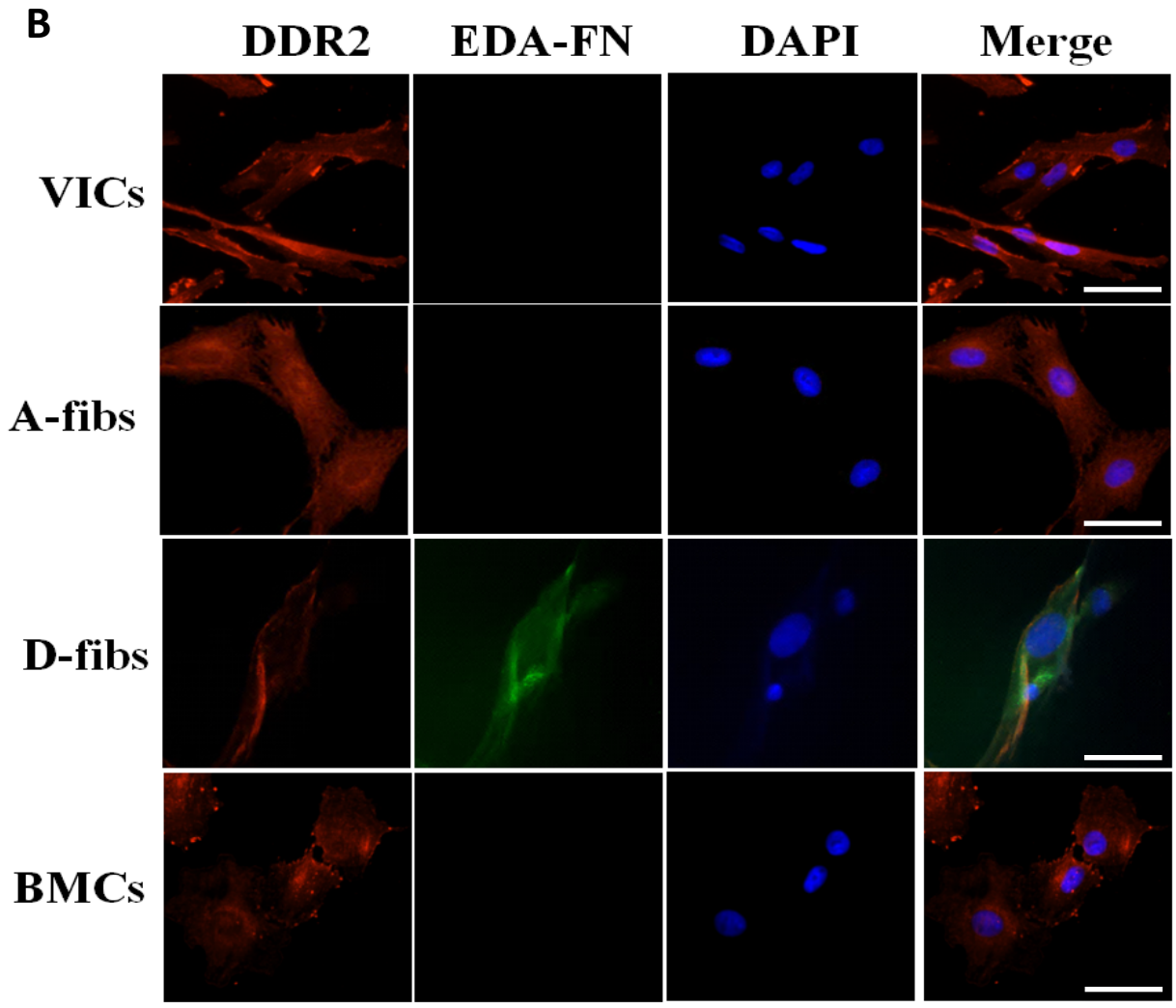

Figure 8B: Immunofluorescent staining probing for cellular markers DDR2 and EDA-FN. Abbreviations: valvular interstitial cells (VICs), atrial fibroblasts (A-fibs), dermal fibroblasts (D-fibs), bone marrow-derived progenitor cells (BMCs), discoidin domain receptor 2 (DDR2) and extra domain A fibronectin (EDA-FN). Scale bar: 50 μm

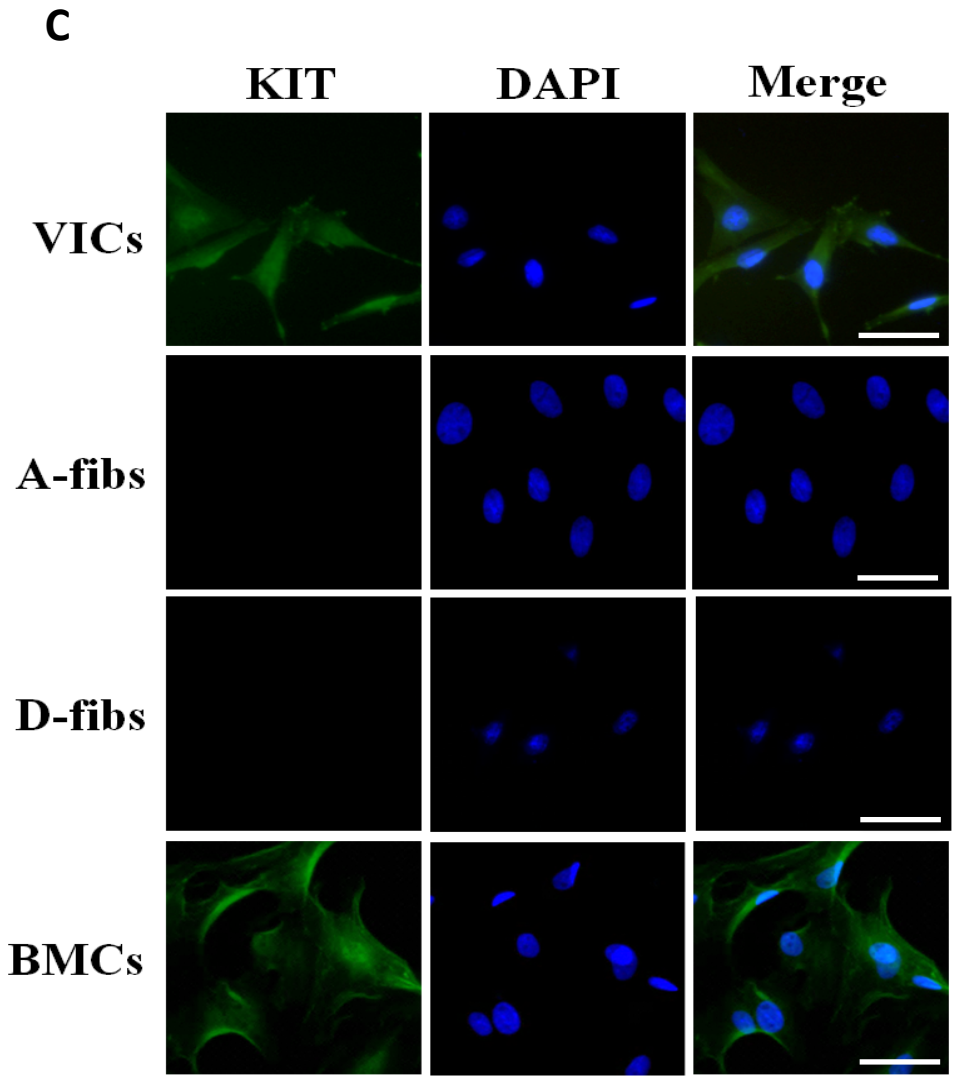

Figure 8C: Immunofluorescent staining probing for cellular marker KIT
Abbreviations: valvular interstitial cells (VICs), atrial fibroblasts (A-fibs), dermal fibroblasts (D-fibs), bone marrow-derived progenitor cells (BMCs) and v-kit Hardy-Zuckerman 4 feline sarcoma viral oncogene (KIT). Scale bar: 50 µm

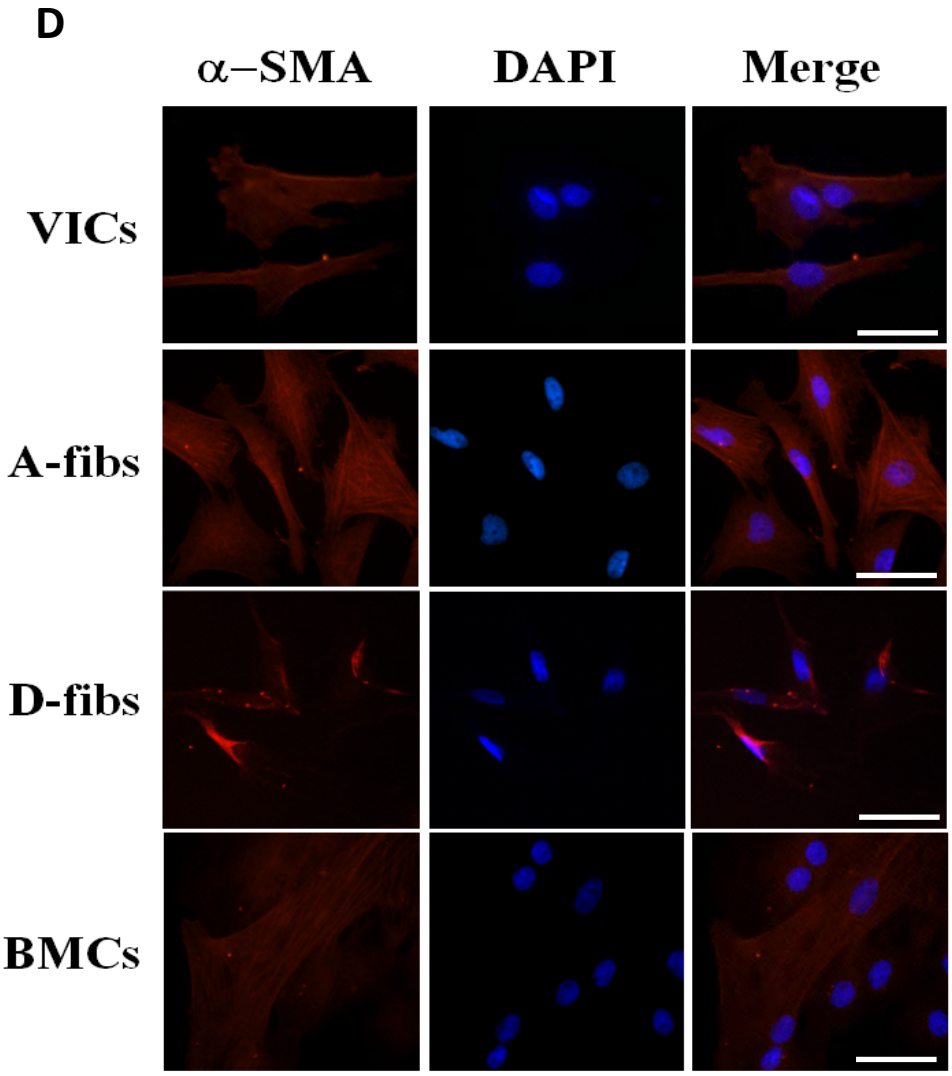

Figure 8D: Immunofluorescent staining probing for cellular marker α-SMA.
Abbreviations: valvular interstitial cells (VICs), atrial fibroblasts (A-fibs), dermal fibroblasts (D-fibs), bone marrow-derived progenitor cells (BMCs), and alpha smooth muscle actin (α-SMA). Scale bar: 50 μm

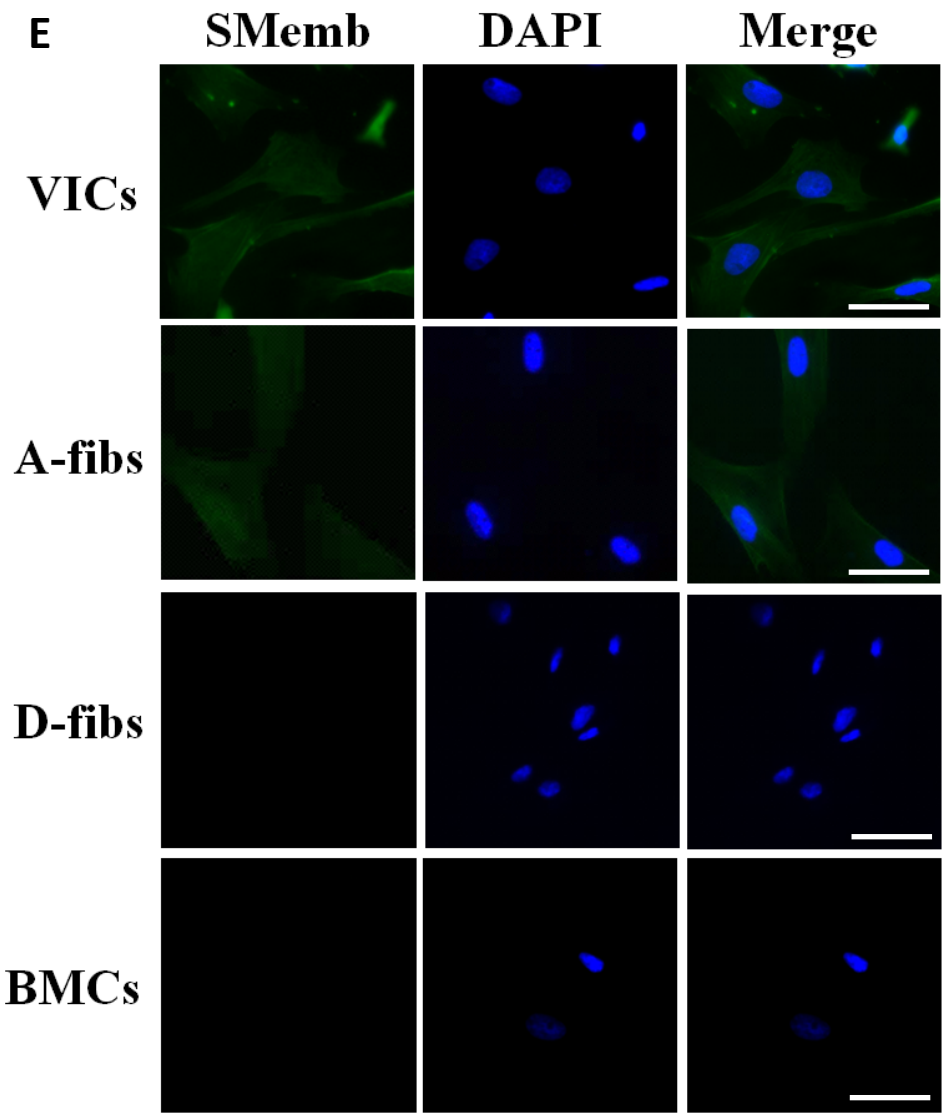

Figure 8E: Immunofluorescent staining probing for cellular marker SMEMB.
Abbreviations: valvular interstitial cells (VICs), atrial fibroblasts (A-fibs), dermal fibroblasts (D-fibs), bone marrow-derived progenitor cells (BMCs), and embryonic smooth muscle myosin heavy chain (SMEMB). Scale bar: 50 μm

F

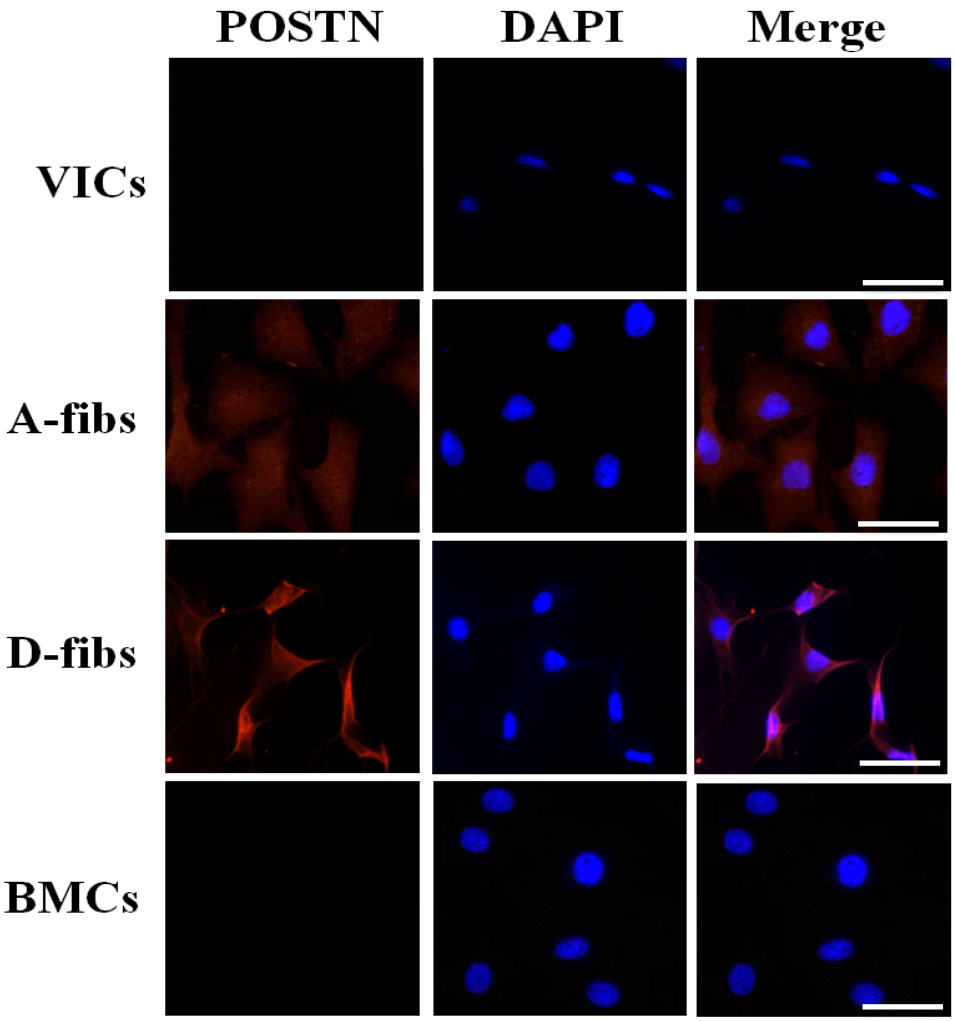

Figure 8F: Immunofluorescent staining probing for cellular marker POSTN.
Abbreviations: valvular interstitial cells (VICs), atrial fibroblasts (A-fibs), dermal fibroblasts (D-fibs), bone marrow-derived progenitor cells (BMCs), and periostin (POSTN). Scale bar: 50 μm

G

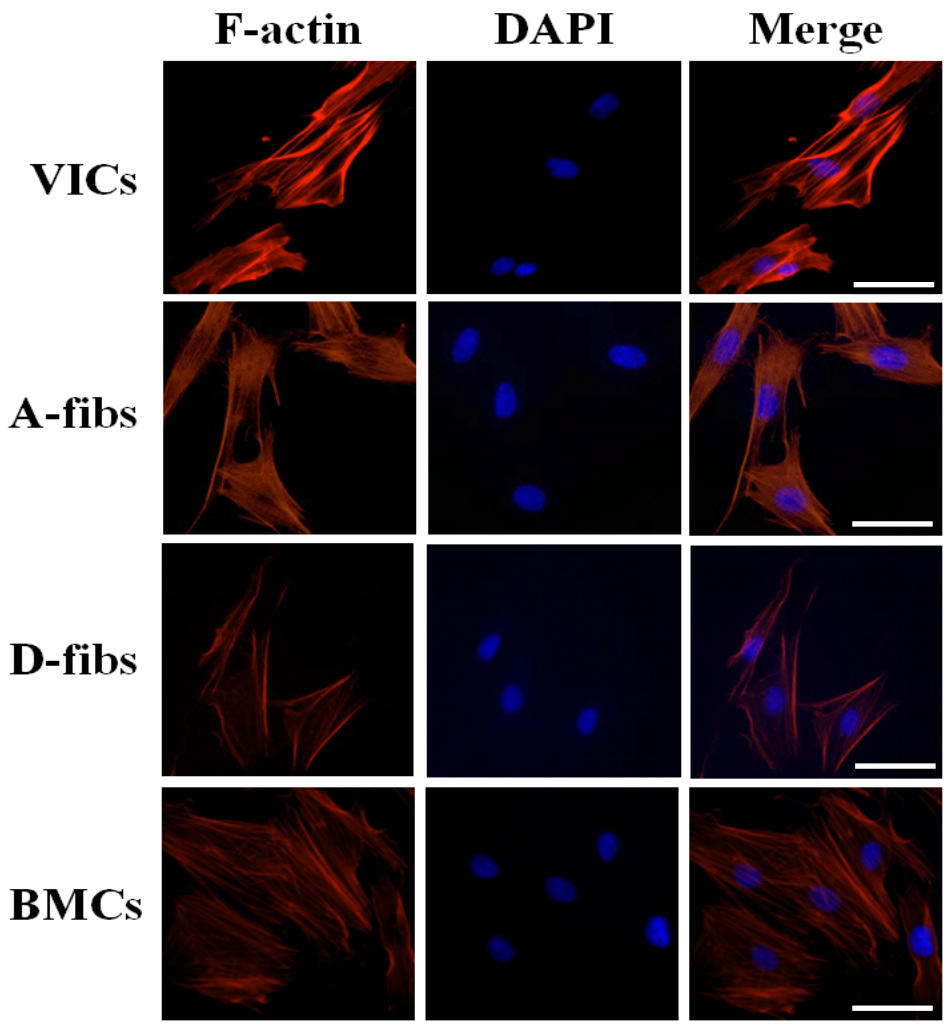

Figure 8G: Immunofluorescent staining probing for cellular marker F-actin.
Abbreviations: valvular interstitial cells (VICs), atrial fibroblasts (A-fibs), dermal fibroblasts (D-fibs), bone marrow-derived progenitor cells (BMCs), filamentous actin (F-actin). Scale bar: 50 μm.

Table 3: Summary of donor cell phenotyping

(A) PI primary porcine VICs, A-fibs, D-fibs and BMCs cultured on standard, rigid plastic dishes were probed for a number of cellular markers; (+) and (-) represent positive or negative staining, respectively. **(B)** VIC staining results were grouped into fibroblast markers, differentiated BMC markers, smooth muscle cell markers and endothelial cell markers; (+) and (-) represent positive or negative staining, respectively. Abbreviations: valvular interstitial cells (VICs), A-fibs (atrial fibroblasts), D-fibs (dermal fibroblasts), bone marrow-derived progenitor cells (BMCs), alpha smooth muscle actin (α-SMA), desmin (DES), discoidin domain receptor 2 (DDR2), extra domain A fibronectin (EDA-FN), filamentous actin (F-actin), v-kit Hardy-Zuckerman 4 feline sarcoma viral oncogene (KIT), osteopontin (OPN), platelet endothelial cell adhesion molecule (PECAM-1), periostin (POSTN), embryonic smooth muscle myosin heavy chain (SMEMB) and vimentin (VIM).

A

Marker	VICs	A-fibs	D-fibs	BMCs
α-SMA	+	+	+	+
DES	-	-	-	-
DDR2	+	+	+	+
EDA-FN	-	-	+	-
F-actin	+	+	+	+
KIT	+	-	-	+
OPN	+	-	-	+
PECAM	-	-	-	-
POSTN	-	+	+	-
SMEMB	+	+	-	-
VIM	+	+	+	+

B

Fibroblast markers						
α-SMA	DDR2	F-actin	SMEMB	VIM	EDA-FN	POSTN
+	+	+	+	+	–	–

BMC markers	
KIT	OPN
+	+

Endothelial markers
PECAM
–

SMC markers
DES
–

4.2.2. Cellular morphology

We examined the cellular morphology the different cell types and found that VICs were most similar in shape and size to dermal fibroblasts. Both exhibited a slender, spindle-like cell body with long cellular projections; however, D-fibs tended to have longer cell bodies and even longer projections. The differentiated BMCs were also similar in shape to that of the VICs and D-fibs, but they were markedly smaller at the same time point. In contrast, A-fibs had larger, cuboidal/cobblestone cell bodies and did not exhibit the same long, slender cellular projections as the VICs and dermal fibroblasts (Figure 9).

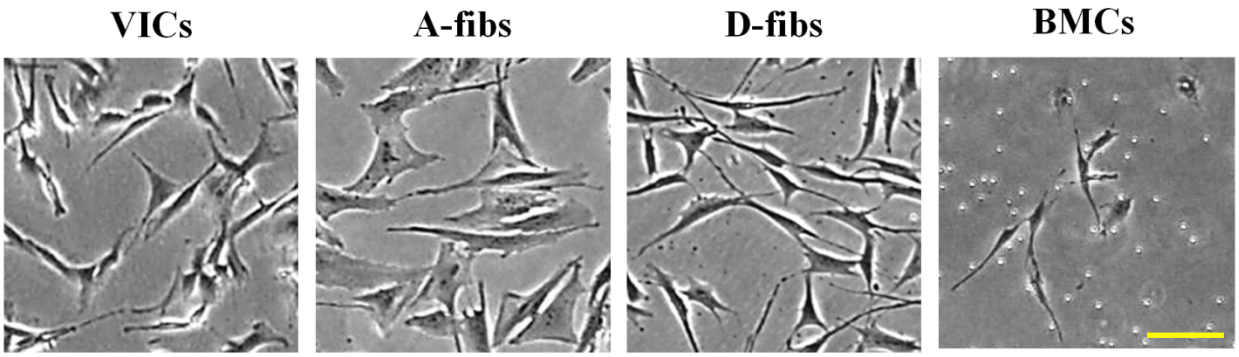

Figure 9: Characterization of VIC morphology
Primary P0 porcine VICs exhibit a similar cellular morphology in comparison to D-fibs and BMCs. Images were taken with a light microscope 72 hours after plating with a magnification of 40x. Representative images show cell cultures plated on fibronectin coated plastic. VICs, as shown, were spindle-shaped, and had elongated processes that protruded from the cell body. D-fibs exhibited a similar shape to VICs, but had longer processes. Differentiated BMCs also exhibited a spindle-shaped cell body after 72 hours of plating, but they were markedly smaller than VICs and D-fibs at the same time point. When compared to VICs, A-fibs had a larger, more cuboidal cell body. Abbreviations: valvular interstitial cells (VICs), A-fibs (atrial fibroblasts), D-fibs (dermal fibroblasts) and bone marrow-derived progenitor cells (BMCs). Scale bar: 200 μm.

4.3. Decreased elastic modulus mitigates cellular activation

4.3.1. Cell culture on 2D compressible matrices

To confirm that the pre-fabricated silicone-based matrices were affective in blocking cellular activation, *in vitro,* we cultured VICs, A-fibs, D-fibs and BMCs 2D matrices with varying stiffness: 5 kPa, 100 kPa, and standard rigid plastic (~1 GPa).

4.3.2. Increased substrate compliance decreases α-SMA expression

Compared to the A-fibs cultured on standard plastic dishes (FN coated and uncoated), A-fibs cultured on soft 2D substrates expressed lower levels of α-SMA, indicating reduced cellular activation. When these cultures were passaged to P1, cells cultured on the soft substrates maintained a significantly lower α-SMA expression when compared to those passage onto the rigid plastic (FN coated and uncoated), p-value ≤ 0.05 (Figure 10). Only those films that did not have over saturated bands, as assessed by the Quantity One software, were used for analysis.

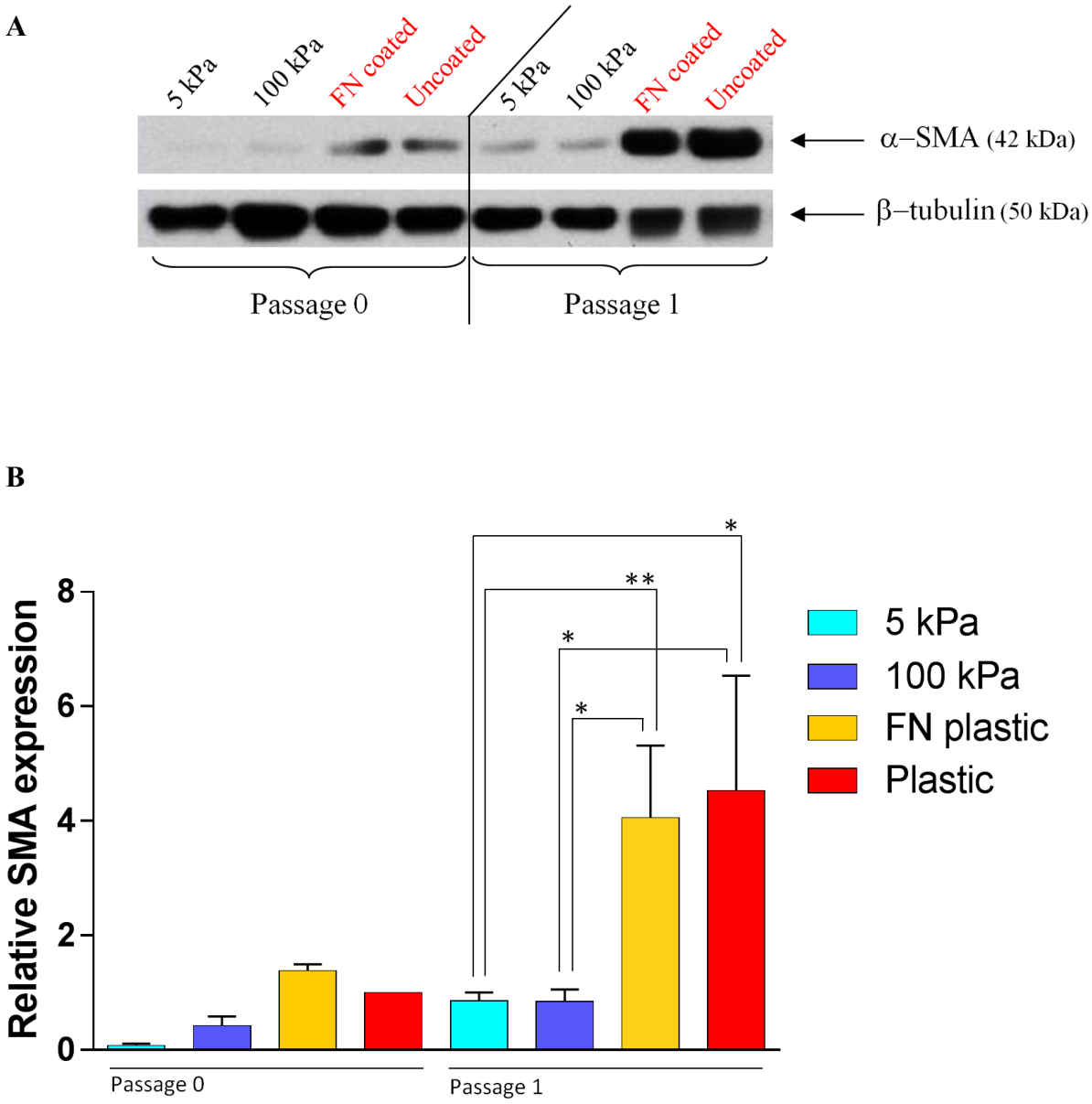

Figure 10: Substrate modulus correlates with cellular α-SMA expression
(A) Representative Western blot of A-fibs from a single Yorkshire pig showing reduced α-SMA expression on soft silicone matrices (5 kPa and 100 kPa), as compared to standard rigid plastic (FN coated and uncoated, substrate modulus ~1 GPa). Lysates were collected once the cell cultures reached 60-70% confluency, or ~72 hours after plating. The soft silicone plates required a fibronectin coating prior to plating, therefore, a fibronectin plastic control was included to account for any variability. β-tubulin was used as a loading control. **(B)** Histogram. n=3, *p<0.05, **p<0.01, ± SEM). Abbreviations: atrial fibroblasts (A-fibs), alpha smooth muscle actin (α-SMA), beta tubulin (β-tubulin), fibronectin (FN), gigapascal (GPa), kilopascals (kPa).

4.3.3. Compressible 2D matrices alter cellular morphology

Compared to rigid controls (FN coated and uncoated), P0 VICs, A-fibs, D-fibs and BMCs plated on 5 kPa and 100 kPa substrates appeared to exhibit reduced cell body size (Figure 11). Additionally, those cells plated on softer matrices appeared to have a more slender, spindle-shaped appearance, whereas those plated on standard rigid plastic had a more cuboidal/cobblestone appearance (e.g. see atrial fibroblasts). BMCs appeared to be less dependent on substrate stiffness, exhibiting a slender cell body on all substrates. To account for any differences that may be due to the FN coating, we compared cells plated on FN coated plastic to the corresponding cell types plated on uncoated rigid plastic. Upon qualitative visual assessment there was no noticeable difference in the cell shape or size between those cells plated on FN coated rigid plastic as compared to uncoated rigid plastic dishes.

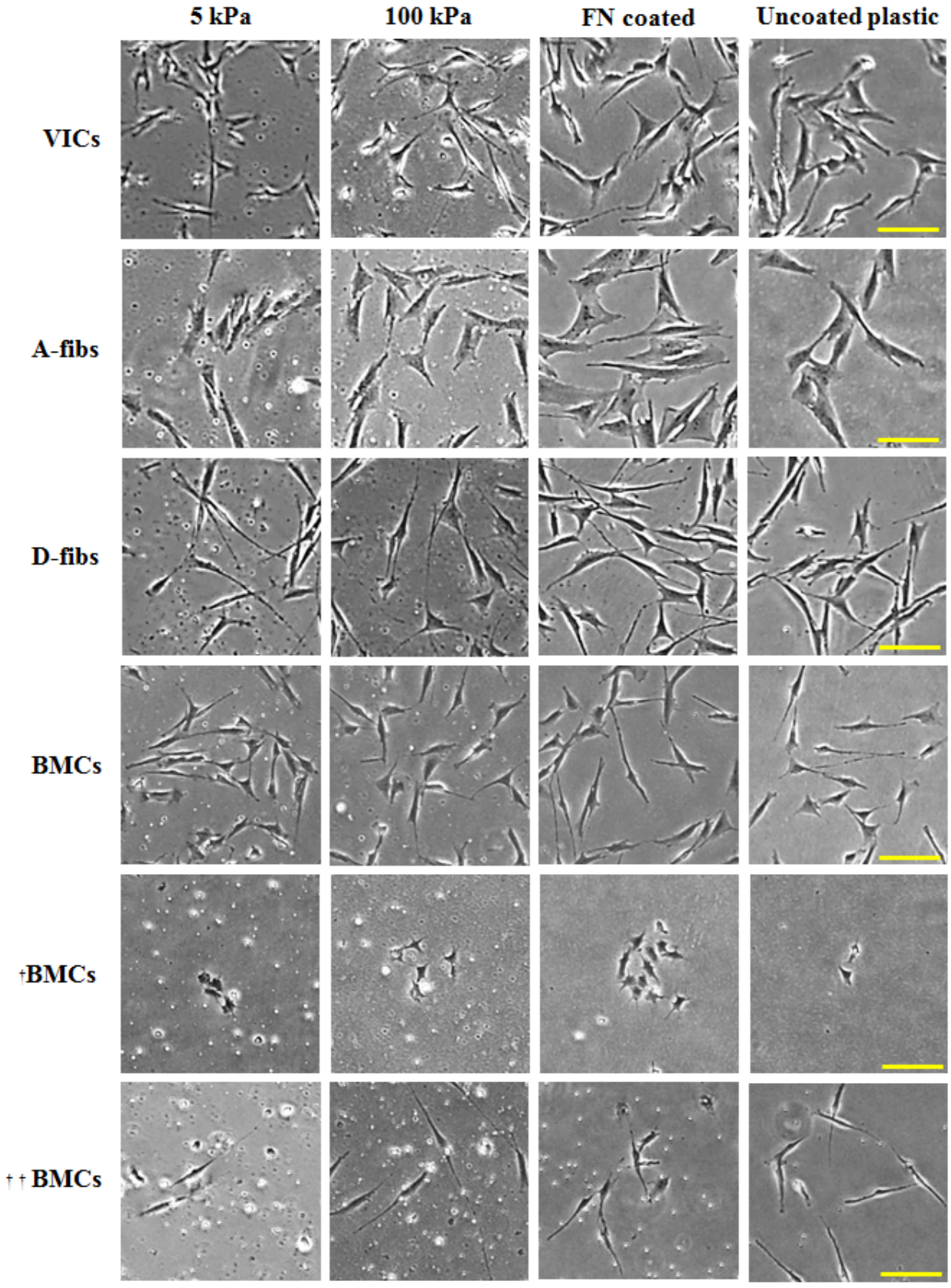
5 kPa
100 kPa
FN coated
Uncoated plastic
VICs
A-fibs
D-fibs
BMCs
†BMCs
† † BMCs

Figure 11: Substrate stiffness modulates cellular morphology

Primary P0 porcine VICs, A-fibs, D-fibs and BMCs were cultured on substrates with varying stiffness. Images were taken with a light microscope at 60-70 confluency (or 72 hours after plating for the A-fibs, D-fibs and VICs, and 120 hours post plating for the BMCs), at 40x magnification. Representative images show cell cultures plated on 5 kPa, 100 kPa, and ~1 GPA (FN coated and uncoated). All cells types, with the exception of BMCs showed an increase in cell body size with increased matrix stiffness. The soft silicone plates (5 and 100 kPa) required a fibronectin coating prior to plating; therefore, a fibronectin plastic control was included to account for any variability. †Representative images showing BMC cultures 24 hours after plating. ††Representative images showing BMC cultures 72 hours after plating. BMCs had a star-shaped morphology early in cell culture, but transitioned into spindle-shaped cells at higher confluency and/or after a longer duration in cell culture. Abbreviations: Atrial fibroblasts (A-fibs), bone marrow-derived progenitor cells (BMCs), dermal fibroblasts (D-fibs), valvular interstitial cells (VICs), fibronectin (FN), gigapascals (GPa) and kilopascals (kPa). Scale bar: 200 μm.

4.4. Microarray analysis of porcine VICs, A-fibs, D-fibs and BMCs

Gene expression was analyzed by Affymetrix GeneChip Porcine Genome 2.0 microarray and a cut-off of a 2-fold change in RNA levels (p-value ≤ 0.05) was used for comparisons between samples. Of the 24 123 gene targets that were analyzed, 1512 transcripts were differentially expressed between VICs and A-fibs (600 up-regulated in A-fibs and 912 down-regulated, representing ~6.3% of the transcripts on the array); 1682 transcripts were differentially expressed between VICs and BMCs (705 up-regulated in BMCs and 977 down-regulated, representing ~7.0% of the transcripts on the array); and 1843 transcripts were differentially expressed between VICs and D-fibs (880 up-regulated in D-fibs and 963 down-regulated, representing ~7.6% of the transcripts on the array). All data were normalized and indicated no sampling bias (Figure 12).

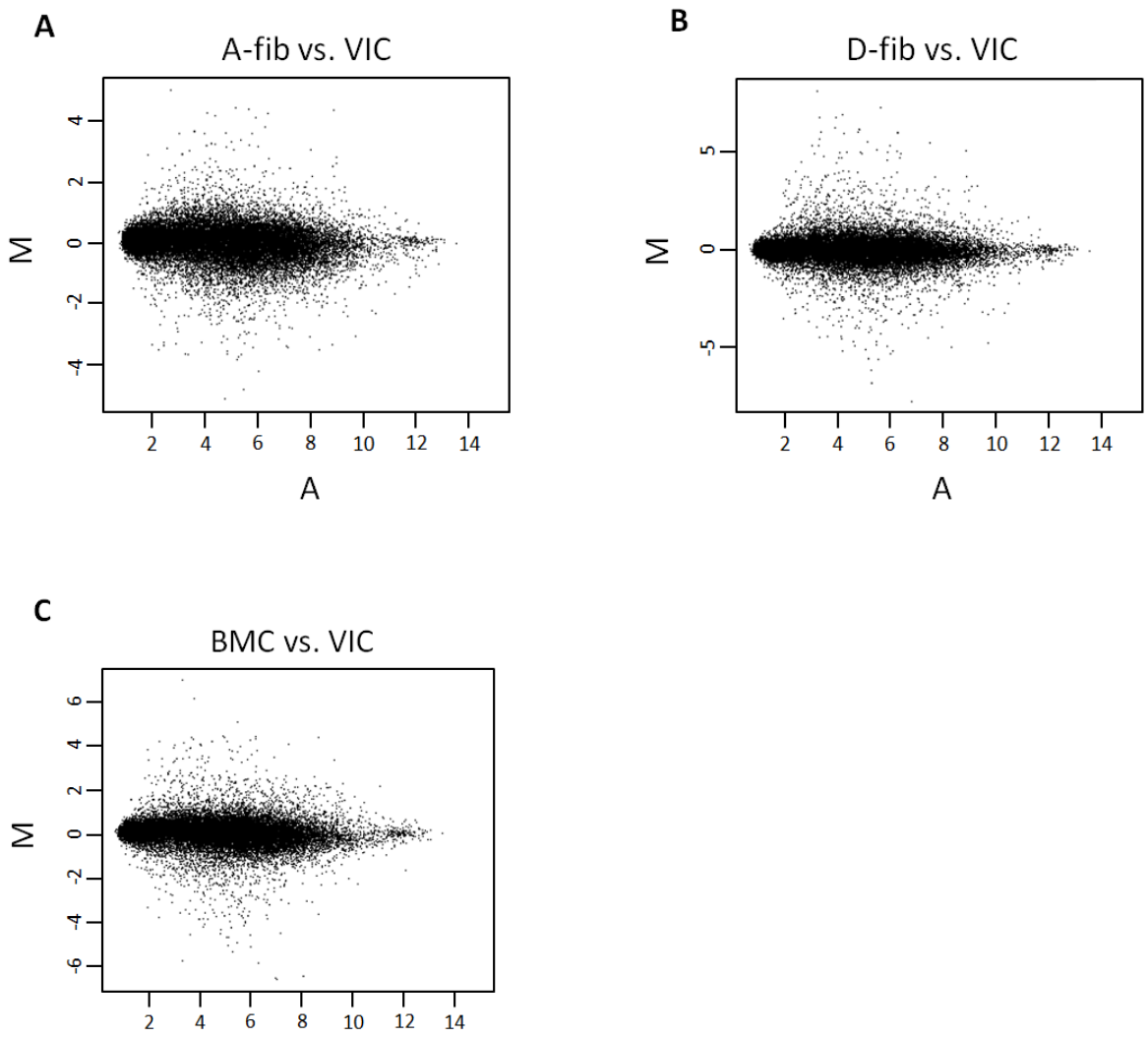

Figure 12: Microarray data quality analysis

MA plot of the microarray data after normalization with signal intensity ratio (M, y-axis) plotted against the average signal intensity (A, x-axis). A distribution of approximately M=0 indicates that the majority of comparative transcripts between the two samples did not differ in expression – this was expected for our sample populations and indicated successful data normalization. **(A)** A-fibs *vs.* VICs, signal intensity ratio (y-axis) vs. average signal ratio (x-axis). **(B)** D-fibs *vs.* VICs, signal intensity ratio (y-axis) vs. average signal ratio (x-axis). **(C)** BMCs *vs.* VICs signal intensity ratio (y-axis) vs. average signal ratio (x-axis). Abbreviations: valvular interstitial cells (VIC), A-fibs (atrial fibroblasts), D-fibs (dermal fibroblasts) and bone marrow-derived progenitor cells (BMCs), average signal intensity (A) and signal intensity ratio (M).

4.4.1. VICs demonstrate differential gene expression in NOTCH signaling proteins

The microarray data revealed differences in relative mRNA levels of several NOTCH signaling targets, relative to VICs (Table 4). *HES1* expression was lower in VICs than all cell types, with A-fibs, D-fibs and BMCs demonstrating fold increases of 3.4, 13.4 and 4.3 relative to VICs, respectively. Conversely, VICs had markedly higher expression of *HEY2* as compared to all other cell types, most notably observed when compared to D-fibs, -216.6-fold change in D-fibs. *HEY2* expression was diminished to a lesser degree in A-fibs and BMCs (-8.0-fold change and -4.0-fold change, respectively). Using a cut-off of a 2-fold change in expression, we did not see any significant difference in *HEY1* expression between VICs and A-fibs, or VICs to BMCs; however, D-fibs had a significantly higher expression of *HEY1* as compared to VICs with a fold increase of 3.3. ADAM-10 and -17, which are proteases that cleave the extracellular NOTCH domain, showed only slight variability in mRNA expression across cell types. The only significant differences observed were between A-fibs/VICs and BMC/VICs, exhibiting slight decreases in expression as compared to VICs (fold-changes -3.0 and -2.4, respectively). There was no significant difference in *RBPJ* across cell types. Due to limitations of the Affymetrix GeneChip Porcine Genome 2.0 microarray, downstream targets of *Hes/Hey* were not available for analysis.

Table 4: Porcine VICs, A-fibs, D-fibs and BMCs show altered expression in NOTCH target genes

Microarray data showing relative mRNA expression for select proteins involved in the NOTCH signaling pathway. Some proteins have multiple expression levels – this is due to multiple target sites for the same gene on the GeneChip. All mRNA expression is normalized to VIC mRNA expression and expressed as fold-change. Abbreviations: atrial fibroblasts (A-fibs), bone marrow-derived progenitor cells (BMCs), dermal fibroblasts (D-fibs), valvular interstitial cells (VIC), a disintegrin and metalloproteinase domain-containing protein 10 (ADAM10), a disintegrin and metalloproteinase domain-containing protein 17 (ADAM17), delta-like 3 (DLL3), delta-like 4 (DLL4), hairy/enhancer-of-split 1 (HES1), hairy/enhancer-of-split related with YRPW motif protein 1 (HEY1), hairy/enhancer-of-split related with YRPW motif protein 2 (HEY2), jagged 1 (JAG1) and recombination signal binding protein for immunoglobulin kappa J region (RBPJ).

Gene	A-fibs/VIC (fold)	D-fibs/VIC (fold)	BMC/VIC (fold)
ADAM10	-1.3, -3.0	-1.1, -1.4	-1.3, -2.4
ADAM17	1.2	1.2	1.0
DLL3	1.2	-1.0	1.2
DLL4	2.8	3.0	1.3
HES1	3.4	13.4	4.3
HEY1	1.8	3.3	-1.8
HEY2	-1.3, -8.0, -6.9	-1.2, -112.4, -216.6	-1.5, -4.0, -2.5
JAG1	1.7, 1.0, -1.2	1.5, 1.1, -1.0	1.4, 2.0, 1.6
RBPJ	-1.1, -1.5, -1.5, -1.2	1.1, -1.1, -1.1, -1.2	-1.2, -1.6, -1.7, -1.4

4.5. Quantitative reverse transcriptase polymerase chain reaction analysis

Validation of the microarray was performed via RT-qPCR. Optimal annealing temperatures were confirmed by preliminary PCRs via temperature gradients.

4.5.1. Porcine VICs demonstrate differential expression of NOTCH target genes

Congruent with the microarray data, A-fibs and D-fibs expressed significantly higher levels of *HEY1* (6.4-fold increase, $p<0.05$; 15.9-fold increase, $p<0.001$, respectively) relative to VICs. Conversely, *HEY2* expression was significantly lower in both A-fibs and D-fibs, relative to VICs (fold-increase of 4.0 and 142, respectively). There was no significant difference in expression of *HES1* and *RBPJ* between VICVs and the other cell types (Figure 12).

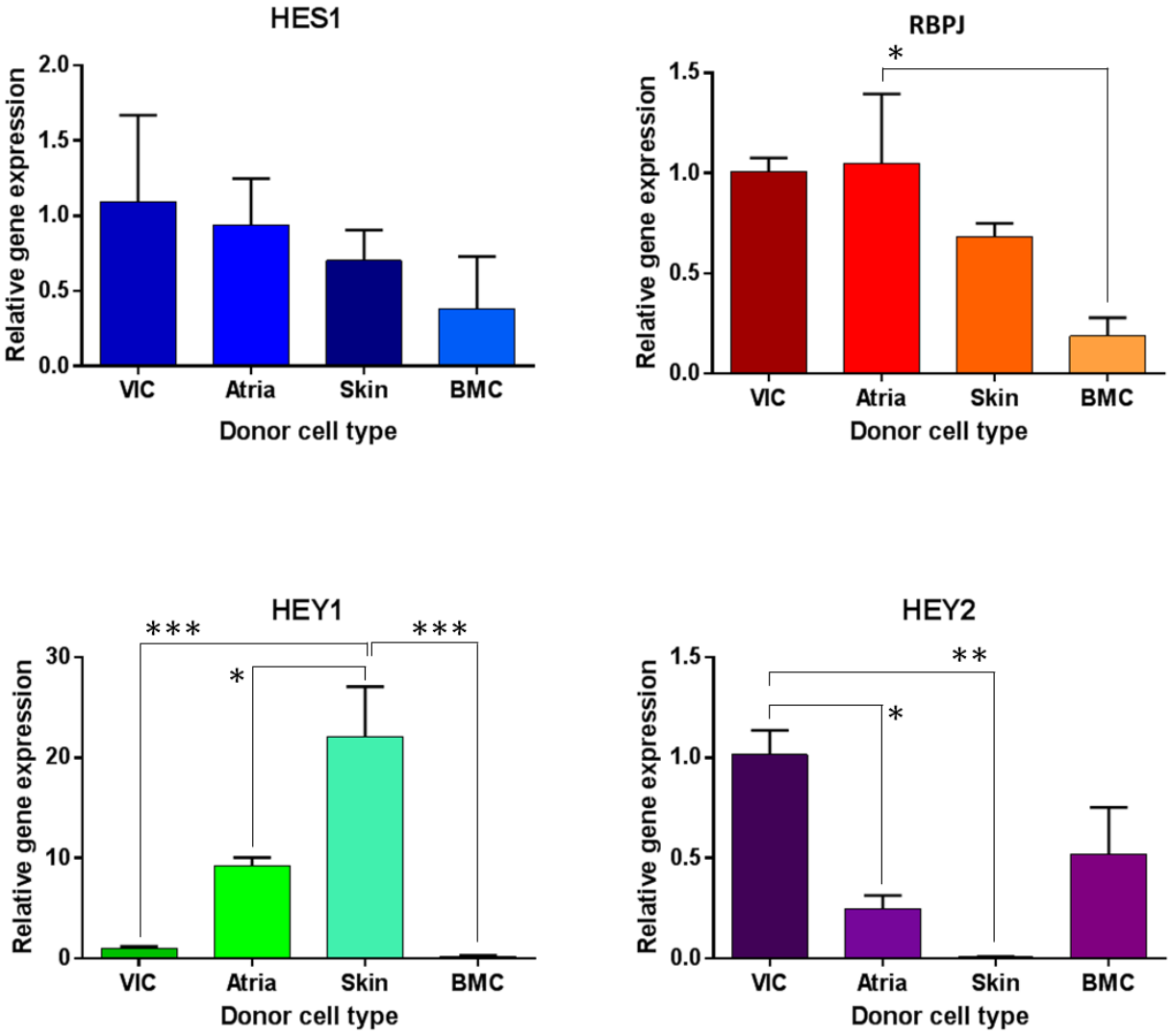

Figure 13: Porcine VICs demonstrate differential expression of NOTCH targets genes

RT-qPCR data showing relative mRNA levels for select proteins involved in the NOTCH signaling pathway. All mRNA expression is normalized to VIC mRNA expression and expressed as fold-change. * $p<0.05$; **$p<0.01$; ***$p<0.001$, n=3.

Abbreviations: valvular interstitial cells (VIC), A-fibs (atrial fibroblasts), D-fibs (dermal fibroblasts) and bone marrow-derived progenitor cells (BMCs), hairy/enhancer-of-split 1 (HES1), hairy/enhancer-of-split related with YRPW motif protein 1 (HEY1), hairy/enhancer-of-split related with YRPW motif protein 2 (HEY2) and recombination signal binding protein for immunoglobulin kappa J region (RBPJ).

4.6. Western blot analysis of NOTCH target genes

Despite attempts to assess relative HEY1 and HEY2 protein levels via Western blot, we were unable to collect usable data. Despite following the manufacturer's protocol for storage, blocking (5% skim milk) and primary antibody concentration (1:200), we had high amounts of background that were incompatible with analysis. We made several attempts to optimize the protocol by testing various blocking agents, and using different concentrations. We found that blocking with 5% skim milk, 10% skim milk, 5% skim milk with 1% BSA or 1% Block-CH were all unsuccessful in preventing high amounts of background. We also increased the primary antibody concentration to 1:100; however, similarly, we were unable to quantify the results with confidence due to high background. We were limited in our options for primary antibodies compatible with porcine epitopes; therefore, we were unable to test antibodies from other manufacturers.

Due to resource limitations were we unable to collect additional cell lysates to attempt other methods for comparing protein levels amongst our selected tissue types. Had more protein been available for analysis a number of other methods for protein quantification could have been attempted. Enzyme-linked immunosorbent assays (ELISAs) are an alternative method for detecting and quantifying proteins; however, similar to Western blots, ELISAs also employ antibodies for protein detection. Therefore, it is likely that we may have encountered similar issues. Another method for protein detection and relative comparison that does not use antibodies is isobaric tagging for relative and absolute quantification (iTRAQ). Instead of using antibodies for protein detection, iTRAQ is a method that involves labeling protein samples with tags of varying mass (298). These samples are then pooled together and fractionated by liquid

chromatography (LC), and then analyzed by tandem mass spectrometry (MS/MS). Although we initially considered iTRAQ as an investigated method for protein quantification – we were unable to pursue that option.

5. DISCUSSION

5.1. Cell culture methods for porcine VICs, A-fibs, D-fibs and BMCs

We investigated the use of pre-fabricated, compliant, silicone-based substrates for culturing porcine tissue, specifically VICs, atrial fibroblasts, dermal fibroblasts and bone marrow-derived progenitor cells. To accomplish this goal, we first standardized protocols for harvesting each organ/tissue type (heart – aortic valve and LAA, bone marrow, and skin), then optimized cell culture methods. To facilitate *in vitro* experiments that would attempt to mimic *in vivo* tissue, our primary experiments required P0 cells that would grow to 60-70% confluency within 48-72 hours (or 5-6 days of BMCs) and required an initial cell seeding time of none more than 2 hours (16 hours for BMCs). These parameters were chosen as we wanted 1) to minimize or prevent the inclusion of cells undergoing senescence, 2) to minimize the influence of the *in vitro* culture environment by minimizing the time in culture, and 3) to limit the number other cell types in our cultures (i.e., non-fibroblast cells and non-VICs). Protocol steps that were empirically established included: duration of enzymatic digestion, enzymes used for tissue digestion, seeding method and initial duration of cell seeding.

The majority of previous studies that investigated porcine VICs *in vitro* performed a 1-6 hour digestion (299-301). However, we found that this length of time was too short and that an overnight digestion resulted in a markedly higher yield. One exception was the BMCs, which were extracted via physical disaggregation and therefore did not required enzymatic digestion. The discrepancy regarding the duration of tissue digestion could be accounted for by the age of

the donors, as older animals have increased matrix protein content and extensive matrix formation. Tissue with a higher percentage of ECM proteins may require a longer exposure to enzymes for sufficient matrix breakdown. Another consideration is the passage number used in our experimental designs versus other studies. The majority of studies studying VICs use P3-P6 cell cultures (240, 302, 303). As our experiments required P0 cell cultures (i.e., we could not expand our cell cultures to increase yield), we had to extract as many cells as possible directly from the tissue to ensure sufficient starting material for our cell cultures. Amongst methods for isolating VICs from valve leaflets, there was substantial variability within the literature regarding the enzymes employed for cellular liberation. Some methods involved the use of collagenase III and dispase II for VIC liberation, whereas others used deoxyribonuclease (DNAse) and hyaluronidase (299, 300). Our lab found did not test collagenase type III, but we found that collagenase type II alone worked quite well and that there was no notable difference when dispase II was included. In addition, we also found that neither DNAse nor hyaluronidase made any noticeable difference to VIC liberation from the leaflets; therefore these enzymes were not included in subsequent isolations. Furthermore, most published methods for culturing porcine VICs include a brief (~10 min) pre-digestion to remove valvular endothelial cells (VECs) (300, 301). Although this was tested in our lab, pre-digestion proved to be redundant as any endothelial contamination was excluded in the subsequent seeding and rinsing steps.

Although we found that the addition of dispase II did not substantially increase the number of VICs extracted from the leaflets, dispase II did markedly increase cellular liberation from the skin tissue. Although several methods for isolating dermal fibroblasts recorded a 24 hour digestion with dispase II alone, we found that a 16 hour (or overnight) digestion with dispase II, along with collagenase II, on tissue that was minced into 2x2x1 mm pieces was sufficient (299,

304, 305). Previous methods for epidermal cell liberation have used 0.2-0.25% trypsin for digestion – this was not examined by our lab (306).

Not all published methods for isolating VICs and dermal fibroblasts involved enzymatic digestion. A direct explant method for culturing either porcine VICs and dermal fibroblasts has been reported (307). Our lab tested the efficacy of culturing dermal fibroblasts using this method and although we were successful in growing colonies of cells, we ultimately opted for enzymatic digestion as we required a method that facilitated an even distribution of cells that would consistently reach 60-70% with 48-72 hours. We did not evaluate the direct explant method with VICs (or atrial fibroblasts) as we anticipated similar issues.

To determine the amount of tissue required to grow our cultures we used trial and error. We opted to not use cell counting as a method for determining how many cells to use for cell seeding as the tissue sample is a heterogeneous mixture of a number of cell types. We recognize that a superior method could include a cell sorting step via flow cytometry to exclude non-fibroblast-like cells followed by cell counting. However, this was not available to us, nor would it have been efficient given our experiment design.

By optimizing our cell cultures methods, we were able to consistently culture porcine VICs, A-fibs, D-fibs and BMCs that were evenly distributed and reached 60-70% confluency 48-72 hours, (or 5-6 days for BMCs).

5.2. Cell culture using pre-fabricated, compliant, silicone-based substrates

Prior to use for *in vitro* cell culture, the pre-fabricated, compliant, silicone-based matrices required a fibronectin coating prior to use. The fibronectin coating increased the adhesivity of the dishes; therefore, seeding times had to be adjusted to optimize cell purity and culture density. We found that an initial seeding time of one hour was adequate for the A-fibs and D-fibs, whereas the VICs required a slightly longer seeding time of two hours, and the BMCs needed to be left overnight. Cellular debris commonly stuck to the fibronectin coating; therefore, additional rinse steps were often required to remove excess debris. A disadvantage to using the compliant, silicone dishes was that cells could not be removed from the plate via scraping. This meant that the collection of cellular lysates demanded the use of trypsin, which could affect cellular gene expression.

5.3. VICs as unique mesenchymal cells

The identity of VICs has long been debated. VICs were previously regarded as a fibroblast with smooth muscle-like characteristics as they demonstrated several phenotypic qualities similar to both fibroblasts and SMCs (203, 227). However, more recently it has been accepted that VICs are a unique cell type that have the ability to activate or differentiate into various phenotypes (i.e. myofibroblast-like and osteoblast-like) (237). Previous studies have shown that VICs in a non-activated state have an elongated, spindle-like morphology, similar to cardiac and dermal fibroblasts (126). Although our cell cultures showed similar trends, we noticed marked differences between the VICs and the A-fibs. We found that the A-fibs appeared to have larger

cell bodies, which more closely resembled a cuboidal/cobblestone appearance, as opposed to a spindle-shaped appearance. VICs, D-fibs and BMCs all exhibited a spindle-shaped cell body with elongated cellular processes, although the BMCs were visibly smaller in size as compared to the VICs and D-fibs.

We also compared the expression of fibroblast and bone marrow progenitor cell markers, between the cell types. All of our experiments included a secondary antibody control to assess the presence of false positive staining, such that we could be confident that any staining we observed was indicative of true protein-antibody binding (i.e. positive protein expression). As expected, both α-SMA and vimentin were expressed in all cell types (228). Although α-SMA staining was weak, some long straight filaments could still be observed. While the cells exhibited a web-like pattern of vimentin, we expected a stronger immunofluorescent signal. However, since all cell-types exhibited weak vimentin staining this could be attributed to efficiency of the antibody. While previous studies have shown that a small percentage of VICs may express low levels of desmin in a diffuse arrangement, this was not observed by our lab. None of our cell cultures, including the VIC cultures exhibited desmin expression. This discrepancy may be due to the difference in passage number used to performed these experiments. Whereas our lab used P1 cells to perform the immunocytochemical analysis, to our knowledge all previous studies used cells isolated from passages 3-6, or higher (300-303). This large difference in passage number could account for discrepancies in protein expression. Discoidin domain receptor II (DDR2), a known marker for fibroblasts, its expression was observed in all cell types (308).

Periostin is a secreted extracellular matrix protein and is commonly used as a marker for fibroblasts (308). It is also found in the mature post-natal heart and is constitutively expressed at

low levels by VICs (309). Periostin is expressed in high levels during valvulogenesis and is vital to embryonic valve development (310, 311). Homozygous deletion of periostin results in serve malformation of the aortic valve and formation of calcific nodules (312). Studies have also shown that periostin expression is increased in the event of aortic valve disease and that elevated levels of periostin in the post-natal heart promotes fibrocalcific remodeling, whereas deletion of periostin attenuates pathological hypertrophy and cardiac remodeling cause by pressure overload (313). We observed periostin staining in the atrial fibroblasts and dermal fibroblasts alone, suggesting that the VICs in culture were not in an activated state. However, VICs stained strongly for OPN – as did BMCs, albeit only weakly. As the VIC cultures stained only weakly for α-SMA, but strongly for OPN, this suggests that our cell cultures were undergoing osteogenic differentiation due to presence of pro-osteogenic factors in the media, rather than through cellular activation. Neither A-fibs nor D-fibs stained positive for osteopontin, suggesting that fibroblasts differ from VICs in their response to factors in the cell culture media.

Kit, a marker for progenitor cells, was present in both BMCs and VICs. Positive staining for VICs has been previously observed and supports the suggestion that circulating progenitor cells replenish VICs.

5.4. Substrate modulus as a regulator of cellular phenotype

It has been well established that cells respond to environmental cues, including mechanical tension (314-318). As such, culturing cells on hard plastic dishes creates an environment that fails to mimic physiological compliance. Stiff substrates have been shown to cause cell

activation and modulate gene expression, whereas biomimetic substrates arrest cells in a physiological, quiescent state (319). To demonstrate this, previous studies have primarily used soft hydrogels and or various in house polymeric compounds (320-324). Our lab sought to investigate the efficacy of pre-fabricated, compliant, silicone-based culture dishes to mitigate cellular activation. To demonstrate this we recorded changes in cellular morphology and α-SMA expression. Congruent with previous studies, VICs and fibroblasts that were cultured on compliant substrates that had a spindle-like morphology, whereas those plated on the stiffer matrices had a cobblestone/cuboidal shape. The softer substrates also reduced α-SMA expression and maintained depressed levels over passage (P0-P1). This finding indicates that cells may be expanded and undergo serial passage without overt activation by using these prefabricated, biomimetic substrates. This may be important in the application of tissue engineering heart valves, in order to grow large numbers of donor cells without causing cellular activation and pathological differentiation.

5.5. NOTCH signaling as a potential regulator of VIC phenotype

We sought to compare the transcriptome of VICs to A-fibs, D-fibs and BMCs and examine any differences of expression in key regulatory pathways that may influence VIC phenotype. The results from our microarray demonstrated significant differences in gene expression of several NOTCH signaling targets, most notably *HEY1* and *HEY2*. NOTCH is an intercellular signaling pathway that is involved in cell fate determination and if left unregulated can lead to oncogenesis (271, 284). It has been well established that this pathway is a key regulator in valvulogenesis and mutations in this gene have been linked to inherited cardiovascular deformities, including

congenital bicuspid valve disease (276, 287, 295, 325-329). More recently, it has been observed that dysfunctional NOTCH leads to VIC osteogenesis and promotes fibrocalcific remodeling in the heart (283, 330). Furthermore, constitutive expression of NOTCH1 in the post-natal heart abrogates the expression of cardiac muscle proteins, such as sarcomeric myosin heavy chain and alpha-actin (331). This suggests that NOTCH may be an important regulator of the VIC phenotype.

Two key downstream targets of NOTCH are HEY1 and HEY2. We found significant differences in *HEY1/HEY2* RNA levels in VICs as compared to fibroblasts. VICs demonstrated markedly higher *HEY2* RNA levels in comparison to cardiac and dermal fibroblasts, whereas dermal fibroblasts had significantly higher levels of *HEY1*. This apparent reciprocal relationship in *HEY1/HEY2* gene expression amongst cell types is of interest. We do recognize, however, that a limitation to our analysis is that all data is reported in relative abundance, not absolute abundance. Therefore, our data may present exaggerated results that are not physiologically relevant. In addition, based on our results we cannot conclude whether the differences in RNA levels amongst cell types is a result of increased or decreased gene expression or due to differences in mRNA stability. Methods including kinetic labeling techniques and transcriptional inhibitors can measure the rate of mRNA decay (332, 333). Similarly, transcriptional pulsing methods such as those based on the *c-fos* inducible promoter and the tetracycline regulated (tet-off) promoter systems can also measure mRNA stability (334). Such experiments would complement our RT-qPCR data. We also acknowledge that our data only provides information for a singular time-point. As such, time course experiments would have provided information regarding relative gene expression over an extended period of time. In addition, while quantitative analysis of relative RNA abundance does provide insight into gene regulation and

may accurately reflect relative protein abundance, we cannot rule-out the possibility of discordant protein and mRNA expression. Unfortunately, we were unable to acquire meaningful data on the relative HEY1 and HEY2 protein levels across cell types via Western blotting, and were unable to pursue alternative methods for protein detection, such as LC/MS/MS. Therefore, without having qualitative data describing relative protein expression, our analysis is limited. Furthermore, studies that investigate HEY1 and HEY2 activity would provide a greater understanding as to the potential functional differences between tissue types in regards to NOTCH/HEY regulation. For example, as HEY 1 and 2 are transcription factors, cellular localization studies establishing differences in regional distribution HEY1 and HEY2 between tissues would be valuable, (however, this technique also requires the use of antibodies). In addition, transcription factor activity assays (e.g., luciferase assays) could be used to measure functional differences in HEY1 and 2 activity between tissue types. These experiments are critical as relative differences in HEY gene expression may not result in physiological differences.

While HEY1 and HEY2 are downstream targets of NOTCH, other signaling pathways may also control expression of these genes in VICs. One study investigating the Organ of Corti has shown that FGF can regulate HEY2 independent of NOTCH signaling (335). Furthermore HES, another downstream target of canonical NOTCH signaling, can also be regulated by pathways other than NOTCH, including: hedgehog, FGF, WNT and STAT. As our results showed that HES1 expression did not differ significantly between cell types and we suggest that the discrepancy in *HEY1* and *HEY2* expression seen across donor cell types may be independent of NOTCH signaling. Unfortunately, due to limitations with the Affymetrix GeneChip Porcine Genome 2.0 microarray, the array did not have other downstream targets of NOTCH1; therefore,

we did not pursue RT-qPCR analysis of NOTCH1. However, further gene analysis targeting *NOTCH1* would likely provide insight as to whether differential expression of HEY proteins is NOTCH mediated. We also observed trends of varying expression of *RBPJ* across cell types, with A-fibs expressing significantly more *RBPJ* than BMCs. Whether this difference has physiological downstream effects is unknown and further tests would be required to elucidate this. As NOTCH activation can affect cell lineage, it may be reasonable to assume that changes in signaling may have a greater effect on the less differentiated and more plastic BMCs (276).

VECs play an important role in regulating VIC phenotype and differentiation (242). Co-culture with VECs has been shown to reduce VIC activation and osteogenic differentiation (242). This paracrine effect is the result of VEC nitric oxide secretion mediating VIC NOTCH1 signaling. Increased NOTCH signaling leading to an upregulation in HEY1/HEY2 expression, which subsequently causes a repression of osteogenic transcription factors BMP-2 and TBX2 (289). Co-culturing effects were abolished via NG-nitro-L-arginine methyl ester (L-NAME), a known NO inhibitor (289, 336). Further investigations showed that inhibition of soluble guanylyl cyclase (sGC) also inhibited VEC effects on VIC activation (242). The cell lysates used in our microarray and subsequent RT-qPCR experiments were derived from VIC cultures without VEC influence. Therefore, our results may oversimplify the complex signaling dynamics that occurs within the valve.

Culture conditions have also been reported to have an effect on cellular gene expression (329). One study reported that primary human endothelial cells exposed to fresh media (containing serum) for two hours had a robust increase in HEY1 and HEY2 expression, which lasted for up to 3 hours (329). Interestingly, concomitant upregulation of other NOTCH target

genes was not observed, and pretreatment of cells with soluble BMP receptors abrogated the increase in HEY protein expression (329). This suggests that factors in the media can induce non-canonical HEY1/HEY2 expression. As our method for collecting cellular lysates includes a trypsinization step, followed by neutralization with fresh media, the cell cultures used in our experiments were exposed to a brief period of serum prior to RNA extraction (less than 5 minutes). Although this is substantially less time than the study in question, we cannot dismiss that a brief exposure to serum may have affected the results if there are cell specific differences in response to serum exposure.

6. CONCLUSIONS

In summary, we have demonstrated the following:

- Successful *in vitro* culturing of porcine valvular interstitial cells, porcine atrial fibroblasts, porcine dermal fibroblasts, and porcine bone marrow-derived progenitor cells
- Porcine VICs express a number of fibroblast and progenitor cell markers, *in vitro*
- Cultured porcine VICs have a morphology similar to dermal fibroblasts and differentiated bone marrow-derived progenitor cells
- Reduced substrate modulus mitigates activation of primary cultured porcine VICs, A-fibs, D-fibs and BMCs
- Reduced substrate modulus maintains a quiescent state in cultured atrial fibroblasts over passage (P0 to P1).
- Stiffer substrates may promote increased cell size and an activated phenotype, in a dose dependent manner
- Porcine VICs, A-fibs, D-fibs and BMCs share unique transcriptomic profiles
- VICs, A-fibs, D-fibs and BMCs have marked differences in NOTCH signaling pathway protein abundance: in particular *HEY1* and *HEY2*

These results provide evidence to support the suggestion that VICs share similarities to both atrial and dermal fibroblasts, as well as bone marrow-derived progenitor cells. Based on our analysis, VICs demonstrated the greatest similarity to differentiated BMCs.

7. SIGNIFICANCE & FUTURE DIRECTIONS

Despite the slow progression of calcific aortic valve disease, medical management of aortic stenosis remains a temporary measure and surgical replacement is the inevitable treatment for patients with severe AS (16, 78). Unfortunately, even with the advances in the design and materials used in aortic valve prostheses, these implants still have substantial limitations, most notably the dependence on anti-coagulant therapy and/or re-operation (57, 65). The development of a heart valve prosthesis that addresses these limitations is imperative. Tissue engineered heart valves are a promising solution; however, progress still needs to be made in regards to finding a suitable, patient autologous cellular alternative for VICs. The majority of research has focused on allogeneic progenitors as a source of cells for engraftment. While non-autologous sources may be more readily available in imminent cases, there is still the major drawback of allograft rejection (97). As aortic valve replacements are commonly elective procedures with a substantial preoperative window, presurgical harvest of autologous cells is a feasible option. The usage of the patient's own cells to recapitulate valve scaffolds would mitigate concerns of immunogenicity. Dermal fibroblasts and bone marrow-derived progenitor cells are readily available and can be harvested in large quantities with ease and relatively little risk to the patient. Similarly, atrial fibroblasts may be a promising source of cells; however harvesting these cells may be more challenging. As seen in previous studies, BMCs share similarities with VICs (337). Our observation was that BMCs cultured in fibroblast growth conditions most closely resembled VICs in regards to phenotypic characteristics and gene expression.

NOTCH signaling plays an important role in regulating VIC activation and may also be vital in providing VICs with their unique phenotype. Our results suggest that the differential

expression of downstream NOTCH target genes, HEY1 and HEY2, may be in part responsible for the uniqueness of VIC characteristics. Based on our preliminary studies, we were unable to determine if the differences in expression were mediated by NOTCH. Therefore, further studies, including RT-qPCR studies examining the expression of *NOTCH1,* as well as putative NOTCH-independent regulators of HEY proteins, such as *WNT, STAT, FGF* and *hedgehog,* are warranted.

In addition, targeting genes downstream of HEY2, such as BMP, RUNX2 and TBX2, or performing a chromatin immunoprecipitation assay to discover HEY2 DNA- or promoter binding sites, may provide insight to the downstream effects of elevated HEY2 expression in VICs. Creating a HEY2 adenoviral vector to synthetically elevate HEY2 expression in BMC, A-fibs and D-fibs, followed by similar characterization studies would be a natural progression towards determining the effects of HEY2 on cellular phenotype. Finally, we only targeted one regulatory pathway from the vast amount of microarray data collected. A more thorough examination of the data set and investigation into other regulatory pathways would likely yield other pathways governing VIC cell fate and novel hypotheses surrounding the issue of valvular tissue engineering.

REFERENCES

1. Silver MA, Roberts WC. Detailed anatomy of the normally functioning aortic valve in hearts of normal and increased weight. Am J Cardiol. 1985;55:454-61.

2. Hutcheson JD, Goettsch C, Rogers MA, Aikawa E. Revisiting cardiovascular calcification: A multifaceted disease requiring a multidisciplinary approach. Semin Cell Dev Biol. 2015;46:68-77.

3. Gross L, Kugel MA. Topographic anatomy and histology of the valve in the human heart. Am J Pathol. 1931;7(5):445-74.

4. Sacks MS, Yoganathan AP. Heart valve function: a biomechanical perspective. Philos Trans R Soc Lond B Biol Sci. 2007;362(1484):1369-91.

5. Buchanan RM, Sacks MS. Interlayer micromechanics of the aortic heart valve leaflet. Biomech Model Mechanobiol. 2014;13(4):813-26.

6. Schoen FJ, Levy RJ, Piehler HR. Pathological considerations in replacement cardiac valves. Cardiovasc Pathol. 1992;1(1):29-52.

7. Sacks MS, Smith DB, Hiester ED. The aortic valve microstructure: effects of transvalvular pressure. J Biomed Mater Res. 1998;41(1):131-41.

8. Tseng H, Grande-Allen KJ. Elastic fibers in the aortic valve spongiosa: a fresh perspective on its structure and role in overall tissue function. Acta Biomater. 2011;7(5):2101-8.

9. Scott M, Vesely I. Aortic valve cusp microstructure: the role of elastin. Ann Thorac Surg. 1995;60(2 Suppl):S391-4.

10. Stephens EH, Chu CK, Grande-Allen KJ. Valve proteoglycan content and glycosaminoglycan fine structure are unique to microstructure, mechanical load and age: Relevance to an age-specific tissue-engineered heart valve. Acta Biomater. 2008;4(5):1148-60.

11. Leopold JA. Cellular mechanisms of aortic valve calcification. Circ Cardiovasc Interv. 2012;5(4):605-14.

12. Rajamannan NM, Evans FJ, Aikawa E, Grande-Allen KJ, Demer LL, Heistad DD, et al. Calcific aortic valve disease: not simply a degenerative process: A review and agenda for research from the National Heart and Lung and Blood Institute Aortic Stenosis Working Group. Executive summary: Calcific aortic valve disease-2011 update. Circulation. 2011;124(16):1783-91.

13. Jelinek VM, McDonald IG, Hale GS. Haemodynamic basis for aortic valve replacement. Br Heart J. 1974;36(1):69-76.

14. Nishimura RA, Otto CM, Bonow RO, Carabello BA, Erwin JP, 3rd, Guyton RA, et al. 2014 AHA/ACC guideline for the management of patients with valvular heart disease: executive

summary: a report of the American College of Cardiology/American Heart Association Task Force on Practice Guidelines. J Am Coll Cardiol. 2014;63(22):2438-88.

15. Czarny MJ, Resar JR. Diagnosis and management of valvular aortic stenosis. Clin Med Insights Cardiol. 2014;8(Suppl 1):15-24.

16. Taniguchi T, Morimoto T, Shiomi H, Ando K, Kanamori N, Murata K, et al. Initial Surgical Versus Conservative Strategies in Patients With Asymptomatic Severe Aortic Stenosis. J Am Coll Cardiol. 2015;66(25):2827-38.

17. Mathieu P, Boulanger MC. Basic mechanisms of calcific aortic valve disease. Can J Cardiol. 2014;30(9):982-93.

18. Thaden JJ, Nkomo VT, Enriquez-Sarano M. The global burden of aortic stenosis. Prog Cardiovasc Dis. 2014;56(6):565-71.

19. Iung B, Vahanian A. Epidemiology of acquired valvular heart disease. Can J Cardiol. 2014;30(9):962-70.

20. Pasipoularides A. Calcific Aortic Valve Disease: Part 1-Molecular Pathogenetic Aspects, Hemodynamics, and Adaptive Feedbacks. J Cardiovasc Transl Res. 2016.

21. Pohle K, Maffert R, Ropers D, Moshage W, Stilianakis N, Daniel WG, et al. Progression of aortic valve calcification: association with coronary atherosclerosis and cardiovascular risk factors. Circulation. 2001;104(16):1927-32.

22. Lindroos M, Kupari M, Valvanne J, Strandberg T, Heikkila J, Tilvis R. Factors associated with calcific aortic valve degeneration in the elderly. Eur Heart J. 1994;15(7):865-70.

23. Iivanainen AM, Lindroos M, Tilvis R, Heikkila J, Kupari M. Calcific degeneration of the aortic valve in old age: is the development of flow obstruction predictable? J Intern Med. 1996;239(3):269-73.

24. Bonow RO, Leon MB, Doshi D, Moat N. Management strategies and future challenges for aortic valve disease. Lancet. 2016;387(10025):1312-23.

25. Abdelbaky A, Corsini E, Figueroa AL, Subramanian S, Fontanez S, Emami H, et al. Early aortic valve inflammation precedes calcification: a longitudinal FDG-PET/CT study. Atherosclerosis. 2015;238(2):165-72.

26. Fernandez-Pisonero I, Lopez J, Onecha E, Duenas AI, Maeso P, Crespo MS, et al. Synergy between sphingosine 1-phosphate and lipopolysaccharide signaling promotes an inflammatory, angiogenic and osteogenic response in human aortic valve interstitial cells. PLoS One. 2014;9(9):e109081.

27. Yutzey KE, Demer LL, Body SC, Huggins GS, Towler DA, Giachelli CM, et al. Calcific aortic valve disease: a consensus summary from the Alliance of Investigators on Calcific Aortic Valve Disease. Arterioscler Thromb Vasc Biol. 2014;34(11):2387-93.

28. Guerraty MA, Chai B, Hsu JY, Ojo AO, Gao Y, Yang W, et al. Relation of aortic valve calcium to chronic kidney disease (from the Chronic Renal Insufficiency Cohort Study). Am J Cardiol. 2015;115(9):1281-6.

29. Islam AK, Majumder AA. Rheumatic fever and rheumatic heart disease in Bangladesh: A review. Indian Heart J. 2016;68(1):88-98.

30. Moloi AH, Watkins D, Engel ME, Mall S, Zuhlke L. Epidemiology, health systems and stakeholders in rheumatic heart disease in Africa: a systematic review protocol. BMJ Open. 2016;6(5):e011266.

31. Carapetis JR. Rheumatic heart disease in developing countries. N Engl J Med. 2007;357(5):439-41.

32. Roth GA, Huffman MD, Moran AE, Feigin V, Mensah GA, Naghavi M, et al. Global and regional patterns in cardiovascular mortality from 1990 to 2013. Circulation. 2015;132(17):1667-78.

33. Roberts KV, Maguire GP, Brown A, Atkinson DN, Remenyi B, Wheaton G, et al. Rheumatic heart disease in Indigenous children in northern Australia: differences in prevalence and the challenges of screening. Med J Aust. 2015;203(5):221 e1-7.

34. Gordon J, Kirlew M, Schreiber Y, Saginur R, Bocking N, Blakelock B, et al. Acute rheumatic fever in First Nations communities in northwestern Ontario: Social determinants of health "bite the heart". Can Fam Physician. 2015;61(10):881-6.

35. Entezari P, Schnell S, Mahadevia R, Malaisrie C, McCarthy P, Mendelson M, et al. From unicuspid to quadricuspid: influence of aortic valve morphology on aortic three-dimensional hemodynamics. J Magn Reson Imaging. 2014;40(6):1342-6.

36. Mookadam F, Thota VR, Garcia-Lopez AM, Emani UR, Alharthi MS, Zamorano J, et al. Unicuspid aortic valve in adults: a systematic review. J Heart Valve Dis. 2010;19(1):79-85.

37. Vallely MP, Semsarian C, Bannon PG. Management of the ascending aorta in patients with bicuspid aortic valve disease. Heart Lung Circ. 2008;17(5):357-63.

38. Siu SC, Silversides CK. Bicuspid aortic valve disease. J Am Coll Cardiol. 2010;55(25):2789-800.

39. Braverman AC, Guven H, Beardslee MA, Makan M, Kates AM, Moon MR. The bicuspid aortic valve. Curr Probl Cardiol. 2005;30(9):470-522.

40. Bekeredjian R, Grayburn PA. Valvular heart disease: aortic regurgitation. Circulation. 2005;112(1):125-34.

41. Lancellotti P, Tribouilloy C, Hagendorff A, Moura L, Popescu BA, Agricola E, et al. European Association of Echocardiography recommendations for the assessment of valvular regurgitation. Part 1: aortic and pulmonary regurgitation (native valve disease). Eur J Echocardiogr. 2010;11(3):223-44.

42. Ortiz JT, Shin DD, Rajamannan NM. Approach to the patient with bicuspid aortic valve and ascending aorta aneurysm. Curr Treat Options Cardiovasc Med. 2006;8(6):461-7.

43. Keane MG, Pyeritz RE. Medical management of Marfan syndrome. Circulation. 2008;117(21):2802-13.

44. Guiney TE, Davies MJ, Parker DJ, Leech GJ, Leatham A. The aetiology and course of isolated severe aortic regurgitation: a clinical, pathological, and echocardiographic study. Br Heart J. 1987;58(4):358-68.

45. Maurer G. Aortic regurgitation. Heart. 2006;92(7):994-1000.

46. Crawford MH, Durack DT. Clinical presentation of infective endocarditis. Cardiol Clin. 2003;21(2):159-66, v.

47. Bashore TM, Cabell C, Fowler V, Jr. Update on infective endocarditis. Curr Probl Cardiol. 2006;31(4):274-352.

48. Miro JM, del Rio A, Mestres CA. Infective endocarditis in intravenous drug abusers and HIV-1 infected patients. Infect Dis Clin North Am. 2002;16(2):273-95, vii-viii.

49. Olaison L, Pettersson G. Current best practices and guidelines. Indications for surgical intervention in infective endocarditis. Cardiol Clin. 2003;21(2):235-51, vii.

50. Petti CA, Fowler VG, Jr. Staphylococcus aureus bacteremia and endocarditis. Cardiol Clin. 2003;21(2):219-33, vii.

51. Thuny F, Grisoli D, Collart F, Habib G, Raoult D. Management of infective endocarditis: challenges and perspectives. Lancet. 2012;379(9819):965-75.

52. Wang A, Athan E, Pappas PA, Fowler VG, Jr., Olaison L, Pare C, et al. Contemporary clinical profile and outcome of prosthetic valve endocarditis. JAMA. 2007;297(12):1354-61.

53. Moreillon P, Que YA. Infective endocarditis. Lancet. 2004;363(9403):139-49.

54. Genereux P, Head SJ, Wood DA, Kodali SK, Williams MR, Paradis JM, et al. Transcatheter aortic valve implantation 10-year anniversary: review of current evidence and clinical implications. Eur Heart J. 2012;33(19):2388-98.

55. Pibarot P, Dumesnil JG. Prosthetic heart valves: selection of the optimal prosthesis and long-term management. Circulation. 2009;119(7):1034-48.

56. Jaquiss RD. Bioprosthetic aortic valve replacement in the young: a cautionary tale. Circulation. 2014;130(1):7-9.

57. Cannegieter SC, Rosendaal FR, Briet E. Thromboembolic and bleeding complications in patients with mechanical heart valve prostheses. Circulation. 1994;89(2):635-41.

58. Ansell J, Hirsh J, Hylek E, Jacobson A, Crowther M, Palareti G, et al. Pharmacology and management of the vitamin K antagonists: American College of Chest Physicians Evidence-Based Clinical Practice Guidelines (8th Edition). Chest. 2008;133(6 Suppl):160S-98S.

59. Nutescu EA, Shapiro NL, Ibrahim S, West P. Warfarin and its interactions with foods, herbs and other dietary supplements. Expert Opin Drug Saf. 2006;5(3):433-51.

60. Wells PS, Holbrook AM, Crowther NR, Hirsh J. Interactions of warfarin with drugs and food. Ann Intern Med. 1994;121(9):676-83.

61. Wild D, Murray M, Donatti C. Patient perspectives on taking vitamin K antagonists: a qualitative study in the UK, USA and Spain. Expert Rev Pharmacoecon Outcomes Res. 2009;9(5):467-74.

62. Flint AC, Lingamneni R, Rao VA, Chan SL, Ren X, Pombra J, et al. Risks of Thrombosis and Rehemorrhage During Early Management of Intracranial Hemorrhage in Patients With Mechanical Heart Valves. J Am Coll Cardiol. 2015;66(15):1738-9.

63. Jaffer IH, Stafford AR, Fredenburgh JC, Whitlock RP, Chan NC, Weitz JI. Dabigatran is Less Effective Than Warfarin at Attenuating Mechanical Heart Valve-Induced Thrombin Generation. J Am Heart Assoc. 2015;4(8):e002322.

64. Ayad SW, Hassanein MM, Mohamed EA, Gohar AM. Maternal and Fetal Outcomes in Pregnant Women with a Prosthetic Mechanical Heart Valve. Clin Med Insights Cardiol. 2016;10:11-7.

65. Chan V, Malas T, Lapierre H, Boodhwani M, Lam BK, Rubens FD, et al. Reoperation of left heart valve bioprostheses according to age at implantation. Circulation. 2011;124(11 Suppl):S75-80.

66. Saleeb SF, Newburger JW, Geva T, Baird CW, Gauvreau K, Padera RF, et al. Accelerated degeneration of a bovine pericardial bioprosthetic aortic valve in children and young adults. Circulation. 2014;130(1):51-60.

67. Shinkawa T, Lu CK, Chipman C, Tang X, Gossett JM, Imamura M. The Midterm Outcomes of Bioprosthetic Pulmonary Valve Replacement in Children. Semin Thorac Cardiovasc Surg. 2015;27(3):310-8.

68. Kidane AG, Burriesci G, Cornejo P, Dooley A, Sarkar S, Bonhoeffer P, et al. Current developments and future prospects for heart valve replacement therapy. J Biomed Mater Res B Appl Biomater. 2009;88(1):290-303.

69. Singh V, Badheka AO, Patel SV, Patel NJ, Thakkar B, Patel N, et al. Comparison of Inhospital Outcomes of Surgical Aortic Valve Replacement in Hospitals With and Without Availability of a Transcatheter Aortic Valve Implantation Program (from a Nationally Representative Database). Am J Cardiol. 2015;116(8):1229-36.

70. Thyregod HG, Steinbruchel DA, Ihlemann N, Nissen H, Kjeldsen BJ, Petursson P, et al. Transcatheter Versus Surgical Aortic Valve Replacement in Patients With Severe Aortic Valve

Stenosis: 1-Year Results From the All-Comers NOTION Randomized Clinical Trial. J Am Coll Cardiol. 2015;65(20):2184-94.

71. Mack MJ, Leon MB, Smith CR, Miller DC, Moses JW, Tuzcu EM, et al. 5-year outcomes of transcatheter aortic valve replacement or surgical aortic valve replacement for high surgical risk patients with aortic stenosis (PARTNER 1): a randomised controlled trial. Lancet. 2015;385(9986):2477-84.

72. Kamperidis V, Delgado V, van Mieghem NM, Kappetein AP, Leon MB, Bax JJ. Diagnosis and management of aortic valve stenosis in patients with heart failure. Eur J Heart Fail. 2016.

73. Ruparelia N, Latib A, Buzzatti N, Giannini F, Figini F, Mangieri A, et al. Long-Term Outcomes After Transcatheter Aortic Valve Implantation from a Single High-Volume Center (The Milan Experience). Am J Cardiol. 2016;117(5):813-9.

74. Walther T, Hamm CW, Schuler G, Berkowitsch A, Kotting J, Mangner N, et al. Perioperative Results and Complications in 15,964 Transcatheter Aortic Valve Replacements: Prospective Data From the GARY Registry. J Am Coll Cardiol. 2015;65(20):2173-80.

75. Al-Halees Z, Pieters F, Qadoura F, Shahid M, Al-Amri M, Al-Fadley F. The Ross procedure is the procedure of choice for congenital aortic valve disease. J Thorac Cardiovasc Surg. 2002;123(3):437-41; discussion 41-2.

76. Mookhoek A, Charitos EI, Hazekamp MG, Bogers AJ, Horer J, Lange R, et al. Ross Procedure in Neonates and Infants: A European Multicenter Experience. Ann Thorac Surg. 2015;100(6):2278-84.

77. Blanchart K, Buklas D, Labombarda F. Restrictive Physiology of Right Ventricle after Ross Procedure. Echocardiography. 2016;33(1):162-3.

78. Bonow RO. Asymptomatic Aortic Stenosis: It Is Not Simple Anymore. J Am Coll Cardiol. 2015;66(25):2839-41.

79. Langer R, Vacanti JP. Tissue engineering. Science. 1993;260(5110):920-6.

80. Arenas-Herrera JE, Ko IK, Atala A, Yoo JJ. Decellularization for whole organ bioengineering. Biomed Mater. 2013;8(1):014106.

81. Langer R, Vacanti J. Advances in tissue engineering. J Pediatr Surg. 2016;51(1):8-12.

82. Weber B, Emmert MY, Hoerstrup SP. Stem cells for heart valve regeneration. Swiss Med Wkly. 2012;142:w13622.

83. Kulig KM, Vacanti JP. Hepatic tissue engineering. Transpl Immunol. 2004;12(3-4):303-10.

84. Davis MW, Vacanti JP. Toward development of an implantable tissue engineered liver. Biomaterials. 1996;17(3):365-72.

85. Simaioforidis V, de Jonge P, Sloff M, Oosterwijk E, Geutjes P, Feitz WF. Ureteral tissue engineering: where are we and how to proceed? Tissue Eng Part B Rev. 2013;19(5):413-9.

86. Arealis G, Nikolaou VS. Bone printing: new frontiers in the treatment of bone defects. Injury. 2015;46 Suppl 8:S20-2.

87. Camarero-Espinosa S, Rothen-Rutishauser B, Foster EJ, Weder C. Articular cartilage: from formation to tissue engineering. Biomater Sci. 2016.

88. Pecha S, Eschenhagen T, Reichenspurner H. Myocardial tissue engineering for cardiac repair. J Heart Lung Transplant. 2016;35(3):294-8.

89. Khademhosseini A, Langer R, Borenstein J, Vacanti JP. Microscale technologies for tissue engineering and biology. Proc Natl Acad Sci U S A. 2006;103(8):2480-7.

90. Jana S, Lerman A. Bioprinting a cardiac valve. Biotechnol Adv. 2015;33(8):1503-21.

91. Kheradvar A, Groves EM, Dasi LP, Alavi SH, Tranquillo R, Grande-Allen KJ, et al. Emerging trends in heart valve engineering: Part I. Solutions for future. Ann Biomed Eng. 2015;43(4):833-43.

92. Namiri M, Ashtiani MK, Mashinchian O, Hasani-Sadrabadi MM, Mahmoudi M, Aghdami N, et al. Engineering natural heart valves: possibilities and challenges. J Tissue Eng Regen Med. 2016.

93. Neuenschwander S, Hoerstrup SP. Heart valve tissue engineering. Transpl Immunol. 2004;12(3-4):359-65.

94. Syedain ZH, Bradee AR, Kren S, Taylor DA, Tranquillo RT. Decellularized tissue-engineered heart valve leaflets with recellularization potential. Tissue Eng Part A. 2013;19(5-6):759-69.

95. Jana S, Tefft BJ, Spoon DB, Simari RD. Scaffolds for tissue engineering of cardiac valves. Acta Biomater. 2014;10(7):2877-93.

96. Simon P, M.T. K, Ried E, Weigel G. Tissue engineering of heart valves-Immunologic and inflammatory challenges of the allograft. Prog Pediatr Cardiol. 2006;21(2):161-65.

97. Badylak SF, Taylor D, Uygun K. Whole-organ tissue engineering: decellularization and recellularization of three-dimensional matrix scaffolds. Annu Rev Biomed Eng. 2011;13:27-53.

98. Badylak SF. Xenogeneic extracellular matrix as a scaffold for tissue reconstruction. Transpl Immunol. 2004;12(3-4):367-77.

99. Manji RA, Lee W, Cooper DK. Xenograft bioprosthetic heart valves: Past, present and future. Int J Surg. 2015;23(Pt B):280-4.

100. Gilbert TW, Sellaro TL, Badylak SF. Decellularization of tissues and organs. Biomaterials. 2006;27(19):3675-83.

101. Manji RA, Menkis AH, Ekser B, Cooper DK. Porcine bioprosthetic heart valves: The next generation. Am Heart J. 2012;164(2):177-85.

102. Badylak SF, Gilbert TW. Immune response to biologic scaffold materials. Semin Immunol. 2008;20(2):109-16.

103. Choi SY, Jeong HJ, Lim HG, Park SS, Kim SH, Kim YJ. Elimination of alpha-gal xenoreactive epitope: alpha-galactosidase treatment of porcine heart valves. J Heart Valve Dis. 2012;21(3):387-97.

104. Lim HG, Kim GB, Jeong S, Kim YJ. Development of a next-generation tissue valve using a glutaraldehyde-fixed porcine aortic valve treated with decellularization, alpha-galactosidase, space filler, organic solvent and detoxification. Eur J Cardiothorac Surg. 2015;48(1):104-13.

105. Lila N, McGregor CG, Carpentier S, Rancic J, Byrne GW, Carpentier A. Gal knockout pig pericardium: new source of material for heart valve bioprostheses. J Heart Lung Transplant. 2010;29(5):538-43.

106. McGregor CG, Carpentier A, Lila N, Logan JS, Byrne GW. Cardiac xenotransplantation technology provides materials for improved bioprosthetic heart valves. J Thorac Cardiovasc Surg. 2011;141(1):269-75.

107. Wilczek P, Lesiak A, Niemiec-Cyganek A, Kubin B, Slomski R, Nozynski J, et al. Biomechanical properties of hybrid heart valve prosthesis utilizing the pigs that do not express the galactose-alpha-1,3-galactose (alpha-Gal) antigen derived tissue and tissue engineering technique. J Mater Sci Mater Med. 2015;26(1):5329.

108. Crapo PM, Gilbert TW, Badylak SF. An overview of tissue and whole organ decellularization processes. Biomaterials. 2011;32(12):3233-43.

109. Daly KA, Liu S, Agrawal V, Brown BN, Johnson SA, Medberry CJ, et al. Damage associated molecular patterns within xenogeneic biologic scaffolds and their effects on host remodeling. Biomaterials. 2012;33(1):91-101.

110. Bayrak A, Tyralla M, Ladhoff J, Schleicher M, Stock UA, Volk HD, et al. Human immune responses to porcine xenogeneic matrices and their extracellular matrix constituents in vitro. Biomaterials. 2010;31(14):3793-803.

111. Liao J, Joyce EM, Sacks MS. Effects of decellularization on the mechanical and structural properties of the porcine aortic valve leaflet. Biomaterials. 2008;29(8):1065-74.

112. Schenke-Layland K, Vasilevski O, Opitz F, Konig K, Riemann I, Halbhuber KJ, et al. Impact of decellularization of xenogeneic tissue on extracellular matrix integrity for tissue engineering of heart valves. J Struct Biol. 2003;143(3):201-8.

113. Zhou J, Fritze O, Schleicher M, Wendel HP, Schenke-Layland K, Harasztosi C, et al. Impact of heart valve decellularization on 3-D ultrastructure, immunogenicity and thrombogenicity. Biomaterials. 2010;31(9):2549-54.

114. Lanza R, Langer R, Vacanti J. Principles of Tissue Engineering. Academic Press: New York. 2011;3rd Edition.

115. Mandrycky C, Wang Z, Kim K, Kim DH. 3D bioprinting for engineering complex tissues. Biotechnol Adv. 2015.

116. Lueders C, Jastram B, Hetzer R, Schwandt H. Rapid manufacturing techniques for the tissue engineering of human heart valves. Eur J Cardiothorac Surg. 2014;46(4):593-601.

117. Seol YJ, Kang HW, Lee SJ, Atala A, Yoo JJ. Bioprinting technology and its applications. Eur J Cardiothorac Surg. 2014;46(3):342-8.

118. Murphy SV, Atala A. 3D bioprinting of tissues and organs. Nat Biotechnol. 2014;32(8):773-85.

119. Duan B, Hockaday LA, Kang KH, Butcher JT. 3D bioprinting of heterogeneous aortic valve conduits with alginate/gelatin hydrogels. J Biomed Mater Res A. 2013;101(5):1255-64.

120. Duan B, Hockaday LA, Kapetanovic E, Kang KH, Butcher JT. Stiffness and adhesivity control aortic valve interstitial cell behavior within hyaluronic acid based hydrogels. Acta Biomater. 2013;9(8):7640-50.

121. Duan B, Kapetanovic E, Hockaday LA, Butcher JT. Three-dimensional printed trileaflet valve conduits using biological hydrogels and human valve interstitial cells. Acta Biomater. 2014;10(5):1836-46.

122. Murphy SV, Skardal A, Atala A. Evaluation of hydrogels for bio-printing applications. J Biomed Mater Res A. 2013;101(1):272-84.

123. Jiang Y, Chen J, Deng C, Suuronen EJ, Zhong Z. Click hydrogels, microgels and nanogels: emerging platforms for drug delivery and tissue engineering. Biomaterials. 2014;35(18):4969-85.

124. Mosadegh B, Xiong G, Dunham S, Min JK. Current progress in 3D printing for cardiovascular tissue engineering. Biomed Mater. 2015;10(3):034002.

125. Argento G, Simonet M, Oomens CW, Baaijens FP. Multi-scale mechanical characterization of scaffolds for heart valve tissue engineering. J Biomech. 2012;45(16):2893-8.

126. Taylor PM, Batten P, Brand NJ, Thomas PS, Yacoub MH. The cardiac valve interstitial cell. Int J Biochem Cell Biol. 2003;35(2):113-8.

127. Capulli AK, MacQueen LA, Sheehy SP, Parker KK. Fibrous scaffolds for building hearts and heart parts. Adv Drug Deliv Rev. 2016;96:83-102.

128. Amoroso NJ, D'Amore A, Hong Y, Rivera CP, Sacks MS, Wagner WR. Microstructural manipulation of electrospun scaffolds for specific bending stiffness for heart valve tissue engineering. Acta Biomater. 2012;8(12):4268-77.

129. Courtney T, Sacks MS, Stankus J, Guan J, Wagner WR. Design and analysis of tissue engineering scaffolds that mimic soft tissue mechanical anisotropy. Biomaterials. 2006;27(19):3631-8.

130. Hobson CM, Amoroso NJ, Amini R, Ungchusri E, Hong Y, D'Amore A, et al. Fabrication of elastomeric scaffolds with curvilinear fibrous structures for heart valve leaflet engineering. J Biomed Mater Res A. 2015;103(9):3101-6.

131. Masoumi N, Larson BL, Annabi N, Kharaziha M, Zamanian B, Shapero KS, et al. Electrospun PGS:PCL microfibers align human valvular interstitial cells and provide tunable scaffold anisotropy. Adv Healthc Mater. 2014;3(6):929-39.

132. Fong P, Shin'oka T, Lopez-Soler RI, Breuer C. The use of polmer based scaffolds in tissue-engineered heart valves. Prog Pediatr Cardiol. 2006;21(2):193-9.

133. Masoumi N, Annabi N, Assmann A, Larson BL, Hjortnaes J, Alemdar N, et al. Tri-layered elastomeric scaffolds for engineering heart valve leaflets. Biomaterials. 2014;35(27):7774-85.

134. Masoumi N, Johnson KL, Howell MC, Engelmayr GC, Jr. Valvular interstitial cell seeded poly(glycerol sebacate) scaffolds: toward a biomimetic in vitro model for heart valve tissue engineering. Acta Biomater. 2013;9(4):5974-88.

135. Sant S, Hwang CM, Lee SH, Khademhosseini A. Hybrid PGS-PCL microfibrous scaffolds with improved mechanical and biological properties. J Tissue Eng Regen Med. 2011;5(4):283-91.

136. Sant S, Iyer D, Gaharwar AK, Patel A, Khademhosseini A. Effect of biodegradation and de novo matrix synthesis on the mechanical properties of valvular interstitial cell-seeded polyglycerol sebacate-polycaprolactone scaffolds. Acta Biomater. 2013;9(4):5963-73.

137. Tseng H, Puperi DS, Kim EJ, Ayoub S, Shah JV, Cuchiara ML, et al. Anisotropic poly(ethylene glycol)/polycaprolactone hydrogel-fiber composites for heart valve tissue engineering. Tissue Eng Part A. 2014;20(19-20):2634-45.

138. Hinderer S, Seifert J, Votteler M, Shen N, Rheinlaender J, Schaffer TE, et al. Engineering of a bio-functionalized hybrid off-the-shelf heart valve. Biomaterials. 2014;35(7):2130-9.

139. Eslami M, Vrana NE, Zorlutuna P, Sant S, Jung S, Masoumi N, et al. Fiber-reinforced hydrogel scaffolds for heart valve tissue engineering. J Biomater Appl. 2014;29(3):399-410.

140. Cebotari S, Lichtenberg A, Tudorache I, Hilfiker A, Mertsching H, Leyh R, et al. Clinical application of tissue engineered human heart valves using autologous progenitor cells. Circulation. 2006;114(1 Suppl):I132-7.

141. Colazzo F, Chester AH, Taylor PM, Yacoub MH. Induction of mesenchymal to endothelial transformation of adipose-derived stem cells. J Heart Valve Dis. 2010;19(6):736-44.

142. Colazzo F, Sarathchandra P, Smolenski RT, Chester AH, Tseng YT, Czernuszka JT, et al. Extracellular matrix production by adipose-derived stem cells: implications for heart valve tissue engineering. Biomaterials. 2011;32(1):119-27.

143. Duan B, Hockaday LA, Das S, Xu C, Butcher JT. Comparison of Mesenchymal Stem Cell Source Differentiation Toward Human Pediatric Aortic Valve Interstitial Cells within 3D Engineered Matrices. Tissue Eng Part C Methods. 2015;21(8):795-807.

144. Forsberg M, Hovatta O. Challenges for the Therapeutic use of Pluripotent Stem Derived Cells. Front Physiol. 2012;3:19.

145. Huang W, Xiao DZ, Wang Y, Shan ZX, Liu XY, Lin QX, et al. Fn14 promotes differentiation of human mesenchymal stem cells into heart valvular interstitial cells by phenotypic characterization. J Cell Physiol. 2014;229(5):580-7.

146. Sales VL, Mettler BA, Engelmayr GC, Jr., Aikawa E, Bischoff J, Martin DP, et al. Endothelial progenitor cells as a sole source for ex vivo seeding of tissue-engineered heart valves. Tissue Eng Part A. 2010;16(1):257-67.

147. Schmidt D, Mol A, Breymann C, Achermann J, Odermatt B, Gossi M, et al. Living autologous heart valves engineered from human prenatally harvested progenitors. Circulation. 2006;114(1 Suppl):I125-31.

148. Simpson DL, Wehman B, Galat Y, Sharma S, Mishra R, Galat V, et al. Engineering patient-specific valves using stem cells generated from skin biopsy specimens. Ann Thorac Surg. 2014;98(3):947-54.

149. Fahrenholtz MM, Liu H, Kearney D, L., Wadhwa L, Fraser CD, Grande-Allen KJ. Characterization of dermal fibroblasts as a cell source for pediatric tissue engineered heart valves. J Cardiovasc Dev Dis. 2014;1(2):146-62.

150. Maienschein J. Stem cell research: a target article collection: Part II--what's in a name: embryos, clones, and stem cells. Am J Bioeth. 2002;2(1):12-9, 30.

151. Reik W, Surani MA. Germline and Pluripotent Stem Cells. Cold Spring Harb Perspect Biol. 2015;7(11).

152. Caplan AI. What's in a name? Tissue Eng Part A. 2010;16(8):2415-7.

153. Siepe M, Akhyari P, Lichtenberg A, Schlensak C, Beyersdorf F. Stem cells used for cardiovascular tissue engineering. Eur J Cardiothorac Surg. 2008;34(2):242-7.

154. Puceat M. TGFbeta in the differentiation of embryonic stem cells. Cardiovasc Res. 2007;74(2):256-61.

155. Nury D, Neri T, Puceat M. Human embryonic stem cells and cardiac cell fate. J Cell Physiol. 2009;218(3):455-9.

156. Dickens BM, Cook RJ. Acquiring human embryos for stem-cell research. Int J Gynaecol Obstet. 2007;96(1):67-71.

157. Juengst E, Fossel M. The ethics of embryonic stem cells--now and forever, cells without end. JAMA. 2000;284(24):3180-4.

158. Menasche P, Vanneaux V, Fabreguettes JR, Bel A, Tosca L, Garcia S, et al. Towards a clinical use of human embryonic stem cell-derived cardiac progenitors: a translational experience. Eur Heart J. 2015;36(12):743-50.

159. Bellamy V, Vanneaux V, Bel A, Nemetalla H, Emmanuelle Boitard S, Farouz Y, et al. Long-term functional benefits of human embryonic stem cell-derived cardiac progenitors embedded into a fibrin scaffold. J Heart Lung Transplant. 2015;34(9):1198-207.

160. Behfar A, Zingman LV, Hodgson DM, Rauzier JM, Kane GC, Terzic A, et al. Stem cell differentiation requires a paracrine pathway in the heart. FASEB J. 2002;16(12):1558-66.

161. Chiu YN, Norris RA, Mahler G, Recknagel A, Butcher JT. Transforming growth factor beta, bone morphogenetic protein, and vascular endothelial growth factor mediate phenotype maturation and tissue remodeling by embryonic valve progenitor cells: relevance for heart valve tissue engineering. Tissue Eng Part A. 2010;16(11):3375-83.

162. Puceat M. Embryological origin of the endocardium and derived valve progenitor cells: from developmental biology to stem cell-based valve repair. Biochim Biophys Acta. 2013;1833(4):917-22.

163. Rivera-Feliciano J, Tabin CJ. Bmp2 instructs cardiac progenitors to form the heart-valve-inducing field. Dev Biol. 2006;295(2):580-8.

164. de Vries RB, Oerlemans A, Trommelmans L, Dierickx K, Gordijn B. Ethical aspects of tissue engineering: a review. Tissue Eng Part B Rev. 2008;14(4):367-75.

165. Dresser R. Ethical issues in embryonic stem cell research. JAMA. 2001;285(11):1439-40.

166. Zoeller K. Science and the lay perspective: lay people's involvement in assessing tissue engineering. Tissue Eng Part A. 2014;20(19-20):2561-6.

167. Guillot PV, Gotherstrom C, Chan J, Kurata H, Fisk NM. Human first-trimester fetal MSC express pluripotency markers and grow faster and have longer telomeres than adult MSC. Stem Cells. 2007;25(3):646-54.

168. J.R S, Pfeifer K, Petry F, Powell N, Delzeit J, Weiss ML. Standardizing umbilical cord mesenchymal stromal cells for translation to clinical use: selection of GMP-compliant medium and a simplified isolation method. Stem Cells Int. 2016;2016:1-14.

169. Bojic M, Worel N, Sperr WR, Schellongowski P, Wohlfarth P, Schwarzinger I, et al. Umbilical Cord Blood Transplantation Is a Feasible Rescue Therapeutic Option for Patients Suffering from Graft Failure after Previous Hematopoietic Stem Cell Transplantation. Oncology. 2016;90(3):160-6.

170. Lee HJ, Kang KS, Kang SY, Kim HS, Park SJ, Lee SY, et al. Immunologic properties of differentiated and undifferentiated mesenchymal stem cells derived from umbilical cord blood. J Vet Sci. 2015.

171. Perea-Gil I, Monguio-Tortajada M, Galvez-Monton C, Bayes-Genis A, Borras FE, Roura S. Preclinical evaluation of the immunomodulatory properties of cardiac adipose tissue progenitor cells using umbilical cord blood mesenchymal stem cells: a direct comparative study. Biomed Res Int. 2015;2015:439808.

172. Roura S, Pujal JM, Galvez-Monton C, Bayes-Genis A. Impant of umbilical cord blood-derived mesenchymal stem cells on cardiovascular research. Biomed Res Int. 2015;2015:1-6.

173. Sodian R, Schaefermeier P, Abegg-Zips S, Kuebler WM, Shakibaei M, Daebritz S, et al. Use of human umbilical cord blood-derived progenitor cells for tissue-engineered heart valves. Ann Thorac Surg. 2010;89(3):819-28.

174. Klimczak A, Kozlowska U. Mesenchymal Stromal Cells and Tissue-Specific Progenitor Cells: Their Role in Tissue Homeostasis. Stem Cells Int. 2016;2016:4285215.

175. Blau HM, Brazelton TR, Weimann JM. The evolving concept of a stem cell: entity or function? Cell. 2001;105(7):829-41.

176. Visconti RP, Ebihara Y, LaRue AC, Fleming PA, McQuinn TC, Masuya M, et al. An in vivo analysis of hematopoietic stem cell potential: hematopoietic origin of cardiac valve interstitial cells. Circ Res. 2006;98(5):690-6.

177. Iop L, Renier V, Naso F, Piccoli M, Bonetti A, Gandaglia A, et al. The influence of heart valve leaflet matrix characteristics on the interaction between human mesenchymal stem cells and decellularized scaffolds. Biomaterials. 2009;30(25):4104-16.

178. Kajbafzadeh AM, Ahmadi Tafti SH, Mokhber-Dezfooli MR, Khorramirouz R, Sabetkish S, Sabetkish N, et al. Aortic valve conduit implantation in the descending thoracic aorta in a sheep model: The outcomes of pre-seeded scaffold. Int J Surg. 2016;28:97-105.

179. Knight RL, Booth C, Wilcox HE, Fisher J, Ingham E. Tissue engineering of cardiac valves: re-seeding of acellular porcine aortic valve matrices with human mesenchymal progenitor cells. J Heart Valve Dis. 2005;14(6):806-13.

180. Ku CH, Johnson PH, Batten P, Sarathchandra P, Chambers RC, Taylor PM, et al. Collagen synthesis by mesenchymal stem cells and aortic valve interstitial cells in response to mechanical stretch. Cardiovasc Res. 2006;71(3):548-56.

181. Latif N, Sarathchandra P, Thomas PS, Antoniw J, Batten P, Chester AH, et al. Characterization of structural and signaling molecules by human valve interstitial cells and comparison to human mesenchymal stem cells. J Heart Valve Dis. 2007;16(1):56-66.

182. Nomura A, Seya K, Yu Z, Daitoku K, Motomura S, Murakami M, et al. CD34-negative mesenchymal stem-like cells may act as the cellular origin of human aortic valve calcification. Biochem Biophys Res Commun. 2013;440(4):780-5.

183. Rath S, Salinas M, Bhatacharjee S, Ramaswamy S. Marrow stem cell differentiation for valvulogenesis via oscillatory flow and nicotine agonists: unusual suspects? J Long Term Eff Med Implants. 2015;25(1-2):147-60.

184. Rath S, Salinas M, Villegas AG, Ramaswamy S. Differentiation and Distribution of Marrow Stem Cells in Flex-Flow Environments Demonstrate Support of the Valvular Phenotype. PLoS One. 2015;10(11):e0141802.

185. Tedder ME, Simionescu A, Chen J, Liao J, Simionescu DT. Assembly and testing of stem cell-seeded layered collagen constructs for heart valve tissue engineering. Tissue Eng Part A. 2011;17(1-2):25-36.

186. Throm Quinlan AM, Sierad LN, Capulli AK, Firstenberg LE, Billiar KL. Combining dynamic stretch and tunable stiffness to probe cell mechanobiology in vitro. PLoS One. 2011;6(8):e23272.

187. Vincentelli A, Wautot F, Juthier F, Fouquet O, Corseaux D, Marechaux S, et al. In vivo autologous recellularization of a tissue-engineered heart valve: are bone marrow mesenchymal stem cells the best candidates? J Thorac Cardiovasc Surg. 2007;134(2):424-32.

188. Yang Y, Fan C, Deng C, Zhao L, Hu W, Di S, et al. Melatonin reverses flow shear stress-induced injury in bone marrow mesenchymal stem cells via activation of AMP-activated protein kinase signaling. J Pineal Res. 2016;60(2):228-41.

189. Ye X, Zhao Q, Sun X, Li H. Enhancement of mesenchymal stem cell attachment to decellularized porcine aortic valve scaffold by in vitro coating with antibody against CD90: a preliminary study on antibody-modified tissue-engineered heart valve. Tissue Eng Part A. 2009;15(1):1-11.

190. Gomes-Alves P, Serra M, Brito C, Ricardo CP, Cunha R, Sousa MF, et al. In vitro expansion of human cardiac progenitor cells: exploring 'omics tools for characterization of cell-based allogeneic products. Transl Res. 2016.

191. Barile L, Messina E, Giacomello A, Marban E. Endogenous cardiac stem cells. Prog Cardiovasc Dis. 2007;50(1):31-48.

192. Bollini S, Smart N, Riley PR. Resident cardiac progenitor cells: at the heart of regeneration. J Mol Cell Cardiol. 2011;50(2):296-303.

193. Bulatovic I, Mansson-Broberg A, Sylven C, Grinnemo KH. Human fetal cardiac progenitors: The role of stem cells and progenitors in the fetal and adult heart. Best Pract Res Clin Obstet Gynaecol. 2016;31:58-68.

194. Drowley L, Koonce C, Peel S, Jonebring A, Plowright AT, Kattman SJ, et al. Human Induced Pluripotent Stem Cell-Derived Cardiac Progenitor Cells in Phenotypic Screening: A Transforming Growth Factor-beta Type 1 Receptor Kinase Inhibitor Induces Efficient Cardiac Differentiation. Stem Cells Transl Med. 2016;5(2):164-74.

195. Okita K, Yamanaka S. Induction of pluripotency by defined factors. Exp Cell Res. 2010;316(16):2565-70.

196. Takahashi K, Tanabe K, Ohnuki M, Narita M, Ichisaka T, Tomoda K, et al. Induction of pluripotent stem cells from adult human fibroblasts by defined factors. Cell. 2007;131(5):861-72.

197. Takahashi K, Yamanaka S. Induction of pluripotent stem cells from mouse embryonic and adult fibroblast cultures by defined factors. Cell. 2006;126(4):663-76.

198. Yamanaka S. A fresh look at iPS cells. Cell. 2009;137(1):13-7.

199. Drews K, Jozefczuk J, Prigione A, Adjaye J. Human induced pluripotent stem cells--from mechanisms to clinical applications. J Mol Med (Berl). 2012;90(7):735-45.

200. Yoshida Y, Yamanaka S. iPS cells: a source of cardiac regeneration. J Mol Cell Cardiol. 2011;50(2):327-32.

201. Zhang Y, Cao N, Huang Y, Spencer CI, Fu JD, Yu C, et al. Expandable Cardiovascular Progenitor Cells Reprogrammed from Fibroblasts. Cell Stem Cell. 2016;18(3):368-81.

202. Lalit PA, Salick MR, Nelson DO, Squirrell JM, Shafer CM, Patel NG, et al. Lineage Reprogramming of Fibroblasts into Proliferative Induced Cardiac Progenitor Cells by Defined Factors. Cell Stem Cell. 2016;18(3):354-67.

203. Mulholland DL, Gotlieb AI. Cell biology of valvular interstitial cells. Can J Cardiol. 1996;12(3):231-6.

204. Moore-Morris T, Cattaneo P, Puceat M, Evans SM. Origins of cardiac fibroblasts. J Mol Cell Cardiol. 2016;91:1-5.

205. Yau JW, Teoh H, Verma S. Endothelial cell control of thrombosis. BMC Cardiovasc Disord. 2015;15:130.

206. Abramochkin DV, Lozinsky IT, Kamkin A. Influence of mechanical stress on fibroblast-myocyte interactions in mammalian heart. J Mol Cell Cardiol. 2014;70:27-36.

207. Howard CM, Baudino TA. Dynamic cell-cell and cell-ECM interactions in the heart. J Mol Cell Cardiol. 2014;70:19-26.

208. Kohl P, Gourdie RG. Fibroblast-myocyte electrotonic coupling: does it occur in native cardiac tissue? J Mol Cell Cardiol. 2014;70:37-46.

209. Hellerstein HK. Endocardial pockets of left atrium. Am Heart J. 1947;34(5):751-7.

210. Park JH, Pak HN, Lee S, Park HK, Seo JW, Chang BC. The clinical significance of the atrial subendocardial smooth muscle layer and cardiac myofibroblasts in human atrial tissue with valvular atrial fibrillation. Cardiovasc Pathol. 2013;22(1):58-64.

211. Stollberger C, Schneider B, Finsterer J. Elimination of the left atrial appendage to prevent stroke or embolism? Anatomic, physiologic, and pathophysiologic considerations. Chest. 2003;124(6):2356-62.

212. Syed FF, DeSimone CV, Friedman PA, Asirvatham SJ. Left atrial appendage exclusion for atrial fibrillation. Cardiol Clin. 2014;32(4):601-25.

213. Syed TM, Halperin JL. Left atrial appendage closure for stroke prevention in atrial fibrillation: state of the art and current challenges. Nat Clin Pract Cardiovasc Med. 2007;4(8):428-35.

214. Yaghi S, Song C, Gray WA, Furie KL, Elkind MS, Kamel H. Left Atrial Appendage Function and Stroke Risk. Stroke. 2015;46(12):3554-9.

215. Romero J, Natale A, L DIB. Left Atrial Appendage Morphology and Physiology: "The Missing Piece in the Puzzle". J Cardiovasc Electrophysiol. 2015.

216. Beigel R, Wunderlich NC, Ho SY, Arsanjani R, Siegel RJ. The left atrial appendage: anatomy, function, and noninvasive evaluation. JACC Cardiovasc Imaging. 2014;7(12):1251-65.

217. Kamohara K, Popovic ZB, Daimon M, Martin M, Ootaki Y, Akiyama M, et al. Impact of left atrial appendage exclusion on left atrial function. J Thorac Cardiovasc Surg. 2007;133(1):174-81.

218. Bartus K, Han FT, Bednarek J, Myc J, Kapelak B, Sadowski J, et al. Percutaneous left atrial appendage suture ligation using the LARIAT device in patients with atrial fibrillation: initial clinical experience. J Am Coll Cardiol. 2013;62(2):108-18.

219. Fahmy P, Spencer R, Tsang M, Gooderham P, Saw J. Left Atrial Appendage Closure for Atrial Fibrillation Is Safe and Effective After Intracranial or Intraocular Hemorrhage. Can J Cardiol. 2016;32(3):349-54.

220. Urena M, Rodes-Cabau J, Freixa X, Saw J, Webb JG, Freeman M, et al. Percutaneous left atrial appendage closure with the AMPLATZER cardiac plug device in patients with nonvalvular atrial fibrillation and contraindications to anticoagulation therapy. J Am Coll Cardiol. 2013;62(2):96-102.

221. Massumi A, Chelu MG, Nazeri A, May SA, Afshar-Kharaghan H, Saeed M, et al. Initial experience with a novel percutaneous left atrial appendage exclusion device in patients with atrial fibrillation, increased stroke risk, and contraindications to anticoagulation. Am J Cardiol. 2013;111(6):869-73.

222. Wiebe J, Franke J, Lehn K, Hofmann I, Vaskelyte L, Bertog S, et al. Percutaneous Left Atrial Appendage Closure With the Watchman Device: Long-Term Results Up to 5 Years. JACC Cardiovasc Interv. 2015;8(15):1915-21.

223. Narine K, DeWever O, Cathenis K, Mareel M, Van Belleghem Y, Van Nooten G. Transforming growth factor-beta-induced transition of fibroblasts: a model for myofibroblast procurement in tissue valve engineering. J Heart Valve Dis. 2004;13(2):281-9; discussion 9.

224. Shinoka T, Shum-Tim D, Ma PX, Tanel RE, Langer R, Vacanti JP, et al. Tissue-engineered heart valve leaflets: does cell origin affect outcome? Circulation. 1997;96(9 Suppl):II-102-7.

225. Neidert MR, Tranquillo RT. Tissue-engineered valves with commissural alignment. Tissue Eng. 2006;12(4):891-903.

226. Filip DA. Mouse atrio-ventricular valve ultrastructure morphometrical correlations. Morphol Embryol (Bucur). 1984;30(3):165-73.

227. Mulholland DL, Goebel N. Cardiac valve interstitial cells: regulator of valve structure and function. Cardiovasc Pathol. 1997;6(3):167-74.

228. Messier RH, Jr., Bass BL, Aly HM, Jones JL, Domkowski PW, Wallace RB, et al. Dual structural and functional phenotypes of the porcine aortic valve interstitial population: characteristics of the leaflet myofibroblast. J Surg Res. 1994;57(1):1-21.

229. Johnson CM, Hanson MN, Helgeson SC. Porcine cardiac valvular subendothelial cells in culture: cell isolation and growth characteristics. J Mol Cell Cardiol. 1987;19(12):1185-93.

230. Chester AH, Taylor PM. Molecular and functional characteristics of heart-valve interstitial cells. Philos Trans R Soc Lond B Biol Sci. 2007;362(1484):1437-43.

231. Filip DA, Radu A, Simionescu M. Interstitial cells of the heart valves possess characteristics similar to smooth muscle cells. Circ Res. 1986;59(3):310-20.

232. Komuro T. Re-evaluation of fibroblasts and fibroblast-like cells. Anat Embryol (Berl). 1990;182(2):103-12.

233. Butcher JT, Nerem RM. Porcine aortic valve interstitial cells in three-dimensional culture: comparison of phenotype with aortic smooth muscle cells. J Heart Valve Dis. 2004;13(3):478-85; discussion 85-6.

234. Della Rocca F, Sartore S, Guidolin D, Bertiplaglia B, Gerosa G, Casarotto D, et al. Cell composition of the human pulmonary valve: a comparative study with the aortic valve--the VESALIO Project. Vitalitate Exornatum Succedaneum Aorticum labore Ingegnoso Obtinebitur. Ann Thorac Surg. 2000;70(5):1594-600.

235. Merryman WD, Lukoff HD, Long RA, Engelmayr GC, Jr., Hopkins RA, Sacks MS. Synergistic effects of cyclic tension and transforming growth factor-beta1 on the aortic valve myofibroblast. Cardiovasc Pathol. 2007;16(5):268-76.

236. Sacks MS, David Merryman W, Schmidt DE. On the biomechanics of heart valve function. J Biomech. 2009;42(12):1804-24.

237. Liu AC, Joag VR, Gotlieb AI. The emerging role of valve interstitial cell phenotypes in regulating heart valve pathobiology. Am J Pathol. 2007;171(5):1407-18.

238. Moraes C, Likhitpanichkul M, Lam CJ, Beca BM, Sun Y, Simmons CA. Microdevice array-based identification of distinct mechanobiological response profiles in layer-specific valve interstitial cells. Integr Biol (Camb). 2013;5(4):673-80.

239. Walker GA, Masters KS, Shah DN, Anseth KS, Leinwand LA. Valvular myofibroblast activation by transforming growth factor-beta: implications for pathological extracellular matrix remodeling in heart valve disease. Circ Res. 2004;95(3):253-60.

240. Xu S, Liu AC, Kim H, Gotlieb AI. Cell density regulates in vitro activation of heart valve interstitial cells. Cardiovasc Pathol. 2012;21(2):65-73.

241. Simmons CA. Aortic valve mechanics: an emerging role for the endothelium. J Am Coll Cardiol. 2009;53(16):1456-8.

242. Gould ST, Matherly EE, Smith JN, Heistad DD, Anseth KS. The role of valvular endothelial cell paracrine signaling and matrix elasticity on valvular interstitial cell activation. Biomaterials. 2014;35(11):3596-606.

243. Jian B, Narula N, Li QY, Mohler ER, 3rd, Levy RJ. Progression of aortic valve stenosis: TGF-beta1 is present in calcified aortic valve cusps and promotes aortic valve interstitial cell calcification via apoptosis. Ann Thorac Surg. 2003;75(2):457-65; discussion 65-6.

244. Monzack EL, Masters KS. Can valvular interstitial cells become true osteoblasts? A side-by-side comparison. J Heart Valve Dis. 2011;20(4):449-63.

245. Hjortnaes J, Shapero K, Goettsch C, Hutcheson JD, Keegan J, Kluin J, et al. Valvular interstitial cells suppress calcification of valvular endothelial cells. Atherosclerosis. 2015;242(1):251-60.

246. O'Brien KD, Kuusisto J, Reichenbach DD, Ferguson M, Giachelli C, Alpers CE, et al. Osteopontin is expressed in human aortic valvular lesions. Circulation. 1995;92(8):2163-8.

247. Cloyd KL, El-Hamamsy I, Boonrungsiman S, Hedegaard M, Gentleman E, Sarathchandra P, et al. Characterization of porcine aortic valvular interstitial cell 'calcified' nodules. PLoS One. 2012;7(10):e48154.

248. Rajamannan NM, Subramaniam M, Rickard D, Stock SR, Donovan J, Springett M, et al. Human aortic valve calcification is associated with an osteoblast phenotype. Circulation. 2003;107(17):2181-4.

249. Hajdu Z, Romeo SJ, Fleming PA, Markwald RR, Visconti RP, Drake CJ. Recruitment of bone marrow-derived valve interstitial cells is a normal homeostatic process. J Mol Cell Cardiol. 2011;51(6):955-65.

250. Wang H, Sridhar B, Leinwand LA, Anseth KS. Characterization of cell subpopulations expressing progenitor cell markers in porcine cardiac valves. PLoS One. 2013;8(7):e69667.

251. Chakraborty S, Cheek J, Sakthivel B, Aronow BJ, Yutzey KE. Shared gene expression profiles in developing heart valves and osteoblast progenitor cells. Physiol Genomics. 2008;35(1):75-85.

252. Rabkin-Aikawa E, Farber M, Aikawa M, Schoen FJ. Dynamic and reversible changes of interstitial cell phenotype during remodeling of cardiac valves. J Heart Valve Dis. 2004;13(5):841-7.

253. Latif N, Sarathchandra P, Taylor PM, Antoniw J, Yacoub MH. Localization and pattern of expression of extracellular matrix components in human heart valves. J Heart Valve Dis. 2005;14(2):218-27.

254. Cushing MC, Jaeggli MP, Masters KS, Leinwand LA, Anseth KS. Serum deprivation improves seeding and repopulation of acellular matrices with valvular interstitial cells. J Biomed Mater Res A. 2005;75(1):232-41.

255. Gu X, Masters KS. Regulation of valvular interstitial cell calcification by adhesive peptide sequences. J Biomed Mater Res A. 2010;93(4):1620-30.

256. Chen JH, Simmons CA. Cell-matrix interactions in the pathobiology of calcific aortic valve disease: critical roles for matricellular, matricrine, and matrix mechanics cues. Circ Res. 2011;108(12):1510-24.

257. Guilak F, Cohen DM, Estes BT, Gimble JM, Liedtke W, Chen CS. Control of stem cell fate by physical interactions with the extracellular matrix. Cell Stem Cell. 2009;5(1):17-26.

258. Spadaccio C, Mozetic P, Nappi F, Nenna A, Sutherland F, Trombetta M, et al. Cells and extracellular matrix interplay in cardiac valve disease: because age matters. Basic Res Cardiol. 2016;111(2):16.

259. Merryman WD, Youn I, Lukoff HD, Krueger PM, Guilak F, Hopkins RA, et al. Correlation between heart valve interstitial cell stiffness and transvalvular pressure: implications for collagen biosynthesis. Am J Physiol Heart Circ Physiol. 2006;290(1):H224-31.

260. Yip CY, Chen JH, Zhao R, Simmons CA. Calcification by valve interstitial cells is regulated by the stiffness of the extracellular matrix. Arterioscler Thromb Vasc Biol. 2009;29(6):936-42.

261. Wu Y, Puperi DS, Grande-Allen KJ, West JL. Ascorbic acid promotes extracellular matrix deposition while preserving valve interstitial cell quiescence within 3D hydrogel scaffolds. J Tissue Eng Regen Med. 2015.

262. Benton JA, Kern HB, Anseth KS. Substrate properties influence calcification in valvular interstitial cell culture. J Heart Valve Dis. 2008;17(6):689-99.

263. Kloxin AM, Benton JA, Anseth KS. In situ elasticity modulation with dynamic substrates to direct cell phenotype. Biomaterials. 2010;31(1):1-8.

264. Tomasek JJ, Gabbiani G, Hinz B, Chaponnier C, Brown RA. Myofibroblasts and mechano-regulation of connective tissue remodelling. Nat Rev Mol Cell Biol. 2002;3(5):349-63.

265. van Putten S, Shafieyan Y, Hinz B. Mechanical control of cardiac myofibroblasts. J Mol Cell Cardiol. 2015.

266. Engler AJ, Sen S, Sweeney HL, Discher DE. Matrix elasticity directs stem cell lineage specification. Cell. 2006;126(4):677-89.

267. Even-Ram S, Artym V, Yamada KM. Matrix control of stem cell fate. Cell. 2006;126(4):645-7.

268. Reilly GC, Engler AJ. Intrinsic extracellular matrix properties regulate stem cell differentiation. J Biomech. 2010;43(1):55-62.

269. Bowers SL, Banerjee I, Baudino TA. The extracellular matrix: at the center of it all. J Mol Cell Cardiol. 2010;48(3):474-82.

270. Abraityte A, Gullestad L, Askevold ET, Nymo S, Dahl CP, Aakhus S, et al. The Notch ligand Delta-like 1 is elevated and associated with mortality in patients with symptomatic aortic stenosis. Int J Cardiol. 2015;180:18-20.

271. Bray S, Bernard F. Notch targets and their regulation. Curr Top Dev Biol. 2010;92:253-75.

272. Kitagawa M, Hojo M, Imayoshi I, Goto M, Ando M, Ohtsuka T, et al. Hes1 and Hes5 regulate vascular remodeling and arterial specification of endothelial cells in brain vascular development. Mech Dev. 2013;130(9-10):458-66.

273. Kokubo H, Miyagawa-Tomita S, Johnson RL. Hesr, a mediator of the Notch signaling, functions in heart and vessel development. Trends Cardiovasc Med. 2005;15(5):190-4.

274. Gazave E, Lapebie P, Richards GS, Brunet F, Ereskovsky AV, Degnan BM, et al. Origin and evolution of the Notch signalling pathway: an overview from eukaryotic genomes. BMC Evol Biol. 2009;9:249.

275. Weber D, Wiese C, Gessler M. Hey bHLH transcription factors. Curr Top Dev Biol. 2014;110:285-315.

276. Carlson ME, Conboy IM. Regulating the Notch pathway in embryonic, adult and old stem cells. Curr Opin Pharmacol. 2007;7(3):303-9.

277. Acharya A, Hans CP, Koenig SN, Nichols HA, Galindo CL, Garner HR, et al. Inhibitory role of Notch1 in calcific aortic valve disease. PLoS One. 2011;6(11):e27743.

278. Fischer A, Gessler M. Delta-Notch--and then? Protein interactions and proposed modes of repression by Hes and Hey bHLH factors. Nucleic Acids Res. 2007;35(14):4583-96.

279. Tao G, Kotick JD, Lincoln J. Heart valve development, maintenance, and disease: the role of endothelial cells. Curr Top Dev Biol. 2012;100:203-32.

280. de la Pompa JL, Epstein JA. Coordinating tissue interactions: Notch signaling in cardiac development and disease. Dev Cell. 2012;22(2):244-54.

281. Rusanescu G, Weissleder R, Aikawa E. Notch signaling in cardiovascular disease and calcification. Curr Cardiol Rev. 2008;4(3):148-56.

282. Fischer A, Gessler M. Hey genes in cardiovascular development. Trends Cardiovasc Med. 2003;13(6):221-6.

283. MacGrogan D, Nus M, de la Pompa JL. Notch signaling in cardiac development and disease. Curr Top Dev Biol. 2010;92:333-65.

284. Fischer A, Steidl C, Wagner TU, Lang E, Jakob PM, Friedl P, et al. Combined loss of Hey1 and HeyL causes congenital heart defects because of impaired epithelial to mesenchymal transition. Circ Res. 2007;100(6):856-63.

285. Kokubo H, Miyagawa-Tomita S, Nakazawa M, Saga Y, Johnson RL. Mouse hesr1 and hesr2 genes are redundantly required to mediate Notch signaling in the developing cardiovascular system. Dev Biol. 2005;278(2):301-9.

286. Kokubo H, Miyagawa-Tomita S, Tomimatsu H, Nakashima Y, Nakazawa M, Saga Y, et al. Targeted disruption of hesr2 results in atrioventricular valve anomalies that lead to heart dysfunction. Circ Res. 2004;95(5):540-7.

287. Nemir M, Pedrazzini T. Functional role of Notch signaling in the developing and postnatal heart. J Mol Cell Cardiol. 2008;45(4):495-504.

288. Schroeder T, Meier-Stiegen F, Schwanbeck R, Eilken H, Nishikawa S, Hasler R, et al. Activated Notch1 alters differentiation of embryonic stem cells into mesodermal cell lineages at multiple stages of development. Mech Dev. 2006;123(7):570-9.

289. Bosse K, Hans CP, Zhao N, Koenig SN, Huang N, Guggilam A, et al. Endothelial nitric oxide signaling regulates Notch1 in aortic valve disease. J Mol Cell Cardiol. 2013;60:27-35.

290. Nigam V, Srivastava D. Notch1 represses osteogenic pathways in aortic valve cells. J Mol Cell Cardiol. 2009;47(6):828-34.

291. Nus M, MacGrogan D, Martinez-Poveda B, Benito Y, Casanova JC, Fernandez-Aviles F, et al. Diet-induced aortic valve disease in mice haploinsufficient for the Notch pathway effector RBPJK/CSL. Arterioscler Thromb Vasc Biol. 2011;31(7):1580-8.

292. Pedrazzini T. Control of cardiogenesis by the notch pathway. Trends Cardiovasc Med. 2007;17(3):83-90.

293. Kostina AS, Uspensky Vcapital Ie C, Irtyuga OB, Ignatieva EV, Freylikhman O, Gavriliuk ND, et al. Notch-dependent EMT is attenuated in patients with aortic aneurysm and bicuspid aortic valve. Biochim Biophys Acta. 2016;1862(4):733-40.

294. van den Akker NM, Caolo V, Molin DG. Cellular decisions in cardiac outflow tract and coronary development: an act by VEGF and NOTCH. Differentiation. 2012;84(1):62-78.

295. Garg V, Muth AN, Ransom JF, Schluterman MK, Barnes R, King IN, et al. Mutations in NOTCH1 cause aortic valve disease. Nature. 2005;437(7056):270-4.

296. Gnecchi M, Melo LG. Bone marrow-derived mesenchymal stem cells: isolation, expansion, characterization, viral transduction, and production of conditioned media. Methods Mol Bio. 2009;482:281-94.

297. Shihabi ZK, Dyer RD. Protein analysis with bicinchoninic acid. Ann Clin Lab Sci. 1988;18(3):235-9.

298. Zhang G, Ueberheide BM, Waldemarson S, Myung S, Molloy K, Eriksson J, et al. Protein quantitation using mass spectrometry. Methods Mol Biol. 2010;673:211-22.

299. Stephens EH, Carroll JL, Grande-Allen KJ. The use of collagenase III for the isolation of porcine aortic valvular interstitial cells: rationale and optimization. J Heart Valve Dis. 2007;16(2):175-83.

300. Witt W, Buttner P, Jannasch A, Matschke K, Waldow T. Reversal of myofibroblastic activation by polyunsaturated fatty acids in valvular interstitial cells from aortic valves. Role of RhoA/G-actin/MRTF signalling. J Mol Cell Cardiol. 2014;74:127-38.

301. Xie C, Shen Y, Hu W, Chen Z, Li Y. Angiotensin II promotes an osteoblast-like phenotype in porcine aortic valve myofibroblasts. Aging Clin Exp Res. 2016;28(2):181-7.

302. Li C, Gotlieb AI. Transforming growth factor-beta regulates the growth of valve interstitial cells in vitro. Am J Pathol. 2011;179(4):1746-55.

303. Rompre P, Auger FA, Germain L, Bouvard V, Lopez Valle CA, Thibault J, et al. Influence of initial collagen and cellular concentrations on the final surface area of dermal and skin equivalents: a Box-Behnken analysis. In Vitro Cell Dev Biol. 1990;26(10):983-90.

304. Fray TR, Molloy JE, Armitage MP, Sparrow JC. Quantification of single human dermal fibroblast contraction. Tissue Eng. 1998;4(3):281-91.

305. Junker JP, Lonnqvist S, Rakar J, Karlsson LK, Grenegard M, Kratz G. Differentiation of human dermal fibroblasts towards endothelial cells. Differentiation. 2013;85(3):67-77.

306. Hentzer B, Kobayasi T. Enzymatic liberation of viable cells of human skin. Acta Derm Venereol. 1978;58(3):197-202.

307. Lester W, Rosenthal A, Granton B, Gotlieb AI. Porcine mitral valve interstitial cells in culture. Lab Invest. 1988;59(5):710-9.

308. Snider P, Standley KN, Wang J, Azhar M, Doetschman T, Conway SJ. Origin of cardiac fibroblasts and the role of periostin. Circ Res. 2009;105(10):934-47.

309. Norris RA, Moreno-Rodriguez RA, Sugi Y, Hoffman S, Amos J, Hart MM, et al. Periostin regulates atrioventricular valve maturation. Dev Biol. 2008;316(2):200-13.

310. Butcher JT, Norris RA, Hoffman S, Mjaatvedt CH, Markwald RR. Periostin promotes atrioventricular mesenchyme matrix invasion and remodeling mediated by integrin signaling through Rho/PI 3-kinase. Dev Biol. 2007;302(1):256-66.

311. Inai K, Norris RA, Hoffman S, Markwald RR, Sugi Y. BMP-2 induces cell migration and periostin expression during atrioventricular valvulogenesis. Dev Biol. 2008;315(2):383-96.

312. Sider KL, Blaser MC, Simmons CA. Animal models of calcific aortic valve disease. Int J Inflam. 2011;2011:364310.

313. Hakuno D, Kimura N, Yoshioka M, Mukai M, Kimura T, Okada Y, et al. Periostin advances atherosclerotic and rheumatic cardiac valve degeneration by inducing angiogenesis and MMP production in humans and rodents. J Clin Invest. 2010;120(7):2292-306.

314. Chowdhury F, Li Y, Poh YC, Yokohama-Tamaki T, Wang N, Tanaka TS. Soft substrates promote homogeneous self-renewal of embryonic stem cells via downregulating cell-matrix tractions. PLoS One. 2010;5(12):e15655.

315. Forte G, Pagliari S, Ebara M, Uto K, Tam JK, Romanazzo S, et al. Substrate stiffness modulates gene expression and phenotype in neonatal cardiomyocytes in vitro. Tissue Eng Part A. 2012;18(17-18):1837-48.

316. Petersen A, Joly P, Bergmann C, Korus G, Duda GN. The impact of substrate stiffness and mechanical loading on fibroblast-induced scaffold remodeling. Tissue Eng Part A. 2012;18(17-18):1804-17.

317. Winer JP, Janmey PA, McCormick ME, Funaki M. Bone marrow-derived human mesenchymal stem cells become quiescent on soft substrates but remain responsive to chemical or mechanical stimuli. Tissue Eng Part A. 2009;15(1):147-54.

318. Yeung T, Georges PC, Flanagan LA, Marg B, Ortiz M, Funaki M, et al. Effects of substrate stiffness on cell morphology, cytoskeletal structure, and adhesion. Cell Motil Cytoskeleton. 2005;60(1):24-34.

319. Horne TE, VandeKopple M, Sauls K, Koenig SN, Anstine LJ, Garg V, et al. Dynamic Heterogeneity of the Heart Valve Interstitial Cell Population in Mitral Valve Health and Disease. J Cardiovasc Dev Dis. 2015;2(3):214-32.

320. Amer LD, Bryant SJ. The In Vitro and In Vivo Response to MMP-Sensitive Poly(Ethylene Glycol) Hydrogels. Ann Biomed Eng. 2016.

321. Engler AJ, Griffin MA, Sen S, Bonnemann CG, Sweeney HL, Discher DE. Myotubes differentiate optimally on substrates with tissue-like stiffness: pathological implications for soft or stiff microenvironments. J Cell Biol. 2004;166(6):877-87.

322. Hjortnaes J, Goettsch C, Hutcheson JD, Camci-Unal G, Lax L, Scherer K, et al. Simulation of early calcific aortic valve disease in a 3D platform: A role for myofibroblast differentiation. J Mol Cell Cardiol. 2016;94:13-20.

323. Mabry KM, Lawrence RL, Anseth KS. Dynamic stiffening of poly(ethylene glycol)-based hydrogels to direct valvular interstitial cell phenotype in a three-dimensional environment. Biomaterials. 2015;49:47-56.

324. Janmey PA, Winer JP, Murray ME, Wen Q. The hard life of soft cells. Cell Motil Cytoskeleton. 2009;66(8):597-605.

325. Garside VC, Chang AC, Karsan A, Hoodless PA. Co-ordinating Notch, BMP, and TGF-beta signaling during heart valve development. Cell Mol Life Sci. 2013;70(16):2899-917.

326. Kerstjens-Frederikse WS, van de Laar IM, Vos YJ, Verhagen JM, Berger RM, Lichtenbelt KD, et al. Cardiovascular malformations caused by NOTCH1 mutations do not keep left: data on 428 probands with left-sided CHD and their families. Genet Med. 2016.

327. Niessen K, Karsan A. Notch signaling in cardiac development. Circ Res. 2008;102(10):1169-81.

328. Timmerman LA, Grego-Bessa J, Raya A, Bertran E, Perez-Pomares JM, Diez J, et al. Notch promotes epithelial-mesenchymal transition during cardiac development and oncogenic transformation. Genes Dev. 2004;18(1):99-115.

329. Woltje K, Jabs M, Fischer A. Serum induces transcription of Hey1 and Hey2 genes by Alk1 but not Notch signaling in endothelial cells. PLoS One. 2015;10(3):e0120547.

330. Wang D, Zeng Q, Song R, Ao L, Fullerton DA, Meng X. Ligation of ICAM-1 on human aortic valve interstitial cells induces the osteogenic response: A critical role of the Notch1-NF-kappaB pathway in BMP-2 expression. Biochim Biophys Acta. 2014;1843(11):2744-53.

331. Chau MD, Tuft R, Fogarty K, Bao ZZ. Notch signaling plays a key role in cardiac cell differentiation. Mech Dev. 2006;123(8):626-40.

332. Chen CY, Ezzeddine N, Shyu AB. Messenger RNA half-life measurements in mammalian cells. Methods Enzymol. 2008;448:335-57.

333. Harrold S, Genovese C, Kobrin B, Morrison SL, Milcarek C. A comparison of apparent mRNA half-life using kinetic labeling techniques vs decay following administration of transcriptional inhibitors. Anal Biochem. 1991;198(1):19-29.

334. Loflin PT, Chen CY, Xu N, Shyu AB. Transcriptional pulsing approaches for analysis of mRNA turnover in mammalian cells. Methods. 1999;17(1):11-20.

335. Doetzlhofer A, Basch ML, Ohyama T, Gessler M, Groves AK, Segil N. Hey2 regulation by FGF provides a Notch-independent mechanism for maintaining pillar cell fate in the organ of Corti. Dev Cell. 2009;16(1):58-69.

336. Pfeiffer S, Leopold E, Schmidt K, Brunner F, Mayer B. Inhibition of nitric oxide synthesis by NG-nitro-L-arginine methyl ester (L-NAME): requirement for bioactivation to the free acid, NG-nitro-L-arginine. Br J Pharmacol. 1996;118(6):1433-40.

337. Ngo MA, Muller A, Li Y, Neumann S, Tian G, Dixon IM, et al. Human mesenchymal stem cells express a myofibroblastic phenotype in vitro: comparison to human cardiac myofibroblasts. Mol Cell Biochem. 2014;392(1-2):187-204.